
Masters Theses

Student Theses and Dissertations

1967

Film boiling from horizontal plates with low thermal capacity

K. M. Ragsdell

Missouri University of Science and Technology, ragsdell@mst.edu

Follow this and additional works at: https://scholarsmine.mst.edu/masters_theses



Part of the [Mechanical Engineering Commons](#)

Department:

Recommended Citation

Ragsdell, K. M., "Film boiling from horizontal plates with low thermal capacity" (1967). *Masters Theses*. 5156.

https://scholarsmine.mst.edu/masters_theses/5156

This thesis is brought to you by Scholars' Mine, a service of the Missouri S&T Library and Learning Resources. This work is protected by U. S. Copyright Law. Unauthorized use including reproduction for redistribution requires the permission of the copyright holder. For more information, please contact scholarsmine@mst.edu.

FILM BOILING FROM HORIZONTAL PLATES
WITH LOW THERMAL CAPACITY

BY

KENNETH M. RAGSDELL

A

THESIS

submitted to the faculty of

THE UNIVERSITY OF MISSOURI AT ROLLA

in partial fulfillment of the requirements for the

Degree of

MASTER OF SCIENCE IN MECHANICAL ENGINEERING

Rolla, Missouri

1967

Approved by

(advisor)

Harry Sawyer Jr.
Ralph E. Schowalter

John K. ...
Jan H. Johnson

ABSTRACT

The object of this investigation was to obtain data for saturated film pool boiling from a low thermal capacity flat plate at atmospheric pressure. A test plate, constructed from resistance strip, was placed horizontally in a pool of liquid, and was heated electrically. Refrigerant-11 and nitrogen were used as the boiling liquids.

Heat transfer results were obtained in both fluids over a temperature range of approximately 1200F^o (400-1600^oF).

Surface size, roughness and orientation effects were observed for flat horizontal heated surfaces with one dimension near the most dangerous wavelength. No surface material effect was observed.

Excellent correlation of the data is achieved by a slight modification to the Berenson equation.

ACKNOWLEDGEMENTS

Thanks are offered to the National Science Foundation for their support of this project.

The professional advice and leadership of my advisor Dr. Harry Sauer is gratefully acknowledged and sincerely appreciated as a significant factor in the successful completion of the project.

The help and advice of Lee Anderson and LeRoy Tipton in the machine shop work is appreciated.

The daily advice of Dick Smith in the Mechanical Engineering Laboratory was very helpful and sincerely appreciated.

The part-time work of Richard Baumann, Paul Shank and Robert Lewis in the laboratory is acknowledged.

The constructive criticism of Dr. Lyle Rhea and Dr. Virgil Flanigan is appreciated.

Thanks go to Mrs. Kathy Taylor for typing the manuscript.

Sincere thanks and appreciation go to my wife Janet for her suggestions and patience throughout the execution of this project. Her wisdom in delaying the birth of our first child until the finished manuscript was ready is appreciated.

TABLE OF CONTENTS

	<u>Page No.</u>
NOMENCLATURE	iv
LIST OF ILLUSTRATIONS	vii
LIST OF TABLES	ix
I. INTRODUCTION	1
II. LITERATURE REVIEW	7
III. EXPERIMENTAL INVESTIGATION	26
IV. RESULTS	40
V. CONCLUSIONS AND RECOMMENDATIONS	69
REFERENCES	70
APPENDICES	73
A. Discussion of Applied Hydrodynamics	73
B. Experimental Data	78
C. Statistical Data Analysis	104
D. Thermophysical Properties	112
VITA	114

NOMENCLATURE

<u>SYMBOL</u>	<u>SIGNIFICANCE</u>	<u>UNITS</u>
<u>CAPITAL LETTERS</u>		
A	Area	ft ²
Gr ₁ [*]	Generalized Grashof Number	---
I	Current	amps
K	Thermal Conductivity	$\frac{\text{BTU}}{\text{hr. ft. } ^\circ\text{F}}$
L	Characteristic Length	---
N	Displacement Perpendicular to Interface	ft.
(Nu ₁) _{co}	Nusselt Number Using Characteristic Length L and Considering Convection Only in Film Boiling	---
P _r [*]	Generalized Prandtl Number	---
ΔT	Temperature of Wall Minus Saturation Temperature of Liquid	°F
ΔT _B	Temperature Drop in Transite Backing	°F
ΔV	Voltage Drop Across Test Section	volts
ΔX	Distance between Thermocouples in Backing	ft.
<u>LOWER CASE LETTERS</u>		
g	Acceleration due to gravity	$\frac{\text{ft.}}{\text{sec.}^2}$
g _c	Gravitational Constant	$\frac{\text{lbs. ft.}}{\text{m. sec.}^2}$
h	Heat Transfer Coefficient	$\frac{\text{BTU}}{\text{hr. ft. } ^2\text{ } ^\circ\text{F}}$
h _{fg}	Average Enthalpy Difference Between Vapor and Liquid	$\frac{\text{BTU}}{\text{lbs. m}}$

<u>SYMBOL</u>	<u>SIGNIFICANCE</u>	<u>UNITS</u>
<u>LOWER CASE LETTERS</u>		
h_{fg}	Latent Heat of Vaporization	$\frac{\text{BTU}}{\text{lbs.}_m}$
m	Wave Number	ft.^{-1}
q or Q	Heat Generated	$\frac{\text{BTU}}{\text{hr.}}$
x	Distance Along Interface	ft.
<u>GREEK LETTERS</u>		
α_c	Equivalent Thermal Diffusivity in Film Boiling by Convection Only	$\frac{\text{ft.}^2}{\text{hr.}}$
λ	Wavelength	ft.
μ	Viscosity	$\frac{\text{lbs.}_f \text{ hr}}{\text{ft.}^2}$
ν	Kinematic Viscosity	$\frac{\text{ft.}^2}{\text{hr.}}$
ω	Wave Frequency	$\frac{\text{rad.}}{\text{sec.}}$
ρ	Density	$\frac{\text{lbs.}_m}{\text{ft.}^3}$
σ	Surface Tension	$\frac{\text{lbs.}_f}{\text{ft.}}$
<u>SUBSCRIPTS</u>		
B. P.	Burnout Point	---
c	Critical	---
d	Most Dangerous	---
f	Film	---

<u>SYMBOL</u>	<u>SIGNIFICANCE</u>	<u>UNITS</u>
<u>SUBSCRIPTS</u>		
l	Liquid	---
L. P.	Leidenfrost Point	---
t	Transite	---
v	Vapor	---

LIST OF ILLUSTRATIONS

	<u>Page No.</u>
FIGURE 1 - Typical Boiling Curve	2
FIGURE 2 - Film Boiling From a Flat Plate	6
FIGURE 3 - Nukiyama' s Boiling Curve	8
FIGURE 4 - Film Correlation from Brentari and Smith.....	18
FIGURE 5 - Experimental Apparatus	27
FIGURE 6 - Schematic of Test Set-Up	28
FIGURE 7 - Heater Assembly.....	30
FIGURE 8 - Thermocouple Spot Welder	31
FIGURE 9 - Power Supply.....	33
FIGURE 10 - Power Generation Curve	34
FIGURE 11 - Heater in Dewar	35
FIGURE 12 - Typical Recorder Output	37
FIGURE 13 - Heat Flux Results for R-11 on 0.5 in. wide Inconel Horizontal Surface	41
FIGURE 14 - Heat Flux Results for R-11 on 1.0 in. wide Kanthal Horizontal Surface	42
FIGURE 15 - Heat Flux Results for R-11 on 2.0 in. wide Inconel Horizontal Surface	43
FIGURE 16 - Heat Transfer Coefficient for R-11 on 1.0 in.wide Kanthal Horizontal Surface	45
FIGURE 17 - Heat Transfer Ccoefficient for R-11 on an Inconel Horizontal Surface	46
FIGURE 18 - H versus q/A for R-11 on Horizontal Surface Showing Heated Surface Size Effect	48
FIGURE 19 - Heat Flux Results for N ₂ on 0.5 in. wide Inconel Horizontal Surface	49
FIGURE 20 - Heat Flux Results for N ₂ on 1.0 in. wide Inconel Horizontal Surface	50
FIGURE 21 - Heat Flux Results for N ₂ on 2.0 in. wide Inconel Horizontal Surface	52

	<u>Page No.</u>
FIGURE 22 - Heat Flux Results for N_2 Showing Heated Surface Size Effect	53
FIGURE 23 - Heat Flux Results for N_2 on 0.5 in. wide Kanthal Horizontal Surface	54
FIGURE 24 - Heat Flux Results for N_2 on 1.0 in. wide Kanthal Horizontal Surface	55
FIGURE 25 - Heat Flux Results for N_2 on 1.0 in. wide sand blasted Kanthal Horizontal Surface	56
FIGURE 26 - Heat Flux Results for N_2 on 1.0 in. wide sand blasted Kanthal Horizontal Surface	57
FIGURE 27 - Heat Flux Results for N_2 on 2.0 in. wide Inconel Surface facing downward	58
FIGURE 28 - Heat Transfer Coefficient Results for N_2 on Inconel Horizontal Surface	60
FIGURE 29 - H versus q/A for N_2 on 1.0 in. wide Horizontal Surface	61
FIGURE 30 - H versus q/A for N_2 on Inconel Horizontal Surfaces ..	62
FIGURE 31 - Modified Berenson Equation	63

LIST OF TABLES

	<u>Page No.</u>
TABLE I - Hydrodynamic Results of Hosler and Westwater	15
TABLE II - Boiling Correlation Equations	25
TABLE III - Listing of Tests.	38
TABLE IV - Boiling Research Data and Results Tabulation, run 529	79
TABLE V - Boiling Research Data and Results Tabulation, run 603	80
TABLE VI - Boiling Research Data and Results Tabulation, run 605	81
TABLE VII - Boiling Research Data and Results Tabulation, run 621	82
TABLE VIII- Boiling Research Data and Results Tabulation, run 623A	83
TABLE IX - Boiling Research Data and Results Tabulation, run 623B	84
TABLE X - Boiling Research Data and Results Tabulation, run 629	86
TABLE XI - Boiling Research Data and Results Tabulation, run 630	87
TABLE XII - Boiling Research Data and Results Tabulation, run 704	89
TABLE XIII- Boiling Research Data and Results Tabulation, run 706	90
TABLE XIV- Boiling Research Data and Results Tabulation, run 711	92
TABLE XV - Boiling Research Data and Results Tabulation, run 717	93
TABLE XVI- Boiling Research Data and Results Tabulation, run 718A	95
TABLE XVII - Boiling Research Data and Results Tabulation, run 718B	97
TABLE XVIII- Boiling Research Data and Results Tabulation, run 719	100
TABLE XIX- Boiling Research Data and Results Tabulation, run 721	103
TABLE XX- Statistical Data for 0.5 in. Inconel in Nitrogen	105

	<u>Page No.</u>
TABLE XXI - Statistical Data for 1.0 in. Inconel in Nitrogen	106
TABLE XXII - Statistical Data for 2.0 in. Inconel in Nitrogen	107
TABLE XXIII- Statistical Data for 0.5 in. Inconcl in Ref rigerant-11.	108
TABLE XXIV- Statistical Data for 1.0 in. Kanthal inRefrigerant-11.	109
TABLE XXV - Statistical Data for 2.0 in. Inconel in Refrigerant-11.	110
TABLE XXVI- Statistical Data for 1.0 in. Kanthal in Refrigerant-11.	111

I. INTRODUCTION

Boiling heat transfer is an intensely interesting field of experimental and theoretical research. At first glance the boiling process, which is often observed in heating water on a kitchen stove, seems deceptively simple. As this boiling process has been subjected to formal investigation, the complexities of the boiling mechanisms have unfolded. In 1934 Nukiyama⁽¹⁾ * published a paper representing his experimental results for pool boiling from a wire and a flat plate to distilled water at atmospheric pressure. Nukiyama displayed three distinct boiling regions, and set in motion the desire to explain the boiling mechanism in each of the three regions. Since this time, a great deal of money and effort has been directed toward a better understanding of boiling heat transfer. This effort is motivated by the application of boiling in steam generators, quenching operations, nuclear reactors and for cooling jet engines, rockets and space vehicles. In the quenching operation of the heat treating of many metals, especially steels, it is very important to have a value for the heat transfer coefficient so that the temperature history of the metal can be predicted.

Since the early work of Nukiyama, many authors have reported experimental and/or theoretical explanations of the different boiling regions. These regions can best be defined and understood with the aid of a heat-flux versus temperature difference graph as shown in Figure 1.

* Numbers in parentheses refer to listings under References.

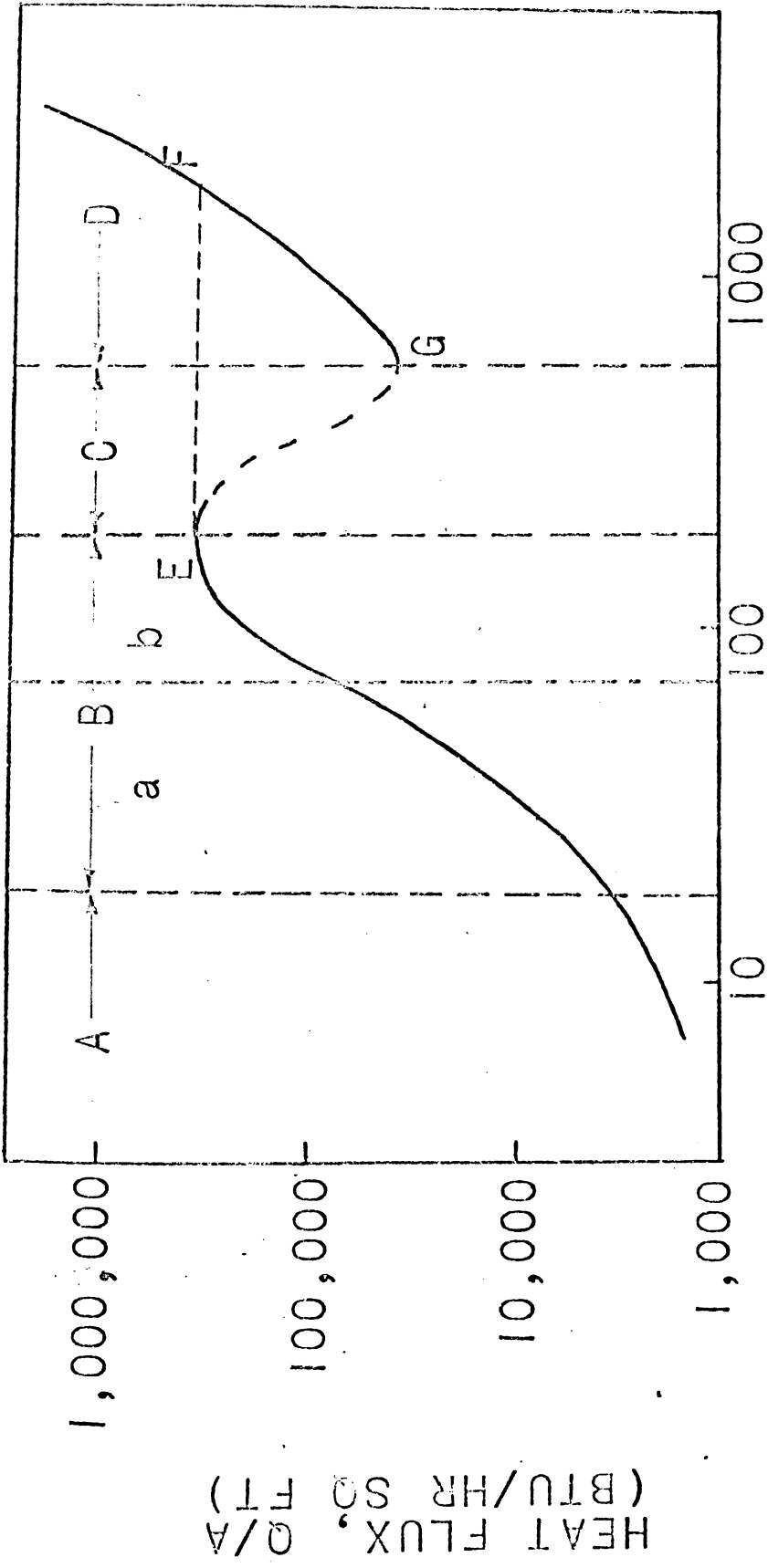


FIGURE 1 - Typical Boiling Curve

In region A steam is produced by vaporization at the liquid vapor interface. The heat transfer from the heater to the liquid takes place by conduction and single phase convection which maintains upward flow of superheated liquid. As the heater surface temperature increases into region B, the formation of bubbles of vapor at discrete points or nuclei on the heating surface gives this region the name, nucleate boiling. The nucleate region can be further divided into the (a) individual bubble, and (b) the continuous column regimes.

As the heater temperature increases, point E is reached where a further increase in temperature will cause a decrease in heat flux. This point is often called the burnout point, the critical excess temperature point, or the hydrodynamic crisis point⁽³⁾. The term burnout point is the most common, because of the destruction of power controlled heaters as the power level is raised above this maximum. Prediction of this burnout point is possible analytically using Helmholtz hydrodynamic instability criteria (See Appendix A). When the power is raised above the level allowed in the nucleate range, the only possibility is for the system to go into region D, film boiling, along a line similar to E - F. Notice that the temperature associated with point F is often above the melting point of the heater, depending on the fluid and the heater material, and therefore burnout occurs.

As the heater surface temperature is increased past point E, region C is entered and transition boiling occurs. There are really only two distinct regions of boiling, nucleate and film. In region C unstable nucleate

and film boiling coexist. The temperatures in region C are too high for stable nucleate but still too low for stable film boiling. Therefore, the mechanism at any one point on the heater alternates between nucleate and film boiling, because the amount of vapor generated by film boiling is too small to support the vapor film and the amount of vapor generated by nucleate boiling is too large to allow enough liquid to reach the heater in a steady stream. Since both of these mechanisms are present the variables that affect each separately should have an effect upon the transition region. An example of this is surface roughness which is known to have a pronounced effect upon nucleate boiling, and does indeed effect the slope of the transition curve.⁽⁴⁾

If the heater surface temperature is increased further in region C, a point G is reached where a further increase in temperature will cause an increase in heat flux. This point G is often referred to as the minimum point or the Leidenfrost point. Prediction of this minimum point is possible analytically using Taylor hydrodynamic instability criteria (See Appendix A). In 1756, Leidenfrost first studied the evaporation of small water droplets on a hot plate.⁽⁵⁾ From this experiment the Leidenfrost point has come into the literature and is defined as "the plate temperature at which the droplet evaporation time is (the) greatest". Or, conversely, as applied to pool boiling, the Leidenfrost point is that temperature at which the heat flux is a minimum in film boiling. Several investigators have offered methods for predicting the location of this minimum point and the rest of the film boiling curve of which point G is the lower limit; the most noteworthy of which are

Berenson,⁽⁴⁾ Bromley,⁽⁶⁾ Chang⁽⁷⁾ and Zuber.⁽⁸⁾

As the temperature of the heater is increased past the Leidenfrost point, stable film boiling occurs. In this region the heater surface is separated from the liquid by a blanket of vapor, as seen in Figure 2. Heat transfer occurs by conduction through the vapor blanket, convection at the liquid-vapor interface and bubble release at selected points along the interface. Several investigators have observed wave-like oscillation of the liquid-vapor interface in film boiling from a flat plate, where bubbles are released at the antinodes of oscillation. As the temperature of the heater surface increases further into the stable film region, radiation heat transfer from the heater surface becomes significant, and must be evaluated to allow calculation of the heat transfer coefficient due to boiling.

It is interesting to note that as recently as 1959 no film boiling data for flat plates had been published.⁽⁷⁾ Needless to say work has been done since this time, but the area is still too thinly populated.

The object of this investigation was to obtain data for saturated film pool boiling from a low thermal capacity flat plate at atmospheric pressure.

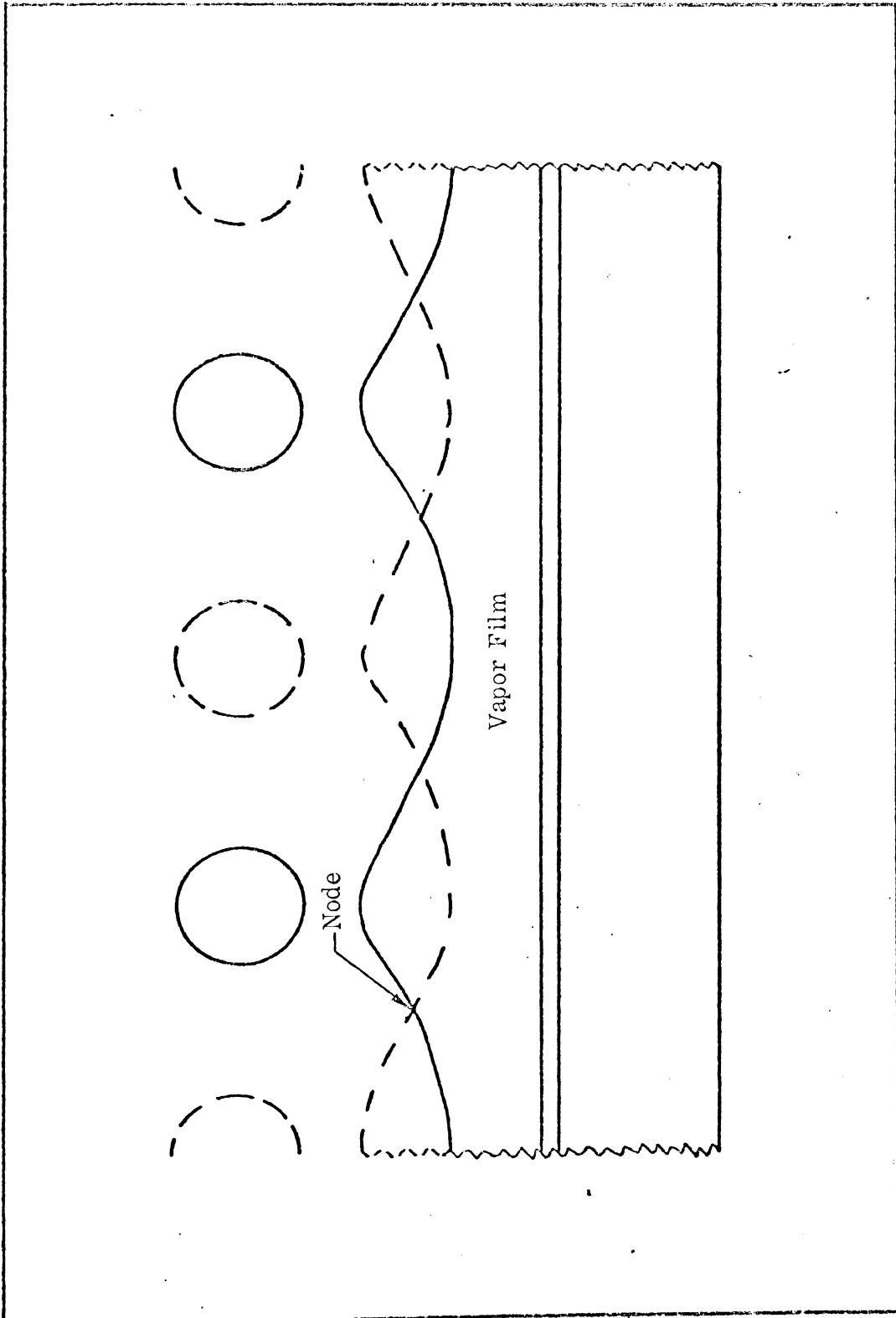


FIGURE 2 - Film Boiling From a Flat Plate

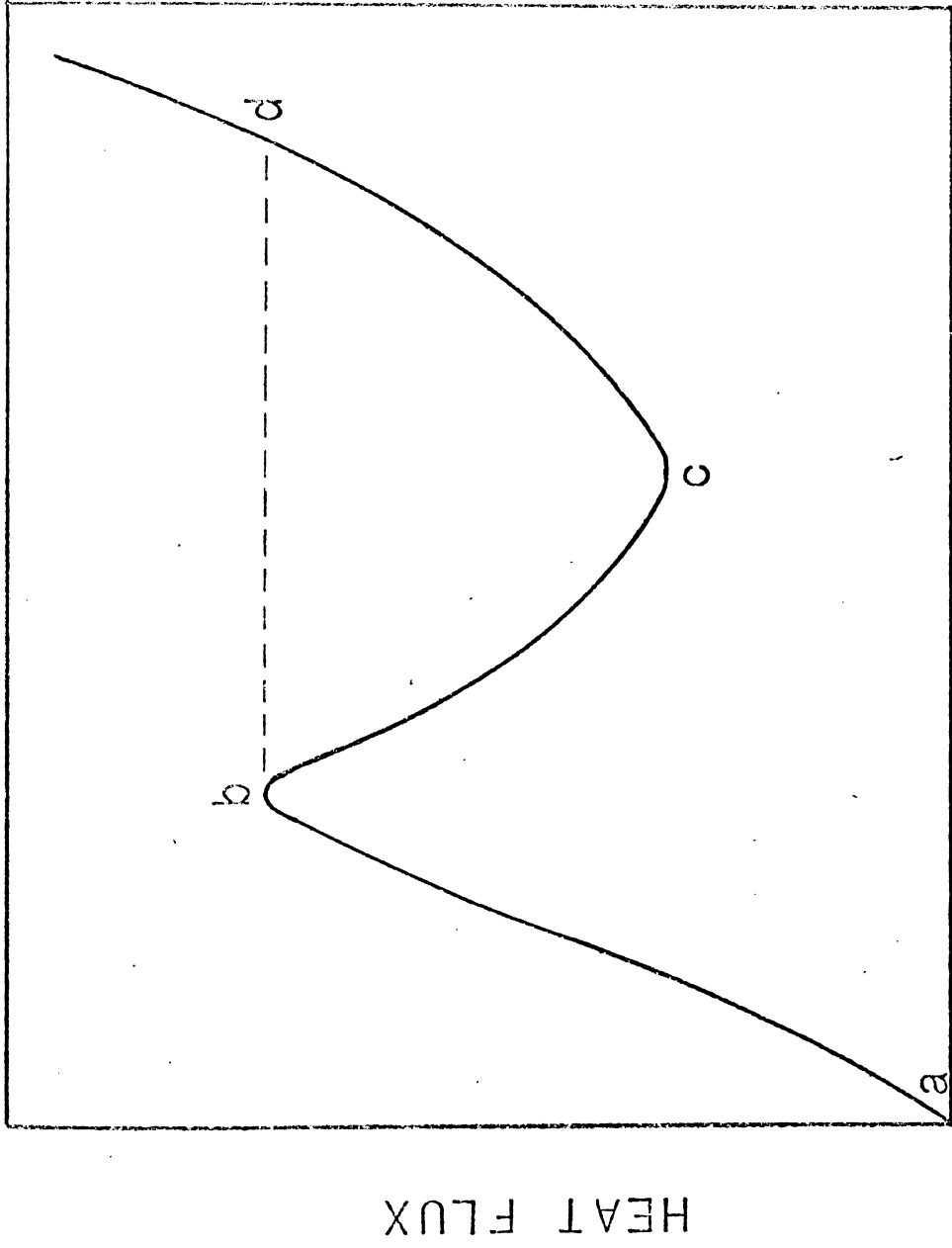
II. LITERATURE REVIEW

The literature of relevance to this investigation is arranged into four main groups, i. e., Film Boiling, Flat Surfaces; Nucleate Boiling, Flat Surfaces; Film Boiling, Other Surfaces; and Nucleate Boiling, Other Surfaces. The groups are listed here in order of decreasing value to this investigation.

Film Boiling, Flat Surfaces

Nukiyama⁽¹⁾ first noted in a paper published in 1934 that there was an upper limit to the heat transferred in the boiling process. He discussed the fact that previous authors had assumed that the heat transfer coefficient approached a fixed value asymptotically, and that the heat flux, q/A , increased with temperature difference without limit. As stated previously, Nukiyama described three distinct regions of boiling, as seen in Figure 3. He described what is now known as the nucleate region up to a maximum point b, and a region from d to c, known now as the film boiling region, as the spheroidal state.

Nukiyama conducted pool boiling experiments with electrically heated wires and flat plates, and presented data to verify the different boiling regions. He proved the existence of maximum and minimum values for q/A . He also postulated in his paper that a small part of the heater surface in nucleate boiling is at an elevated temperature forming nucleation sites, and the rest of the heater stays wetted and at the saturation temperature of the boiling liquid. The temperature that is recorded (for instance with a wire heater) using resistance thermometry is simply the weighted average of this elevated



TEMPERATURE DIFFERENCE

FIGURE 3 - Nukiyama's Boiling Curve

temperature and the lower saturation temperature.

Berenson^{(4), (9), (10)} has given much insight into the mechanisms of heat transfer occurring in nucleate and film boiling. In his investigation of the transition boiling region Berenson has concluded that there are only two distinct regions of boiling heat transfer and that transition boiling is a combination of nucleate boiling and film boiling over that range of temperature difference where neither is stable. Berenson also concluded that the burn-out flux is independent of surface material, roughness, and cleanliness and that the film boiling curve is independent of surface material, cleanliness, and roughness provided the roughness height is less than the film thickness. An interesting phenomenon occurs at the Leidenfrost point. Several minimum points may be observed depending upon the cleanliness of the heater material. Dirty surfaces cause the system to drop into nucleate boiling at higher temperature differences. A similar phenomenon occurs when a wetting agent is added to the boiling liquid, that is, the minimum point occurs at a higher temperature.

Berenson offers the following equations for the predictions of the Leidenfrost point:

$$(q/A)_{L.P.} = .09\rho_v h_{fg} \left[\frac{(\rho_l - \rho_v)}{\rho_l + \rho_v} \right]^{1/2} \left[\frac{g_c \sigma}{g(\rho_l - \rho_v)} \right]^{1/4}, \quad (1)$$

and

$$(\Delta T)_{L.P.} = .127 \frac{\rho_v h'_{fg}}{K_{vf}} \left[\frac{g(\rho_1 - \rho_v)}{\rho_1 + \rho_v} \right]^{2/3} \left[\frac{g_c \sigma}{g(\rho_1 - \rho_v)} \right]^{1/2} \left[\frac{\mu_f}{g_c (\rho_1 - \rho_v)} \right]^{1/3}, \quad (2)$$

which agree with his data within $\pm 10\%$. Also presented is the following equation for stable film boiling:

$$h = .425 \left[\frac{K_{vf}^3 h'_{fg} \rho_{vf} g (\rho_1 - \rho_v)}{\mu_{vf} \Delta T_g \left[\frac{g_c \sigma}{g(\rho_1 - \rho_v)} \right]} \right]^{1/4}. \quad (3)$$

Chang⁽⁷⁾ in a paper published in 1959 offers a theoretical model for film boiling from flat plates. By means of the concepts of equivalent thermal diffusivity a generalized Prandtl number is recommended. Thus, a general formula is obtained for both convection and boiling. In his paper, Chang investigates film boiling from horizontal and vertical flat plates. Of interest to this investigation are his results for the horizontal flat plate.

Chang suggests that a standing wave exists over a plane surface experiencing film boiling. Since the temperature of the flat heating surface is higher than the vapor that surrounds it, heat is transmitted to the vapor film causing it to thicken.

The vapor film grows to a thickness that will no longer support the boiling liquid, therefore, the film ruptures and heat and mass transfer occur at the anti-node of the standing wave.

This mechanism takes into account the fact that film boiling will not exist in a given liquid at a wave length above a certain critical value as

discussed in Appendix A.

Chang analyzes the problem as set forth in the above mechanism to arrive at a relation between film thickness and time. Comparing the resulting equation with the conduction equation for a homogeneous substance, he is able to formulate an equivalent thermal diffusivity;

$$\alpha_c = \frac{K_v \Delta T}{2 h_{fg} \rho_v} \quad (4)$$

Chang further defines generalized Prandtl and Grashof number as

$$P_r^* = \frac{\nu}{\alpha_c} \quad \text{and} \quad Gr_1^* = \frac{g \rho_v^2 L^3}{\mu_v^2} \cdot \frac{\rho_l - \rho_v}{\rho_v} \quad (5)$$

and therefore reduces his analysis to the following equation:

$$(Nu_1)_{co} = 0.234 (P_r^* Gr_1^*)^{1/3} \quad (6)$$

which he suggests is a general equation for film boiling on a horizontal surface, similar to the equation for simple convection. In this analysis the effect of radiation was not considered, but its effect could be realized by considering the added thickness of the vapor film due to the radiation.

It is interesting to note that Chang states that experimental data for film boiling from flat plates is very scarce, and that he is therefore forced to compare his theory with data from horizontal tubes. It is interesting to note also that in the discussion of Chang's paper, Zarwyn brings up the question of validity for the above analysis for a flat horizontal plate facing downwards. Chang states that the application of his theory would depend

heavily upon the size of the flat plate.

Zuber ⁽⁸⁾ discusses extensively the three regions of boiling heat transfer. He approaches the burnout point analysis from the transition boiling region. The burnout point is the maximum point in nucleate, but also corresponds to the maximum point in transitional boiling. Zuber maintains that the burnout point is located on a q/A vs. temperature difference graph by the application of Taylor-Helmholtz hydrodynamic instability criteria. Helmholtz instability is characterized by that condition when the vapor generated by the heater corresponds to the maximum counterflow of vapor and liquid normal to the heating surface which can occur in steady flow and remain stable. Taylor instability occurs as a result of the fact that in film boiling a liquid of high density is above a comparatively lower density vapor film. The result of the mathematics associated with the above instabilities is the following equation for the burnout flux :

$$(q/A)_{B.P.} = .157h_{fg}\rho_v \left[\frac{\sigma m \rho_l}{\rho_v (\rho_l + \rho_v)} \right]^{1/2} \quad (7)$$

The Leidenfrost point is the minimum point in stable film boiling. This point is extremely interesting because of the applicability of hydrodynamic principles, and because this point corresponds to the transfer position from film to nucleate boiling for power controlled heaters. Zuber has developed the following formula for the heat flux at the Leidenfrost point:

$$(q/A)_{L.P.} = .177h_{fg}\rho_v \left[\frac{\sigma g(\rho_l - \rho_v)}{(\rho_l + \rho_v)^2} \right]^{1/4} \quad (8)$$

The works of Chang and Zuber are mainly theoretical, relying primarily upon mathematics of hydrodynamics to furnish relations between q/A and temperature difference. Several authors find fault with their work, because of the simplifications made in developing an analytical model to represent film boiling. With this in mind Hosler and Westwater⁽¹¹⁾ have investigated film boiling from a flat plate with the objective of determining the actual validity of these different theories.

Hosler and Westwater present data for film boiling from a flat eight by eight inch aluminum plate. Conventional q/A vs. temperature difference plots are presented, and photographic data is given to support hydrodynamic calculations for the two test fluids; water and Freon-11. Hosler and Westwater state that significant edge effects will exist in film boiling in most liquids with a heat transfer surface as small as 2 inches in diameter, as used by Berenson.

The authors present relations often used when discussing film boiling, that is the critical wave length and the most dangerous wave length:

$$\lambda_c = 2\pi \left[\frac{g_c \sigma}{g(\rho_l - \rho_v)} \right]^{1/2} \quad \text{and} \quad (9)$$

$$\lambda_d = 2\pi \left[\frac{3g_c \sigma}{g(\rho_l - \rho_v)} \right]^{1/2} \quad (10)$$

Also presented is a simplified relation attributed to Chang for stable film boiling,

$$h = \left[K_v^3 (\rho_l - \rho_v) g / 8\pi^2 \mu_v \alpha_c \right]^{1/3}, \quad (6a)$$

where

$$\alpha_c = \frac{K_v \Delta T}{2h_{fg} \rho_v} \quad \text{for saturated pool boiling.}$$

Hosler and Westwater locate the Leidenfrost point at 11,000 $\frac{\text{BTU}}{\text{hr. ft.}^2}$ and 285^oF, and 5700 $\frac{\text{BTU}}{\text{hr. ft.}^2}$ and 160^oF for water and Freon-11 respectively. In the investigation by Hosler and Westwater, hydrodynamic measurements were taken from high speed motion pictures of the boiling. This information is presented in Table I. This photographic investigation shows that a square or rectangular array of bubble release areas does not exist in film boiling. A very irregular array was observed. Of particular interest is the fact that Hosler and Westwater observed that the average spacing between bubbles of the same size was approximately equal to λ_d , and the minimum spacing was equal to λ_c . The observed breakoff diameters were 73% of λ_d .

Hosler and Westwater go on to state that the method of Chang for predicting the film boiling curve is not reliable. Also, the method of Berenson for predicting the film boiling curve is good, except the temperature difference values at the Leidenfrost point are not generally reliable.

Class, et al. ⁽¹²⁾ have published data for film boiling from a flat electrically heated plate to liquid hydrogen. An interesting observation made by the authors concerns surface roughness. They observed that the

TABLE I

HYDRODYNAMIC RESULTS OF HOSLER AND WESTWATERSummary of Bubble Measurements at Minimum Point
for Freon-11

Diameter at Breakoff

observed: average	0.38 in.
maximum	0.47 in.
minimum	0.30 in.

Center to Center Spacing

observed: average	0.57 in
maximum	1.25 in.
minimum	0.25 in.

Bubble Period

observed: average	0.17 sec.
maximum	0.26 sec.
minimum	0.08 sec.

burnout point could be raised 100% in some instances by covering the heat transfer surface with silicon grease. In the film region the curve was displaced to the right slightly.

Manson⁽¹³⁾ expresses concern about the present theories of film boiling and contends that present theories, hydrodynamic analysis included, fail to consider the effect of surface material. This surface material effect must be taken into account when heaters are coated with thermally nonconducting materials such as Teflon. Manson obtained the following minimum points for film boiling in Nitrogen for coated and uncoated copper plates:

coated (.001 in. Teflon)	6500	$\frac{\text{BTU}}{\text{hr. ft}^2}$, 300°R
uncoated	2500	"	, 60°R

Manson offers an analog computer method for prediction of a non-uniform heat transfer coefficient which takes into account the surface material effect.

Gottfried, Lee and Bell⁽⁵⁾ have investigated film boiling of liquid droplets on a flat plate, which has peripheral importance to this investigation. The authors conclude that the Leidenfrost point is independent of droplet size, therefore suggesting its application to pool boiling. The authors define the Leidenfrost point as the plate temperature at which the droplet evaporation time is greatest.

Brentari and Smith⁽¹⁴⁾ have made a significant contribution to the literature with their paper on correlation of pool boiling data for cryogenic fluids. The authors have gathered together the works of many of the eminent researchers in the field. The synthesis of ideas which results is miraculously

not confusing. Correlations are offered for the major cryogenic fluids including nitrogen in nucleate and film boiling.

The burnout point is a favorite area for analytical investigators, because of its prediction with fluid properties only. The authors offer the following equation attributed to Kutateladze:

$$(q/A)_{B.P.} = 15.7 h_{fg} \left[\rho_v \right]^{1/2} \left[\sigma (\rho_l - \rho_v) \right]^{1/4} \quad (11)$$

The Leidenfrost point is represented by the following equation attributed to Zuber,

$$(q/A)_{L.P.} = .177 h_{fg} \rho_v \left[\frac{\sigma g (\rho_l - \rho_v)}{(\rho_l + \rho_v)^2} \right]^{1/4} \quad (8a)$$

Of particular interest to this investigation are the predictive film pool boiling correlations offered for nitrogen. This information can be seen in Figure 4. The stable film region is given by correlations attributed to Breen and Westwater, and the minimum points are attributed to Lienhard and Wong, or Berenson.

Brentari and Smith have a section devoted to the discussion of several variables which effect boiling performance. They say that a major subcooling effect may occur in normal film boiling, as a result of the increased rate of condensation.

The effect of external force fields such as gravity are expected to have a large influence on the boiling phenomena in the film region. This supports the change in heat transfer characteristics as reported by Lyon for a horizontal surface facing downward.

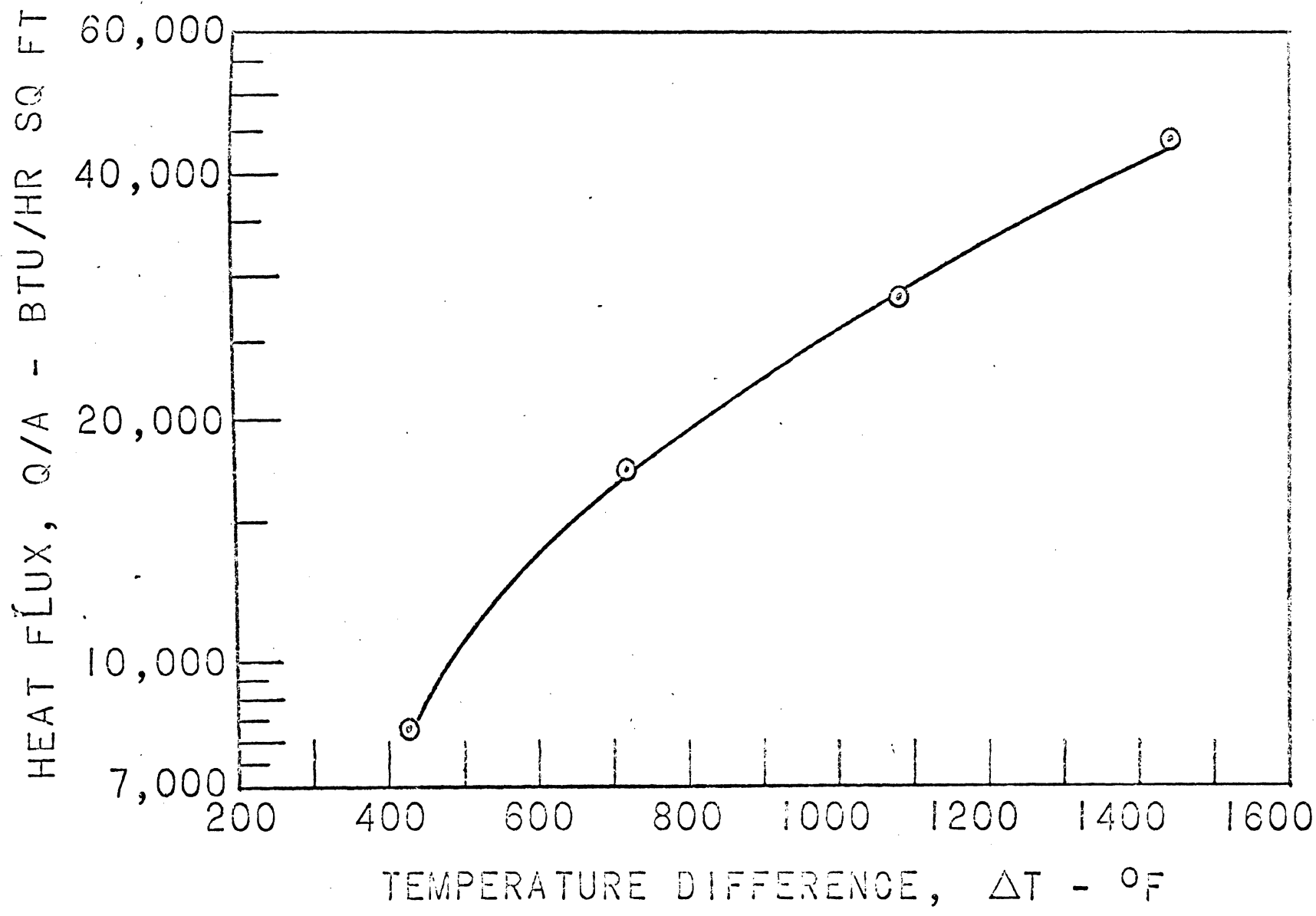


FIGURE 4 - Film Correlation From Brentari and Smith

Of particular interest to this investigation are the authors' comments concerning surface temperature variations. The authors state that, "It is possible that surface temperature differences may occur which may be attributed to the heater surface and not to the boiling phenomena. Heaters with a small mass per unit of heater surface, such as very thin materials, may produce such temperature variations and subsequently a lower peak flux... The source of energy for the heater may also influence the surface temperature variations. Kutateladze reports that electrically heated surfaces have slightly different heat transfer characteristics than those heated by vapor condensation..."

The authors further note that chemical composition of the heat transfer surface, especially its wetting characteristics, may have a marked effect upon the boiling curve.

Cole⁽¹⁵⁾ has studied pool boiling due to sudden large power surge with a nickel ribbon, which was electrically heated by a direct power surge of 30 millisecond duration. For heat generation rates above that required for stable film boiling, the ribbon temperature could be predicted by assuming it to be completely insulated.

Several informative heat transfer texts are available today which cover film boiling in general. Good examples of this are the texts by McAdams,⁽¹⁶⁾ Rohsenow and Choi,⁽¹⁷⁾ Kreith,⁽³⁾ Holman,⁽¹⁸⁾ Jacob,⁽¹⁹⁾ Parker and Boggs,⁽²⁰⁾ and Tong.⁽²¹⁾

Nucleate Boiling, Flat Surfaces

Houchin and Lienhard⁽²²⁾ have conducted experiments with low thermal capacity flat plates to determine their burnout points. Up to the publication of this paper it was generally considered that the burnout point was predictable using hydrodynamic considerations. The authors maintain that a thin ribbon flat plate, therefore one of low thermal capacity, constitutes a special case. The authors state that such heaters display a burnout point that is below the hydrodynamic crisis point.

As previously stated, there is a portion of the nucleate boiling region where continuous columns of vapor exist. The burnout mechanism proposed by Houchin and Lienhard functions in this regime. Burnout, that is a transfer into the film region, will occur locally at isolated circular points at the base of selected vapor columns when the power generated is at a level which will generate the Leidenfrost temperature at these isolated points. Observation of the boiling curve indicates that, for heaters that function in this manner, there should be little difference in the power level at which a heater goes into film as compared to the level at which it drops back into nucleate.

Usiskin and Siegel⁽²³⁾ have reported data for boiling in reduced gravity fields. They found that the critical heat flux in water varied approximately with g to the one quarter power. Therefore, the burnout flux decreases with decreasing gravity as predicted by theory. The authors also observed that the bubbles ascended more slowly as gravity was decreased; the bubble diameter increased as gravity decreased; and at zero gravity film and nucleate

boiling take on a similar appearance.

Chang⁽²⁴⁾ presents a general wave theory for boiling. He presents the theory in detail for nucleate boiling and makes some general remarks concerning film boiling.

Several of the authors, whose works have been previously mentioned, have presented excellent data in the nucleate range. Trends or points of interest to this investigation will be included here.

Berenson⁽⁹⁾ discusses the effect of surface roughness on the nucleate boiling region. It has long been assumed that a rough surface will produce a smaller temperature difference for a given power setting than a smooth surface of equal size. But what does the word "roughness" mean when used in relation to nucleate boiling? Surface A is rougher than surface B if it has more likely nucleation sites. Therefore, rms values of roughness are not always a reliable indication of "roughness". This can be verified by the data presented by Berenson for nucleate boiling. Berenson also observed that surface roughness does not effect the magnitude of the burnout flux.

Brentari and Smith⁽¹⁴⁾ present a great deal of information concerning correlation equations available today for predicting nucleate boiling curves at various pressures in cryogenic fluids. The authors state that, in reviewing the available literature and experimental data, correlation equations which predict q/A as a function of temperature difference cubed are the most reliable.

Film Boiling, Other Surfaces

Bromley⁽⁶⁾ has made significant theoretical and experimental investigations of stable film boiling. Bromley's theory and experimental data represent stable film boiling from a horizontal tube.

Bromley admits in the development of his theory for stable film boiling, that very different situations do occur around the periphery of a horizontal tube. He makes assumptions which seem to fit approximately two-thirds of the heat transfer area; leaving out the top and bottom of the tube. Bromley justifies this procedure by assuming that the greatest part of the heat transfer occurs on the two-thirds of the tube previously mentioned.

DiCicco and Schoenhals⁽²⁵⁾ have published works showing the effect of pressure pulsation upon stable film boiling. They used a .030 inch diameter platinum wire, which was calibrated as a resistance thermometer, in Freon-11 for their boiling experiments.

The authors state that a substantial increase in heat flux at a particular temperature in film boiling is attained by applying a pulsating pressure to the boiling liquid. Theoretically, in every boiling fluid, there is a certain pressure which will completely collapse the vapor film. DiCicco and Schoenhals applied an approximately square pressure wave, with the peak pressure being one-third of the value required for collapse of the film. The lower limit was atmospheric pressure. Surprisingly the heat transfer rate for the pulsating pressure was above the rate for the peak pressure at steady state. The authors also offer data for film boiling at atmospheric pressure.

Grassmann and Hauser⁽²⁶⁾ have conducted film boiling experiments with wires submerged in water.

Flynn, Draper and Roos⁽²⁷⁾ have presented experimental data for nucleate, transition and film boiling from a horizontal tube in liquid nitrogen.

Rhea⁽²⁸⁾ has recently presented data for nucleate and film boiling from oscillating spheres to liquid nitrogen. The author suggests the addition of a vibrational Froude number to the film boiling correlation of Frederking and Clark to account for the effect of oscillation upon the heat transfer performance.

There has been a great deal of work done on film boiling from surfaces other than flat plates. The authors and works discussed here therefore represent only a cross section of the literature available.

Nucleate Boiling, Other Surfaces

Nucleate boiling is a very efficient method of transferring heat at high heat fluxes and low temperatures. Because of this, very much attention has been given to nucleate boiling. For the sake of brevity only a few works will be cited.

Jens⁽²⁾ covers the known facts concerning boiling heat transfer to about 1954. He discusses the fact that such a wide range of nomenclature is used in the literature to discuss a relatively small number of important ideas that confusion sometimes results. Jens makes an interesting comment in conclusion. He suggests that the status of boiling in 1954 was at a stage where the obvious variables had been sufficiently investigated, and the more

subtle variables would now be defined and investigated.

Levy⁽²⁹⁾ has developed a generalized correlation for nucleate boiling. "The derivation is based upon bubble growth rate close to the heated surface and an empirical determination of the relation between heat transfer rate at the heated surface and that at the bubble surface."

Engelberg-Forster⁽³⁰⁾ and Greif have investigated the different mechanisms advocated in the literature for nucleate boiling and developed correlations for each.

Many other authors have presented correlation equations for saturated pool boiling; one of the most noteworthy being Rohsenow.⁽³¹⁾

The correlation equations presented in the literature are collected in Table II.

TABLE II
BOILING CORRELATION EQUATIONS

Stable Film

$$h = .425 \left[\frac{K_{vf}^3 h_{fg} \rho_{vf} g(\rho_1 - \rho_v)}{\mu_{vf} \Delta T g_c} \right]^{1/4} \quad (3)$$

Berenson

$$h = .234 \left[\frac{2K_v^2 \rho_v h_{fg} g(\rho_1 - \rho_v)}{\Delta T \mu_{vf} g_c} \right]^{1/3} \quad (6b)$$

Chang

Leidenfrost Point

$$(q/A)_{L.P.} = .09 \rho_v h_{fg} \left[\frac{(\rho_1 - \rho_v)^{1/2}}{\rho_1 + \rho_v} \right] \left[\frac{g_c \sigma}{g(\rho_1 - \rho_v)} \right]^{1/4} \quad (1)$$

Berenson

$$(\Delta T)_{L.P.} = .127 \frac{\rho_v h_{fg}}{K_{vf}} \left[\frac{g(\rho_1 - \rho_v)}{\rho_1 + \rho_v} \right]^{2/3} \left[\frac{g_c \sigma}{g(\rho_1 - \rho_v)} \right]^{1/2} \left[\frac{\mu_{vf}}{g_c(\rho_1 - \rho_v)} \right]^{1/3} \quad (2)$$

Berenson

$$(q/A)_{L.P.} = .177 h_{fg} \rho_v \left[\frac{\sigma g(\rho_1 - \rho_v)}{(\rho_1 + \rho_v)^2} \right]^{1/4} \quad (8)$$

Zuber

Burnout Point

$$(q/A)_{B.P.} = .157 h_{fg} \rho_v \left[\frac{\sigma m \rho_1}{\rho_v (\rho_1 + \rho_v)} \right]^{1/2} \quad (7)$$

Zuber

$$(q/A)_{B.P.} = 15.7 h_{fg} \left[\rho_v \right]^{1/2} \left[\sigma (\rho_1 - \rho_v) \right]^{1/4} \quad (11)$$

Kutateladze

III. EXPERIMENTAL INVESTIGATION

Method

A test plate, constructed from a resistance strip, was placed horizontally in a pool of liquid, and was heated electrically. Thermocouples were spot welded to the unwetted side of the test plate, and the same side was in turn cemented to transite as an insulating backing. Thus, the fluid was essentially heated from one side of the test plate only. Direct current power was supplied to the test plate from a welding generator. For added power control to the test plate a carbon-pile rheostat was used. A potentiometer measured the voltage drop across the test plate, and a voltmeter was used to monitor the output voltage of the power supply. A potentiometer in conjunction with a precision resistor was used to measure the current. An ammeter was also used to indicate the current. The test plate temperatures and the bulk temperature of the fluid were recorded on a multichannel recording potentiometer.

Equipment

The main components of the boiling apparatus in the laboratory are shown in Figure 5. The instrumentation is shown mounted in the console. The dewar containing the heater and test fluid can be seen on the table. A schematic of the apparatus is given as Figure 6. This schematic serves as a listing of the equipment and shows the relationship of the components. More detailed descriptions of the test sections, power supply and control, and instrumentation are presented in the following sections.

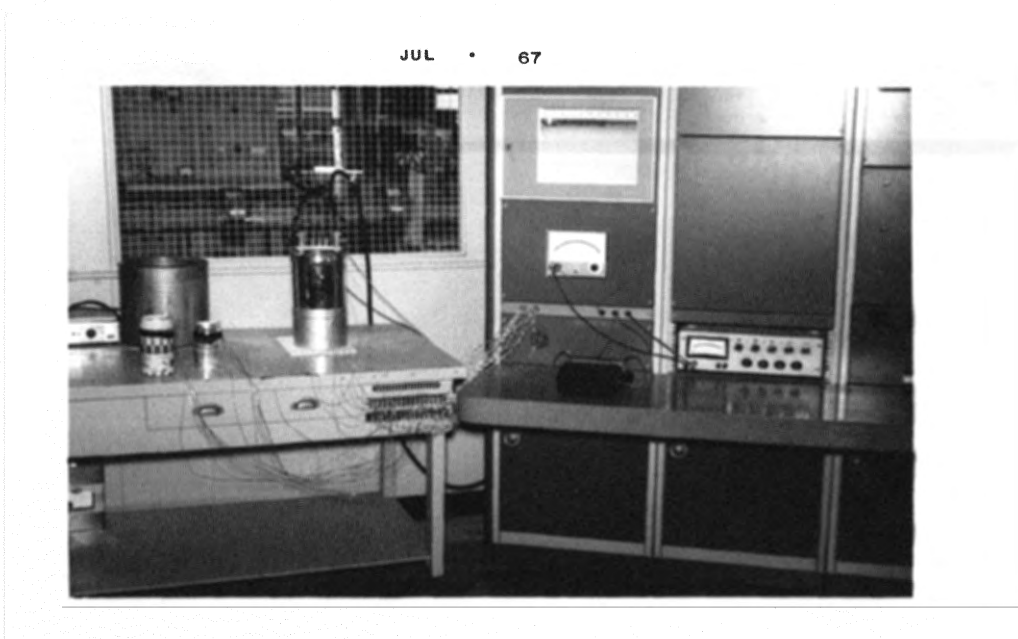


FIGURE 5 - Experimental Apparatus

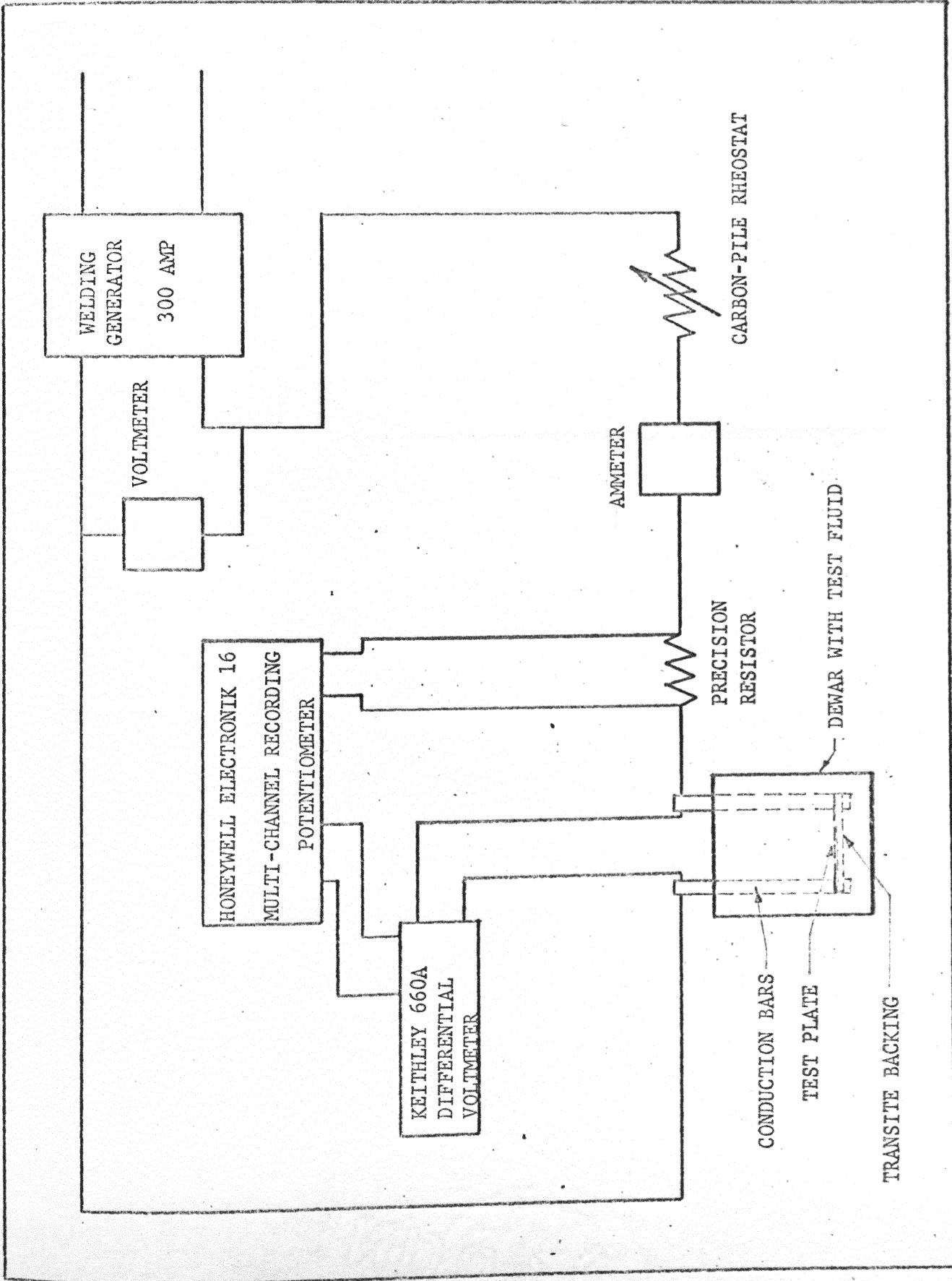


FIGURE 6 - Schematic of Test Set-up

Test Sections. The test sections were fabricated in three widths; one-half, one, and two inches. The thickness of the test plate was either .005 or .010 inches depending on the material, and all test sections were approximately four inches long when installed. The heater materials were Kanthal A-1 and Inconel-600. The surfaces were roughened by sand blasting in some tests.

The heater material was cut to a length of approximately five inches. This allowed one-half inch on each side of the four inch heat transfer surface to connect the test section into the conduction bars, as shown in Figure 7. Six thirty-gage chromel-alumel thermocouples were spot welded to the back of the heat transfer surface using the miniature solid state spot welder shown in Figure 8. A piece of one-half inch thick transite insulation was grooved out to accommodate the thermocouples on the back side of the heater plate. The transite backing was then cemented with high temperature epoxy to the metal heat transfer surface. Using this method a heater was constructed that would deliver heat to a boiling liquid from essentially one side. There was, of course, heat loss out the insulated side. To account for this, two thermocouples were placed in the backing perpendicular to the heater surface and $3/16$ of an inch apart. With the resulting temperature difference, and the value of K_t for transite ($.47 \text{ BTU/hr.ft.}^{\circ}\text{F}$), the one-dimensional Fourier Law was used to calculate the heat loss. The reference junctions of all thermocouples were placed in an ice bath for the Refrigerant-11 tests, and in a liquid nitrogen bath for the nitrogen tests.

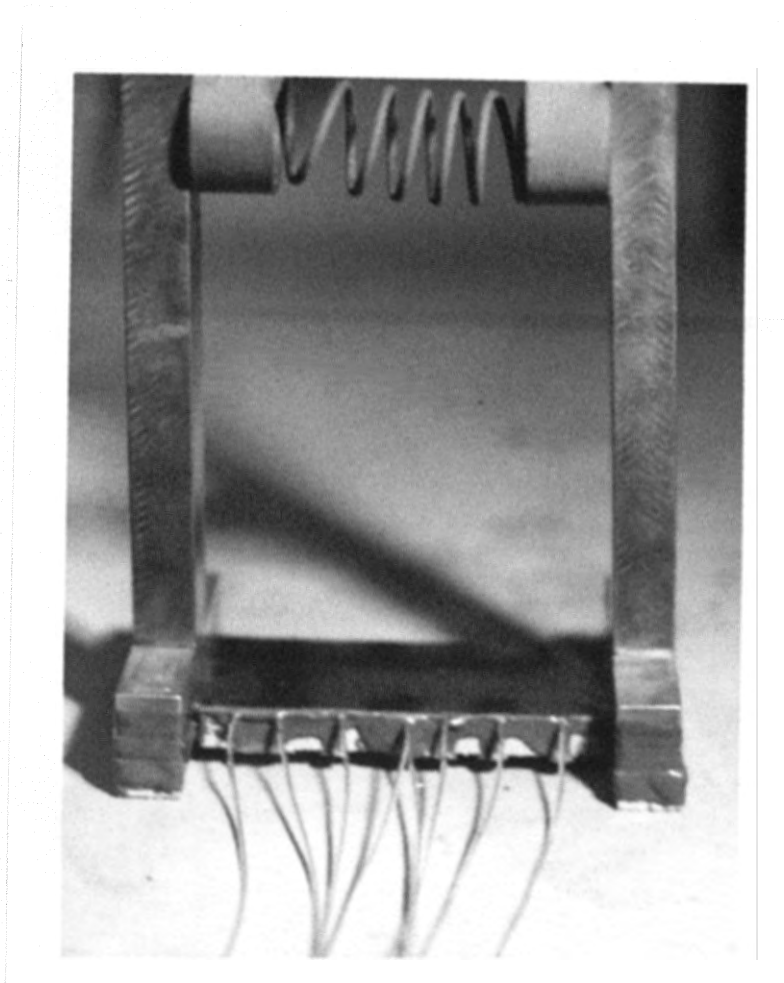


FIGURE 7 - Heater Assembly

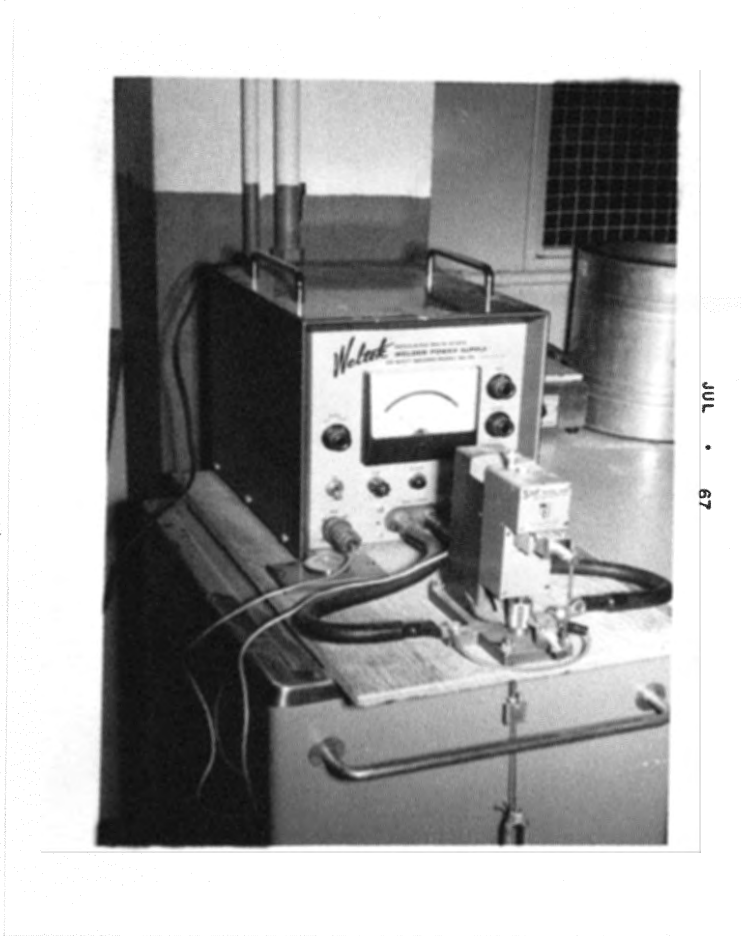


FIGURE 8 - Thermocouple Spot Welder

Power Supply and Control. The power was supplied to the heat transfer surface by a Lincoln 300 ampere direct current welding generator, as seen in Figure 9. Number 2 welding cable carried the power to the conduction bars, which held the test section. The power delivered to a typical heater is displayed in Figure 10. The output of the welder was controllable at the welder by adjusting a fine and a coarse setting. This power supply had sufficient capacity to destroy all of the heaters tested. At the lowest setting, the welder would deliver approximately 42 amperes to the test section. It was therefore desirable to add another source of power control in the line. This was accomplished by adding a one thousand watt carbon-pile rheostat. The carbon-pile rheostat was a satisfactory method of controlling the current delivered to the heater, especially at low power settings.

Instrumentation. As previously mentioned, the output of the power supply was displayed on a Weston voltmeter and a Weston ammeter. The voltage drop across the heater was measured with a Keithley 600A differential voltmeter capable of measuring voltages to five significant figures. An attenuated voltage signal was then fed into an Elektronik-16 potentiometric multichannel recorder. The voltage drop across a Weston precision resistor was fed into the recorder to give a record of the current through the test plate. Figure 11 shows a one-half inch heater in position in the dewar. The thermocouple wires can be seen coming out the top of the dewar. The eight thermocouples associated with each heater plus the bulk temperature thermocouple were fed into the recorder.

JUL • 67



FIGURE 9 - Power Supply

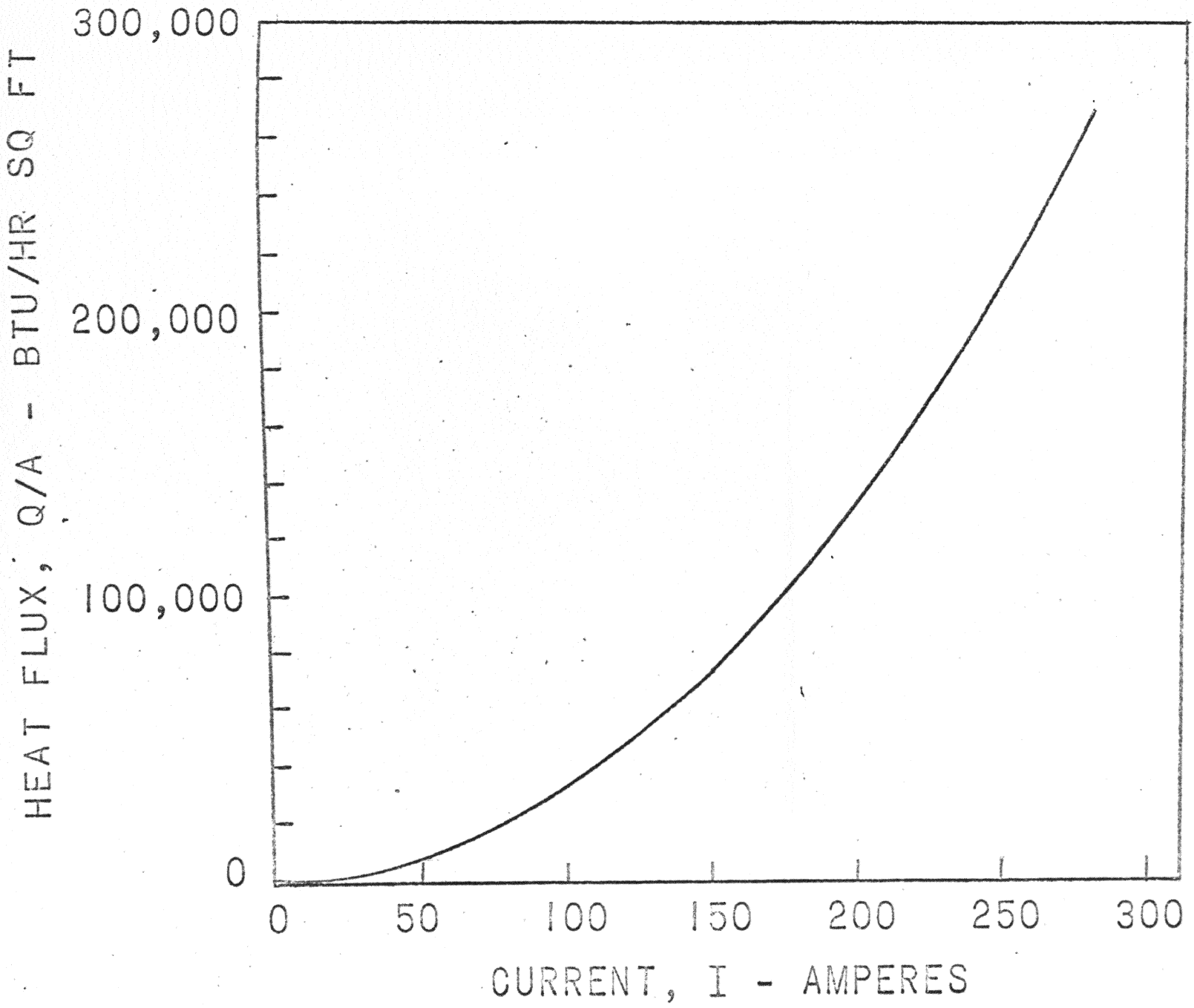


FIGURE 10 - Power Generation Curve

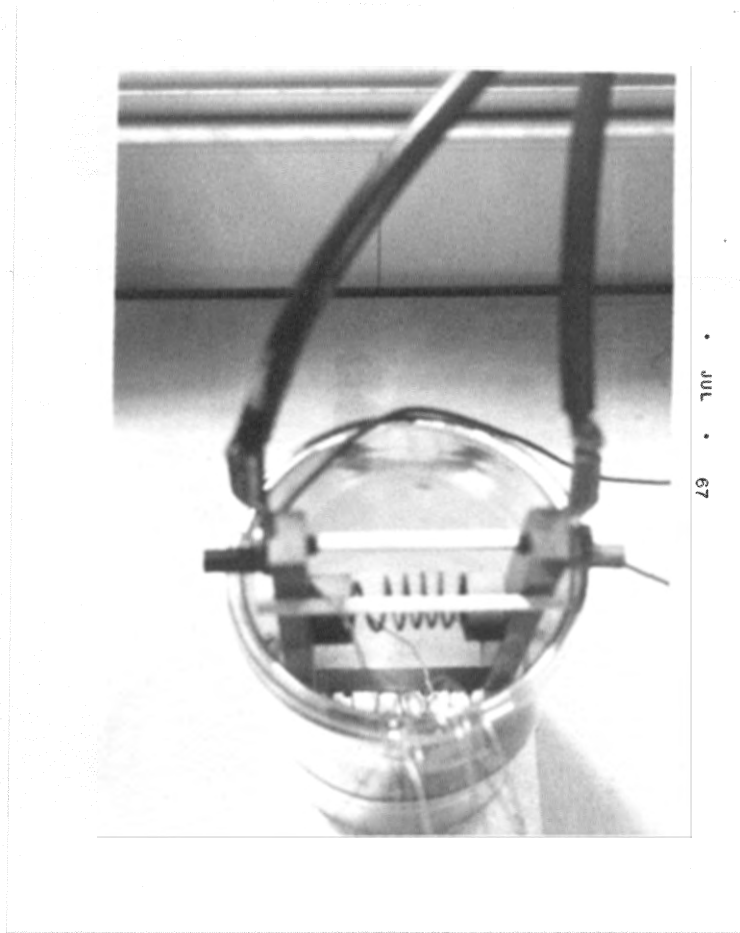


FIGURE 11 - Heater in Dewar

Procedure

The heat transfer surface was cleaned with acetone, and the instrumentation was turned on to allow a sufficient warm-up prior to each test. The heater and conduction bar assembly was then placed into the filled dewar. All of the electrical and thermocouple circuits were checked, and after equilibrium had been reached the welder was turned on at its lowest setting. The welder was turned up in small increments until the burnout point was passed and the system went into film boiling. The system was observed, and when equilibrium was reached a data set was taken. The welder output was decreased in small increments, and a data set obtained at each stable point, until the minimum point was reached. The welder output was increased in small increments until the test plate was at a predetermined maximum temperature or until destruction of the heater occurred. The power was shut off and the heater assembly was inspected for separation. If it was in good shape, the above process was repeated.

The following items were taken at each data point; the six plate temperatures, the bulk temperature, temperatures in the backing for the calculation of heat loss, and the current through and voltage drop across the test plate. Figure 12 is a typical recorder output sheet. All of the items previously mentioned that were necessary in the calculations can be seen in this figure. Table III is a list of the tests that were run.

Data Reduction

The reduced data can be found in Appendix B. The tests are

TABLE III

LISTING OF TESTS

TEST NO. (DATE)	TEST FLUID	HEATER		
		MATERIAL	SIZE	FINISH
529	Refrigerant-11	Kanthal A-1	1.0 inch	5- μ in. rms.
603	Refrigerant-11	Kanthal A-1	1.0 inch	5- μ in. rms.
605	Refrigerant-11	Kanthal A-1	1.0 inch	5- μ in. rms.
621	Nitrogen	Kanthal A-1	1.0 inch	5- μ in. rms.
623A	Nitrogen	Inconel-600	2.0 inch	Mirror Finish
623B	Nitrogen	Inconel-600	2.0 inch	Mirror Finish
629	Nitrogen	Kanthal A-1	1.0 inch	5- μ in. rms.
630	Nitrogen	Inconel-600	2.0 inch	Mirror Finish
704	Nitrogen	Inconel-600	2.0 inch	Mirror Finish
706	Nitrogen	Kanthal A-1	1.0 inch	sand blasted 40-60 μ in. rms.
711	Nitrogen	Kanthal A-1	0.5 inch	5- μ in. rms.
717	Refrigerant-11	Kanthal A-1	1.0 inch	sand blasted 50-90 μ in. rms.
718A	Nitrogen	Inconel-600	0.5 inch	Mirror Finish
718B	Refrigerant-11	Inconel-600	0.5 inch	Mirror Finish
719	Nitrogen	Inconel-600	1.0 inch	Mirror Finish
721	Refrigerant-11	Inconel-600	2.0 inch	Mirror Finish

1-6 PLATE TEMPERATURES

7 BULK TEMPERATURE.

8,9 BACKING TEMPERATURES

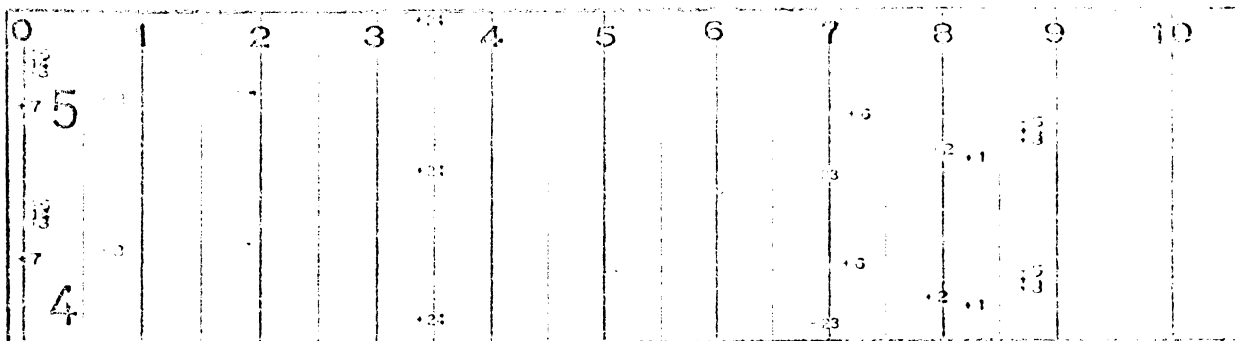


FIGURE 12 - Typical Recorder Output

arranged in chronological order with the test number actually reflecting the date of the test. Important information concerning each test, such as reference junction temperature, fluid, heater material, size and surface finish can be found at the top of each page. The run numbers within each test run consecutively with each stable film boiling point obtained.

The average of the six heater thermocouple emf's was obtained and converted to the average heater temperature, T_h , using the National Bureau of Standards Circular No. 561. The average bulk temperature was obtained in a similar manner. The millivolt outputs from the thermocouples in the insulated backing were converted to temperatures and subtracted to get the temperature drop in the backing.

The expression for the power supplied to the test section is as follows;

$$(q/A)_{\text{supplied}} = \frac{I\Delta V}{A} \quad (3.4129) ,$$

The heat loss through the backing is calculated using,

$$(q/A)_{\text{loss}} = K_t \frac{\Delta T_B}{\Delta X} ,$$

where $K_t = .47$ (BTU/hr.ft.⁰F). The heat flux associated with boiling from the flat plate was obtained by subtracting the heat lost out the backing from the power delivered to the test section. The heat transfer coefficient, h , was obtained using the standard relationship

$$h = \frac{(q/A)}{T} .$$

IV. RESULTS

General

Two test fluids were employed in the experiments, refrigerant-11 and nitrogen. There are significant differences in the characteristics of these fluids, therefore, the results of tests in each fluid will be presented separately.

Refrigerant-11. Figures 13, 14 and 15 show the heat flux results of the 0.5, 1.0 and 2.0 in. wide Inconel horizontal heated surfaces, respectively. In Figure 13 the data taken in run 718B on a 0.5 inch mirror finished Inconel surface is displayed. In Figure 14 several runs are displayed. Runs 529, 603 and 605 are for smooth, 5-8 μ in. rms. 1.0 in. Kanthal horizontal surfaces. Also included in Figure 14 is run 717 for a sand blasted; 50-90 μ in. rms, 1.0 in. Kanthal horizontal surface, and heat flux data from Hosler and Westwater. (11)

In this figure as in several others presented different heated surface materials were used on different days and good reproducibility of the data was obtained. The physical set-up of the experimental apparatus did not lend itself to investigation of the film boiling curve near the Leidenfrost point as presented by Hosler and Westwater. But the trend indicated by the Hosler and Westwater's data agrees very closely with the data presented over the larger temperature range in this investigation. The trend as suggested by the data of Hosler and Westwater is slightly to the right of the best fit curve for the data presented for the 1.0 in. heated surface. This is to be expected, because of the larger heated surface used by Hosler and Westwater. This will be discussed more fully later. The data as presented in Figure 14 including the roughened test

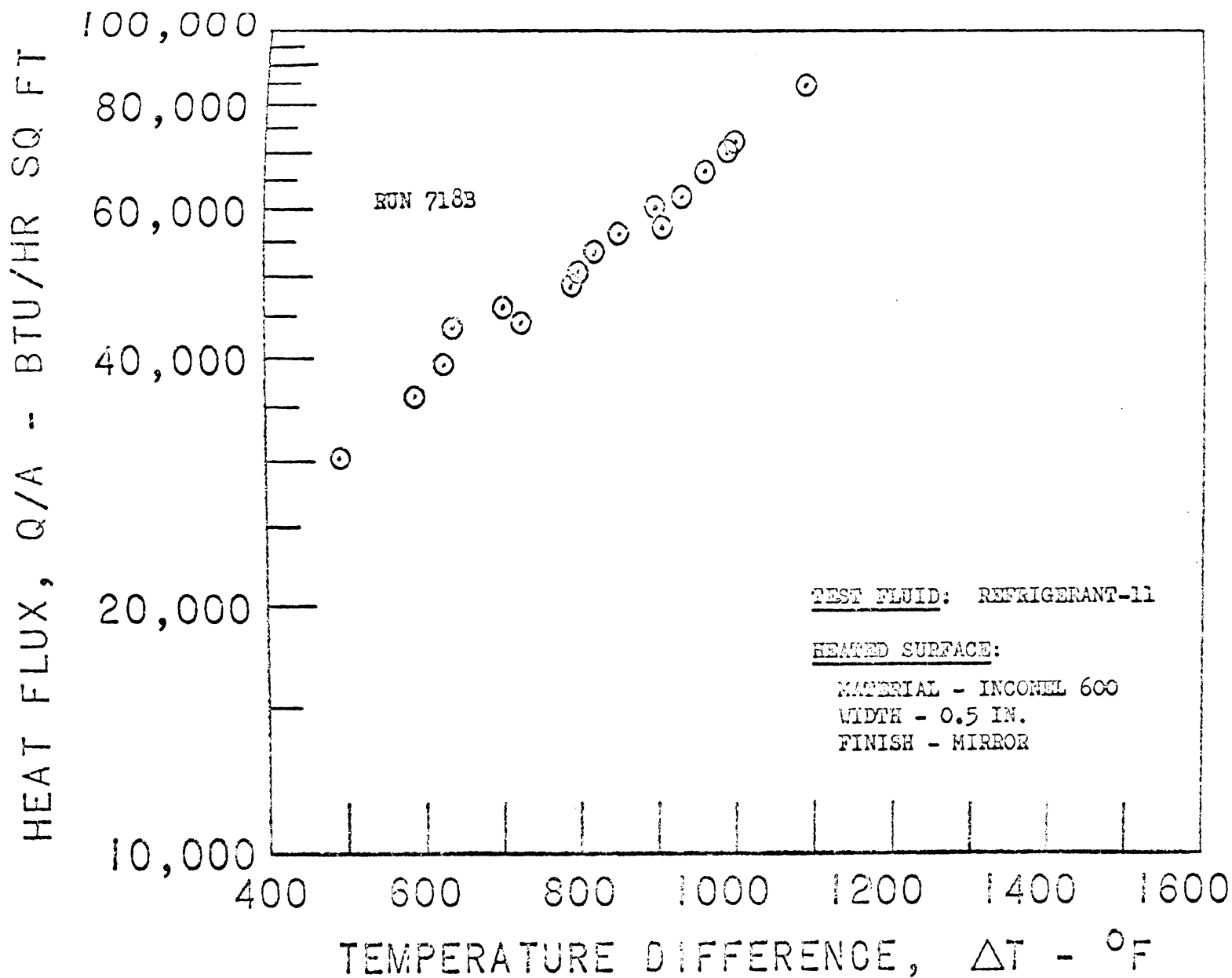


FIGURE 13 - Heat Flux Results for R-11 on 0.5 in. wide Inconel Horizontal Surface

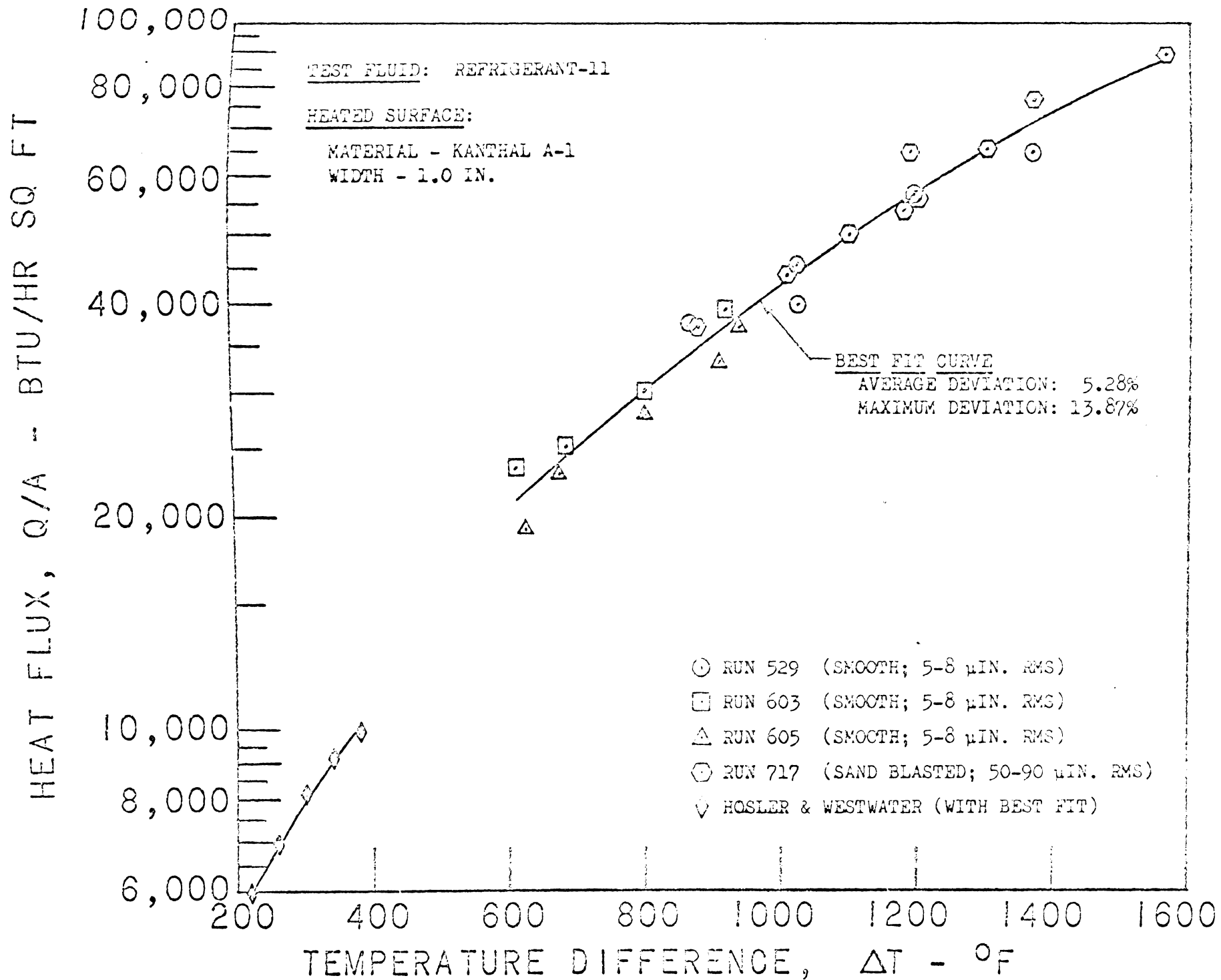


FIGURE 14 - Heat Flux Results for R-11 on 1.0 in. wide Kanthal Horizontal Surface

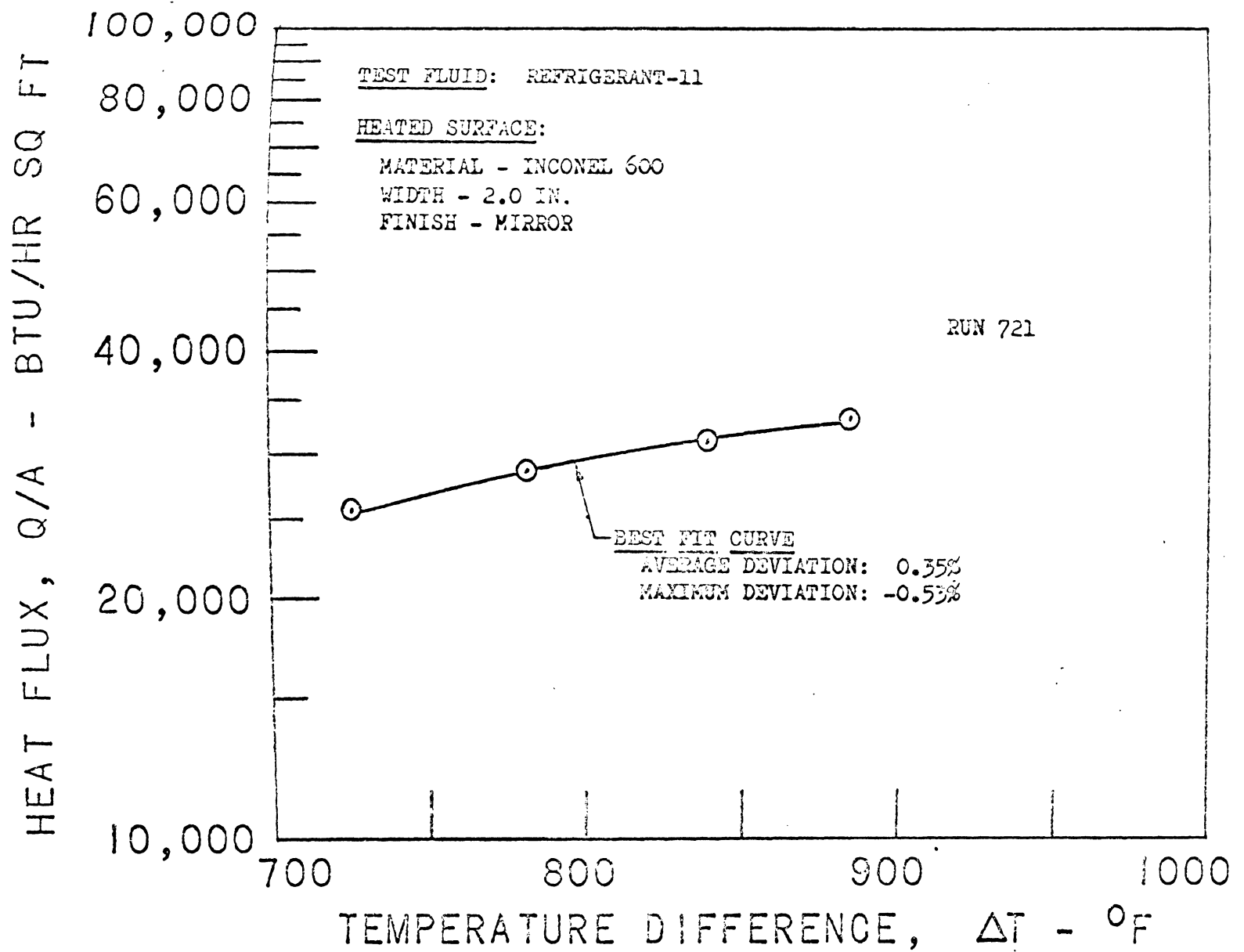


FIGURE 15 - Heat Flux Results for R-11 on 2.0 in. wide Inconel Horizontal Surface

has an average deviation of 5.28% from the best polynomial fit. Representative results from the application of the least squares method for the best polynomial fit to the data can be found in Appendix C.

Figure 15 displays the heat flux results for a 2.0 in. wide Inconel heated surface with a mirror-finish. The average deviation of the data from the best fit polynomial curve is 0.35%.

Figure 16 is interesting for several reasons. Presented in Figure 16 is the heat transfer coefficient results for 1.0 in. Kanthal horizontal surfaces. Also included are the plots of the correlation equations of Chang and Berenson, and the data of Hosler and Westwater. Again the data presented verifies the trend suggested by Hosler and Westwater. In considering this figure it should be noted that the correlation equations of Chang and Berenson are for infinite horizontal flat plates with the effect of radiation not included. The effect of radiation was not considered in the presentation of the data set forth in Figure 16. But the effect could be qualitatively realized by rotating the best fit curve clockwise about its left end slightly. With this in mind it can be seen that the equations as set forth by Chang and Berenson, when applied to refrigerant-11, form good upper and lower limits to the actual results. The data presented has an average deviation of 5.26% from the best polynomial fit curve.

Figure 17 includes the data from runs 718B and 721 for 0.5 in. and 2.0 in. wide mirror-finish Inconel surfaces. The heat transfer coefficient results are presented in this figure.

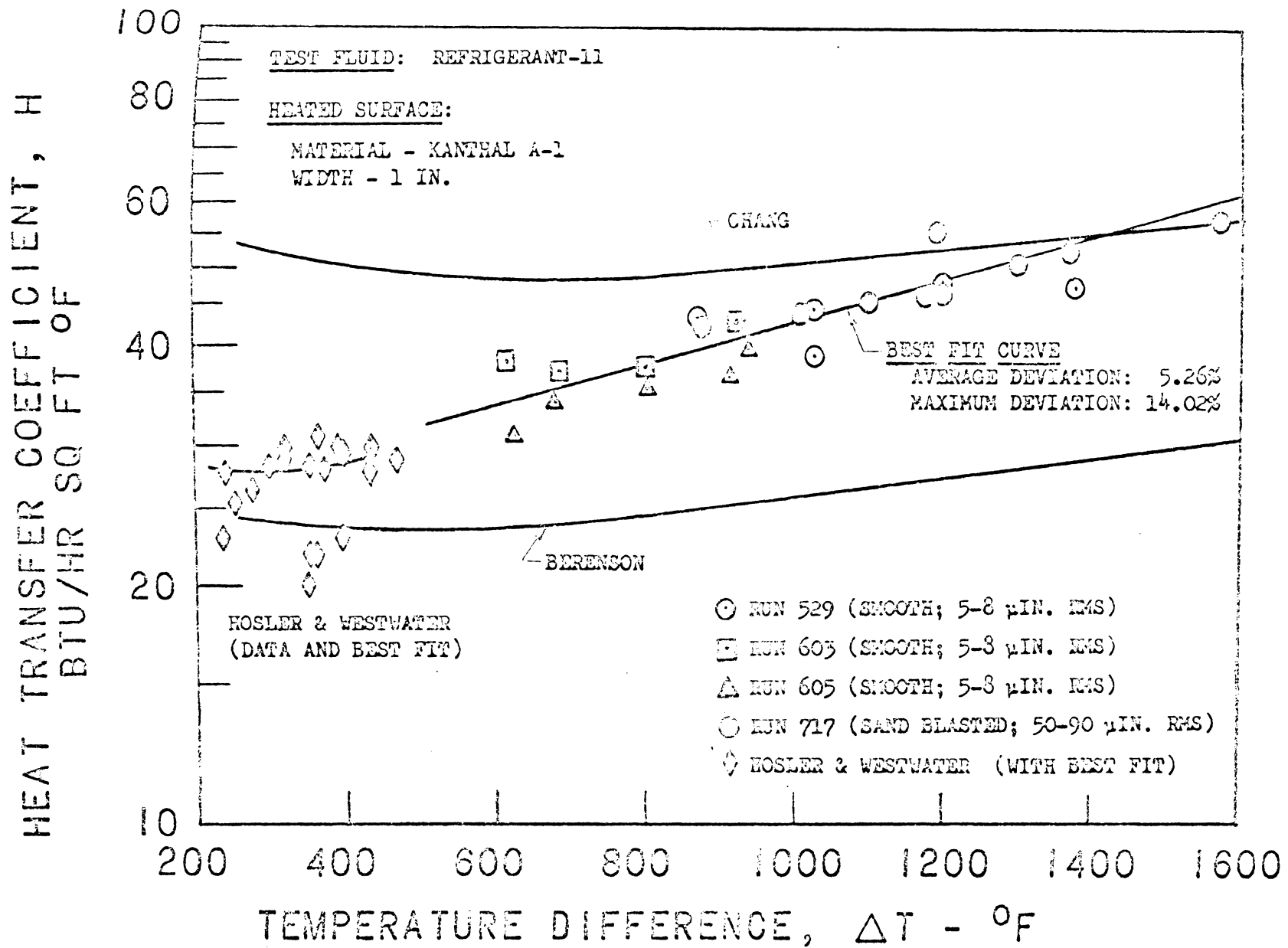


FIGURE 16 - Heat Transfer Coefficient for R-11 on 1.0 in. wide Kanthal Horizontal Surface

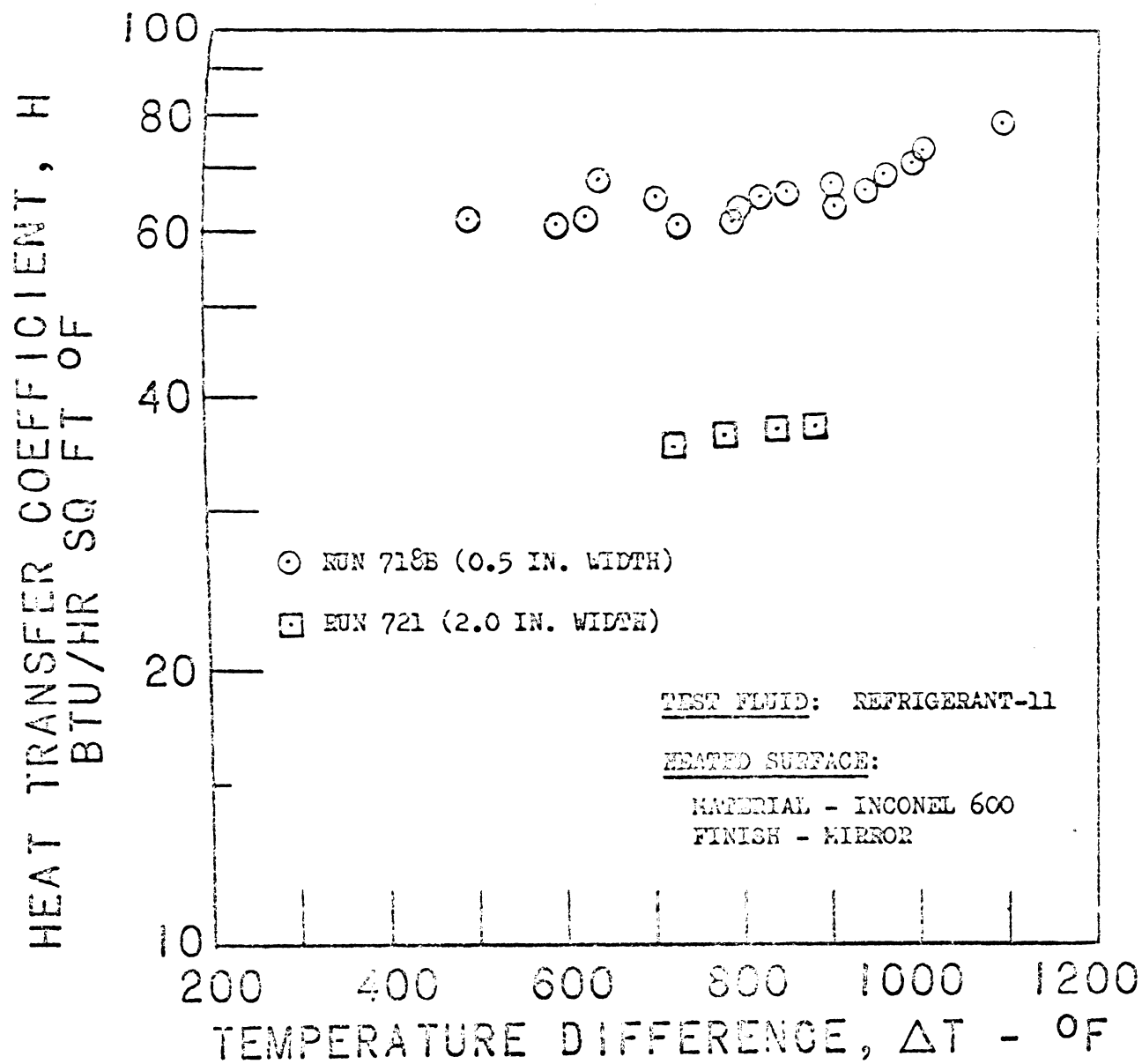


FIGURE 17 - Heat Transfer Coefficient for R-11 on an Inconel Horizontal Surface

The data in Figure 18 is presented somewhat differently than that usually found in the literature. Included in the presentation is the heat transfer coefficient versus heat flux for 0.5, 1.0 and 2.0 in. wide heated surfaces. This type of plot is significant when a power controlled heat transfer element is used, as was the case in this investigation. The best polynomial fit curves are included for each of the three widths presented. The average deviations for the 0.5, 1.0 and 2.0 in. wide heated surface data are 2.06%, 3.32% and 0.23% respectively.

Nitrogen. Figures 19, 20, and 21 show the heat flux results of the 0.5, 1.0 and 2.0 wide Inconel horizontal heated surfaces, respectively. In Figure 19 the heat flux results for run 718A are presented. It can be seen that the first three data points do not correspond with the general trend of the bulk of the data. They were not included in the best fit calculations because it is believed that air was entrained upon the heated surface during the beginning of these runs, causing the high heat flux values.⁽¹⁴⁾ The other data has an average deviation of 3.01% from the best polynomial fit curve. In Figure 20 the heat flux results for a 1.0 in. mirror-finish Inconel horizontal surface are presented. Notice that the only difference between the heated surfaces described in Figures 19 and 20 is the width. Again the first five data points in Figure 20 do not correspond with the trend of the rest of the data and were not included in the best fit calculations for the reason previously mentioned. These points and the ones discussed in Figure 19 suggest a trend. For the points included in the best fit calculations the average deviation is

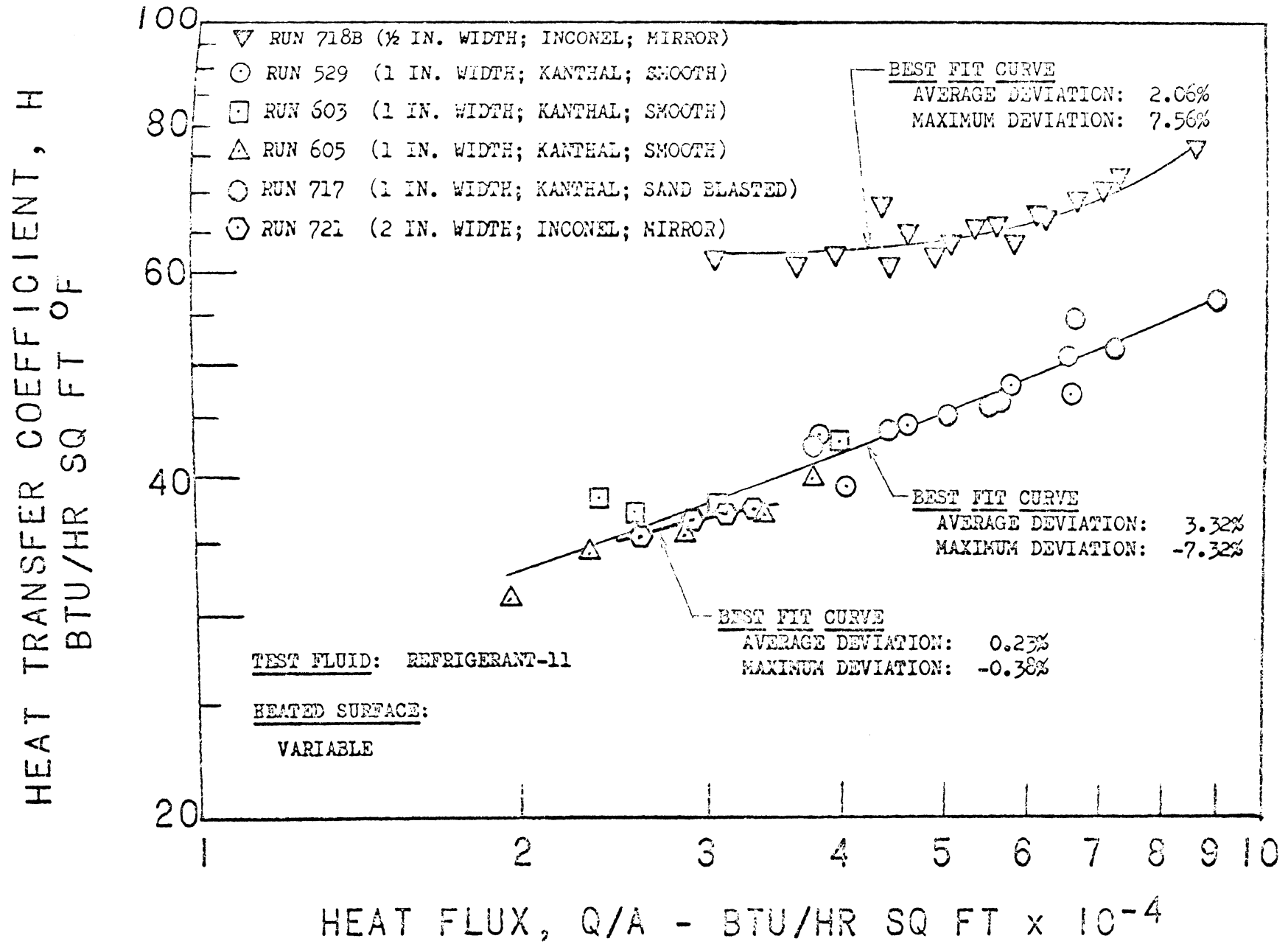


FIGURE 18 - H versus q/A for R-11 on Horizontal Surface Showing Heated Surface Size Effect

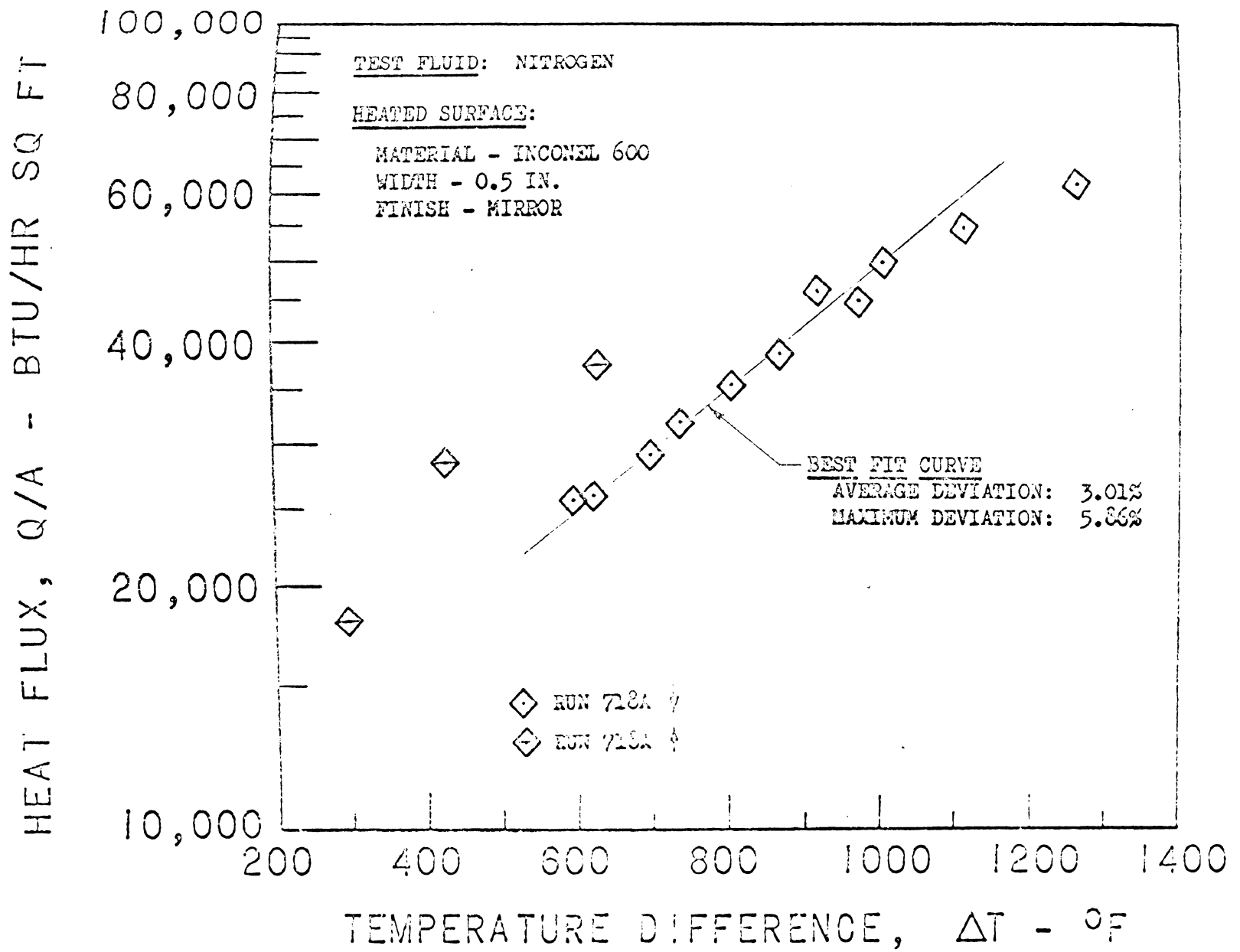


FIGURE 19 - Heat Flux Results for N_2 on 0.5 in. wide Inconel Horizontal Surface

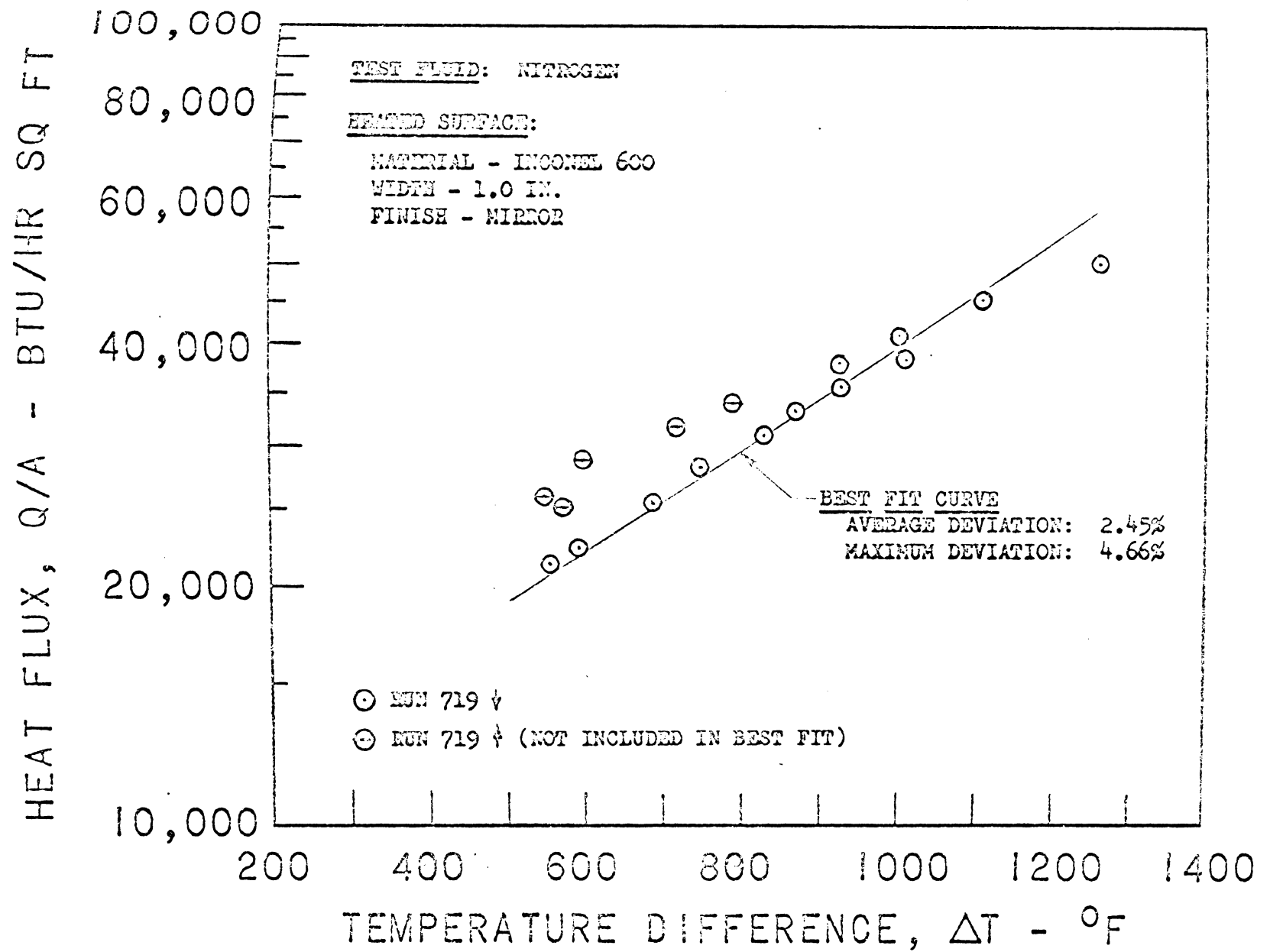


FIGURE 20 - Heat Flux Results for N_2 on 1.0 in. wide Inconel Horizontal Surface

2.45% in Figure 20.

Figure 21 is a presentation of the heat flux results for 2.0 in. wide mirror-finished Inconel horizontal heated surfaces. One of the heaters tested was cycled repeatedly from nucleate to film to nucleate etc. . . . , with the darkened points obtained on the last return to film. It is believed that the high heat flux values observed for these three points were due to a small separation of the heat transfer surface from the backing. The rest of the data has an average deviation of 1.78% from the best polynomial fit.

Figure 22 gives a comparison of the best polynomial fit curves for the 0.5, 1.0 and 2.0 in. wide mirror-finish Inconel horizontal heated surfaces.

Figure 23 and 24 present the results for 0.5 and 1.0 in. wide smooth Kanthal horizontal heated surfaces.

Figure 25 contains the heat flux results for a 1.0 in. wide Kanthal, sand blasted, 40-60 μ in. rms., horizontal heated surface.

In Figure 26 all of the heat flux results for the 1.0 in. heaters in nitrogen are presented. The best polynomial fit was applied to all points except the ones representing the roughened surface. The average deviation of the points included from the best fit curve is 5.01%.

In Figure 27 the results with a 2.0 in. wide Inconel horizontal surface with the heated surface facing downward, are presented. For comparison the best fit curve for a similar heater with the heated surface facing upward is included.

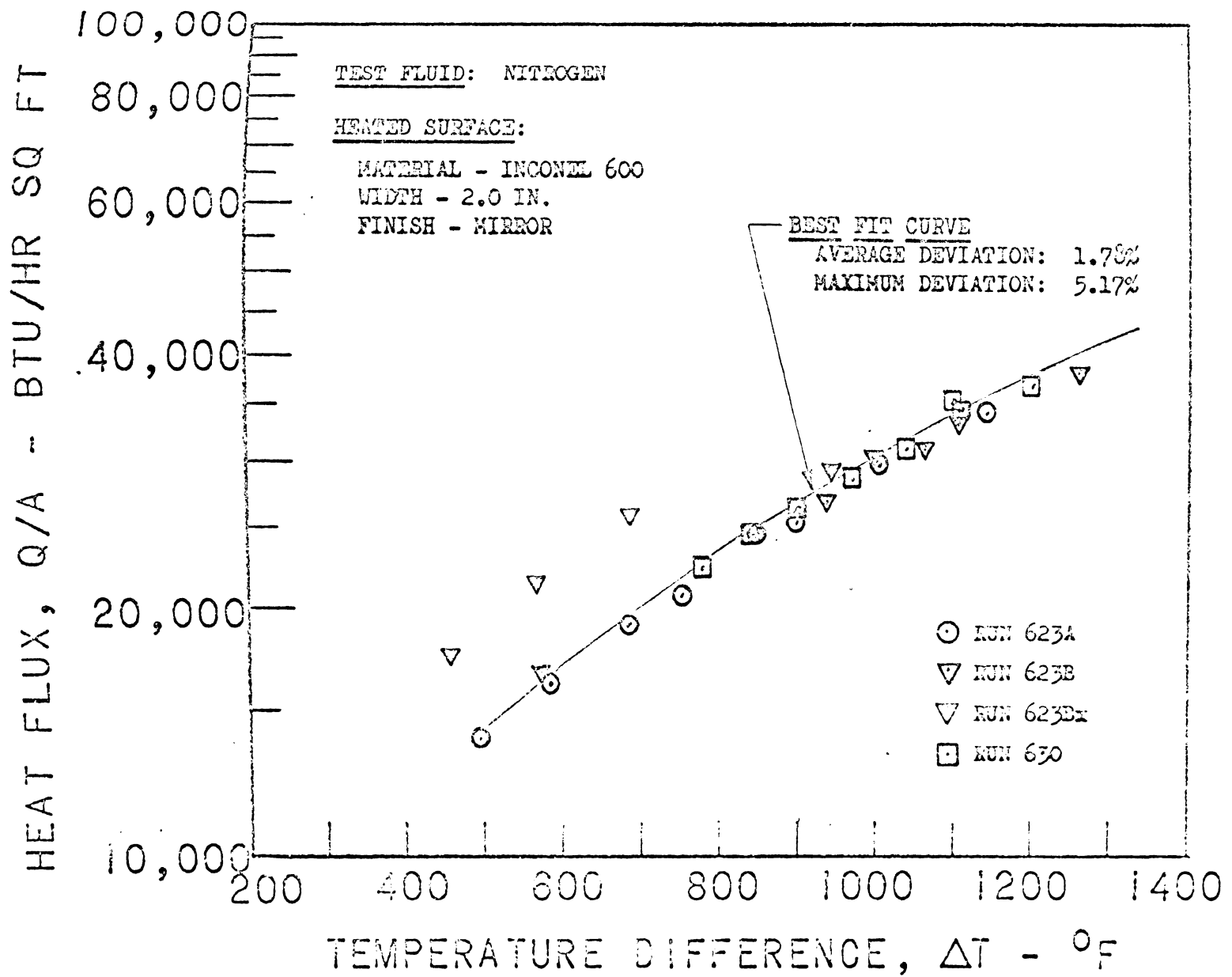


FIGURE 21 - Heat Flux Results for N_2 on 2.0 in. wide Inconel Horizontal Surface

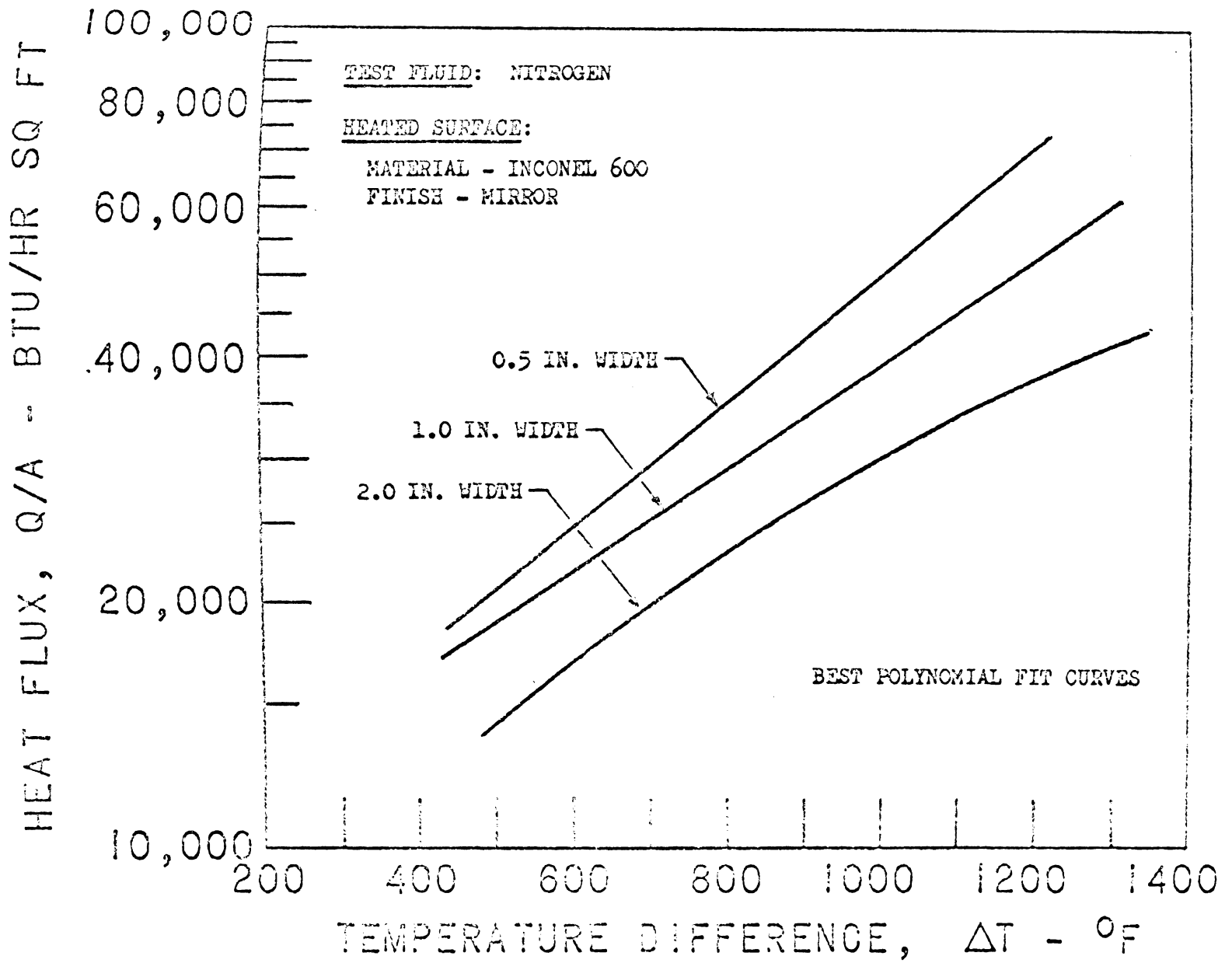


FIGURE 22 - Heat Flux Results for N_2 Showing Heated Surface Size Effect

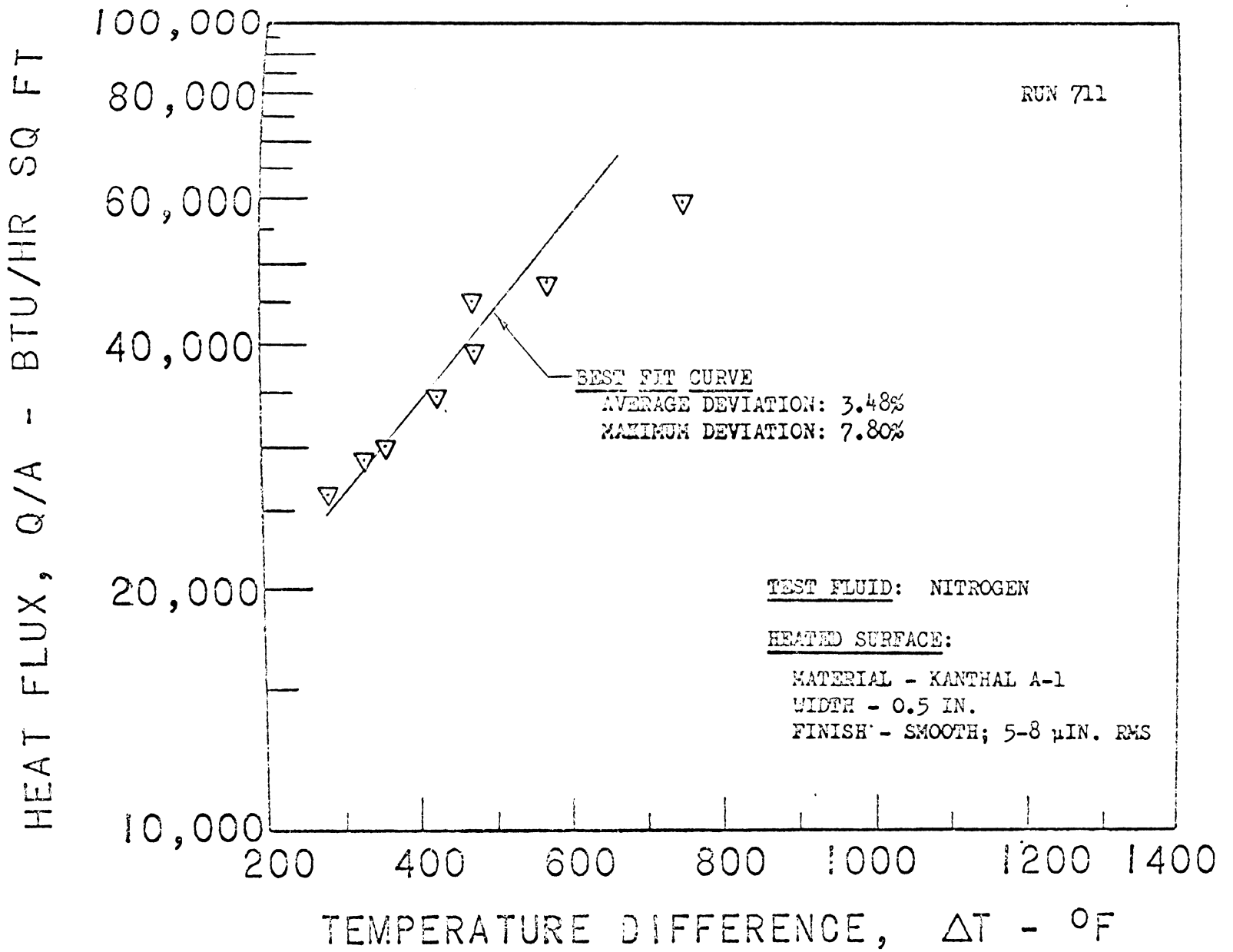


FIGURE 23 - Heat Flux Results for N₂ on 0.5 in. wide Kanthal Horizontal Surface

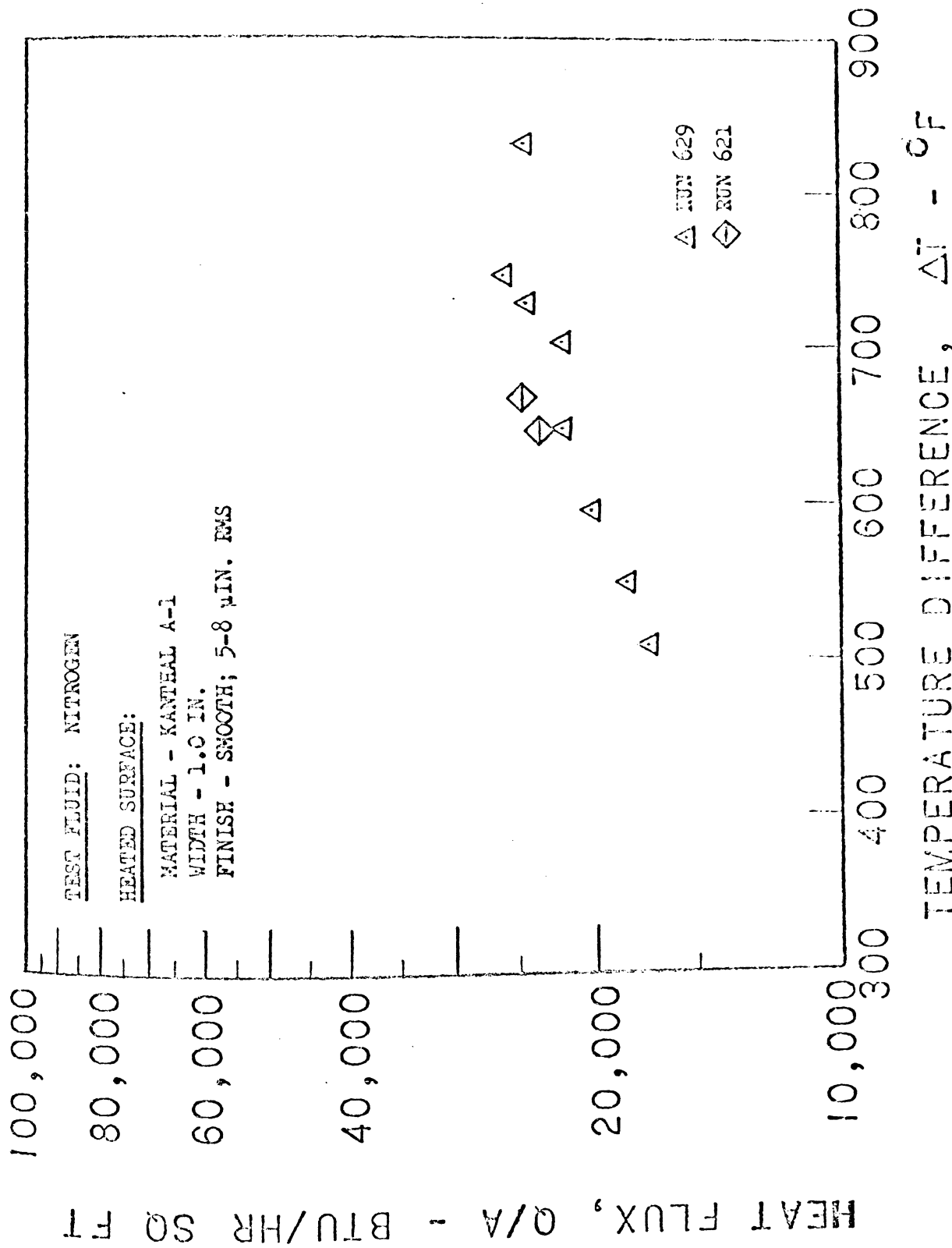


FIGURE 24 - Heat Flux Results for N₂ on 1.0 in. wide Kanthal Horizontal Surface

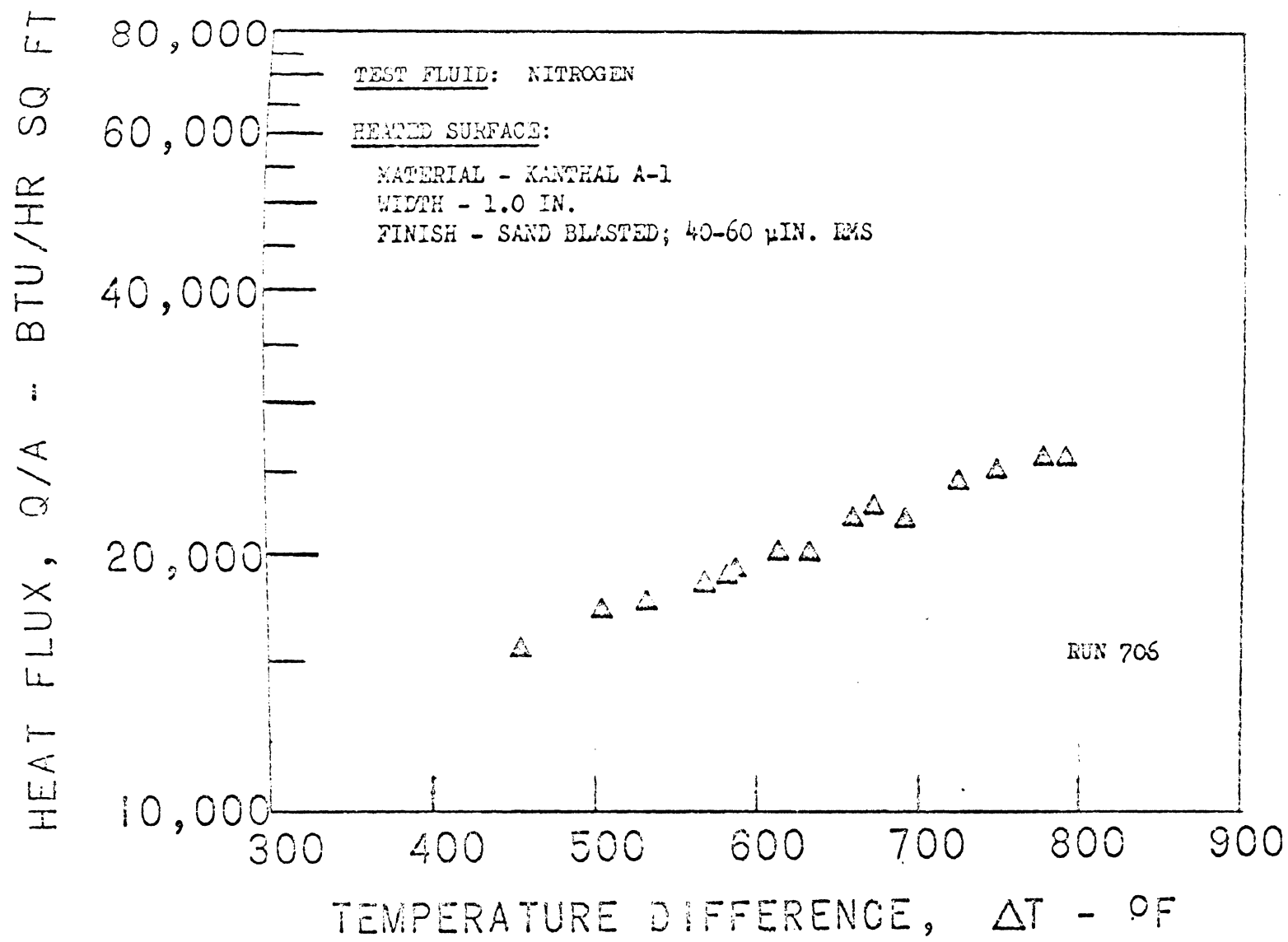


FIGURE 25 - Heat Flux Results for N₂ on 1.0 in. wide sand blasted Kanthal Horizontal Surface

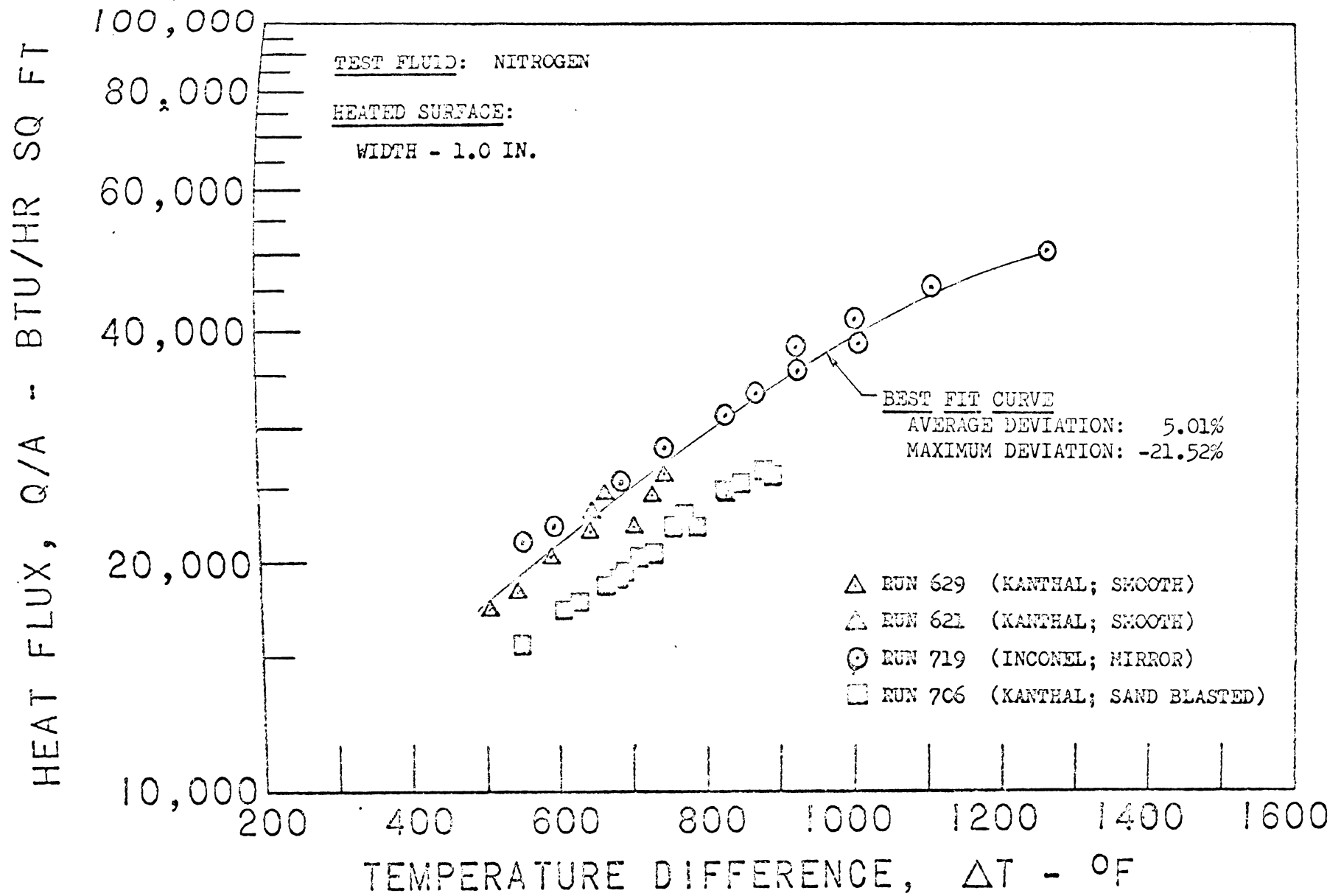


FIGURE 26 - Heat Flux Results for N_2 on 1.0 in. wide sand blasted Kanthal Horizontal Surface

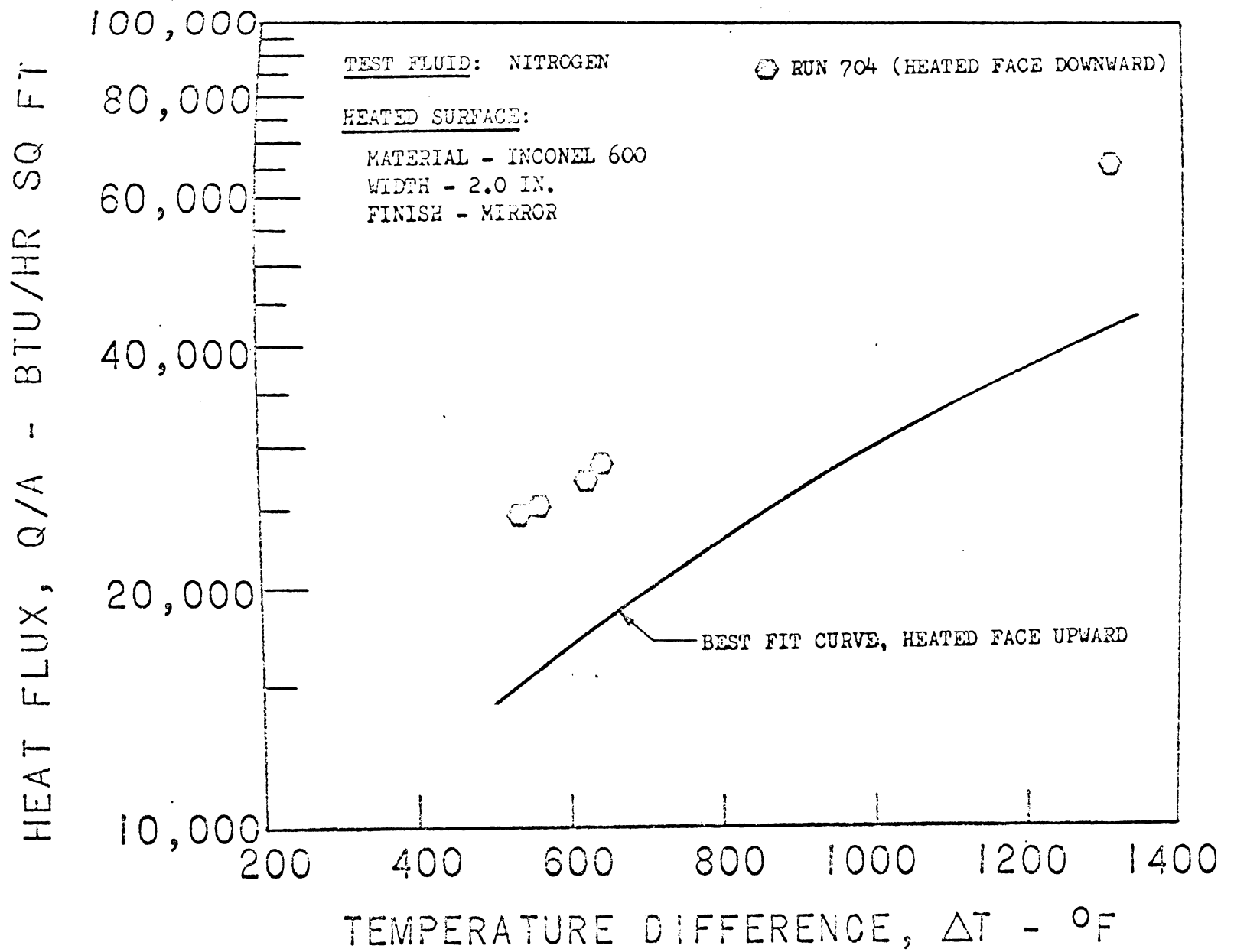


FIGURE 27 - Heat Flux Results for N_2 on 2.0 in. wide Inconel Surface facing downward

Figure 28 contains the heat transfer coefficient results for the 0.5, 1.0 and 2.0 in. wide Inconel horizontal heated surfaces. Included for comparison are the predicted results as presented by Chang and Berenson. Berenson's equation seems to serve well as a lower limit to the heat transfer coefficients that can be experimentally expected.

Figure 29 presents the heat transfer coefficient versus heat flux results for the 1.0 in. wide heated surfaces. The results for the roughened surface are included for comparison, but not in the best fit calculations. The average deviation of the points included from the best polynomial fit is 4.04%

Figure 30 shows the heat transfer coefficient versus heat flux results for the 0.5, 1.0 and 2.0 in. wide Inconel heated surfaces.

Correlation With Modified Berenson Equation

Examination of Figures 16 and 28 display a favorable trend for the Berenson correlation equation in two fluids of very different nature. The Berenson equation does not include the effect of radiation heat transfer to the vapor film. Brentari and Smith have published radiation heat transfer rates for nitrogen.⁽¹⁴⁾ Using these values, the 2.0 in. heat flux curve in Figure 22 was adjusted for radiation loss. The heat transfer coefficient shown in Figure 31 results from this adjustment. Although this data still does not agree with the Berenson equation a slight modification of Berenson's coefficient from .425 to .512 results in excellent correlation. The resulting equation is therefore;

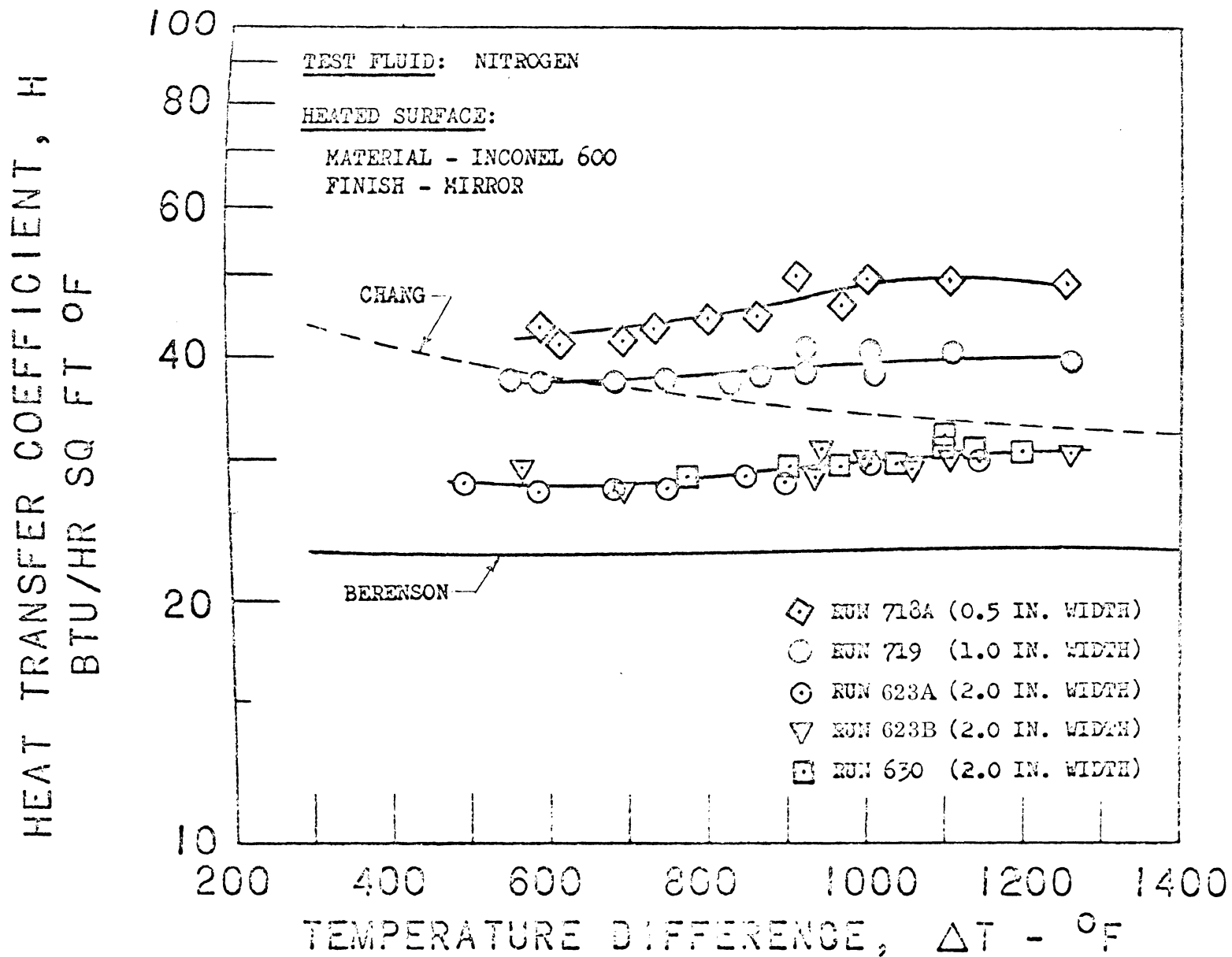


FIGURE 28 - Heat Transfer Coefficient Results for N_2 on Inconel Horizontal Surface

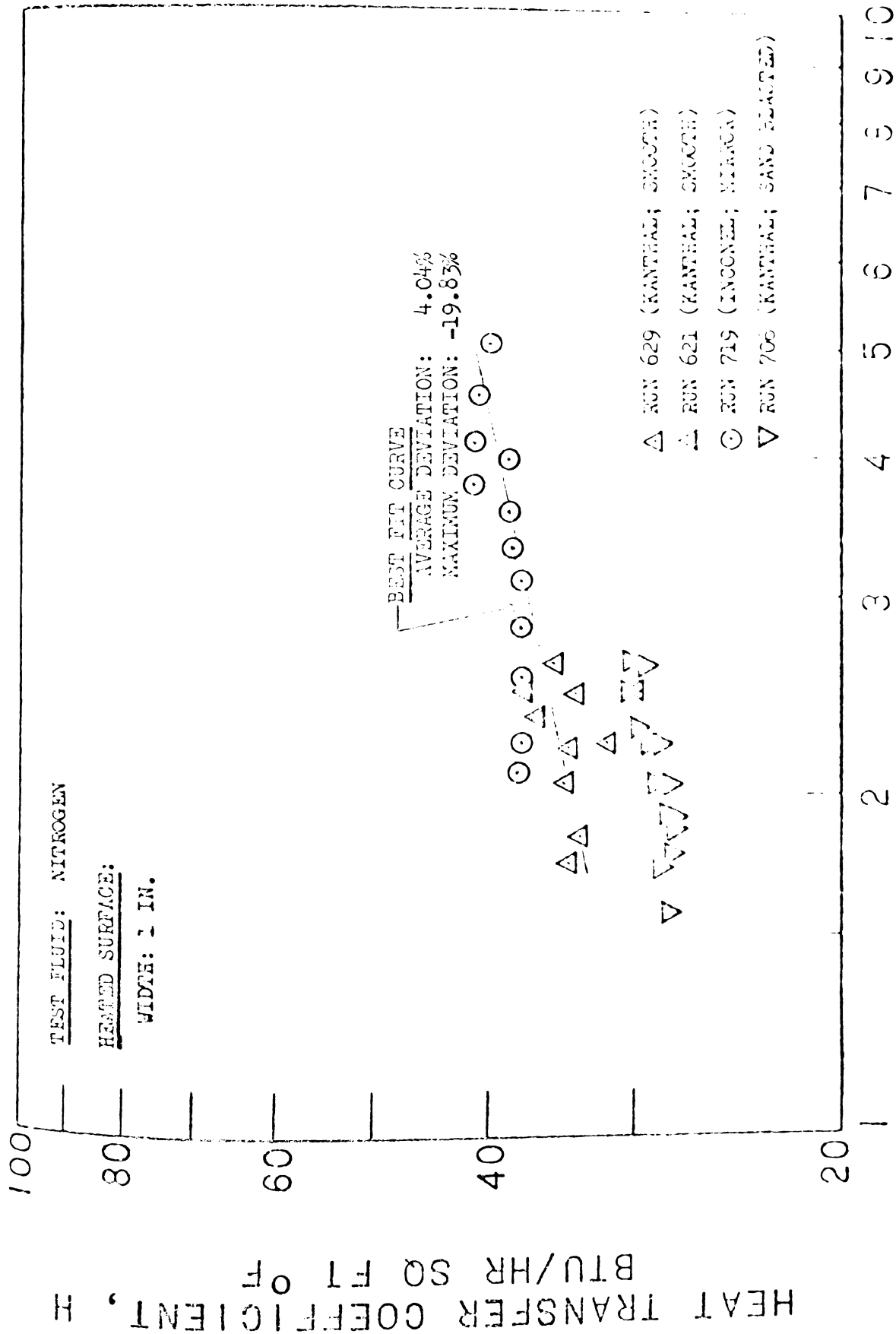


FIGURE 29 - H versus G/A for N₂ on 1.0 in. wide Hemmed Surface

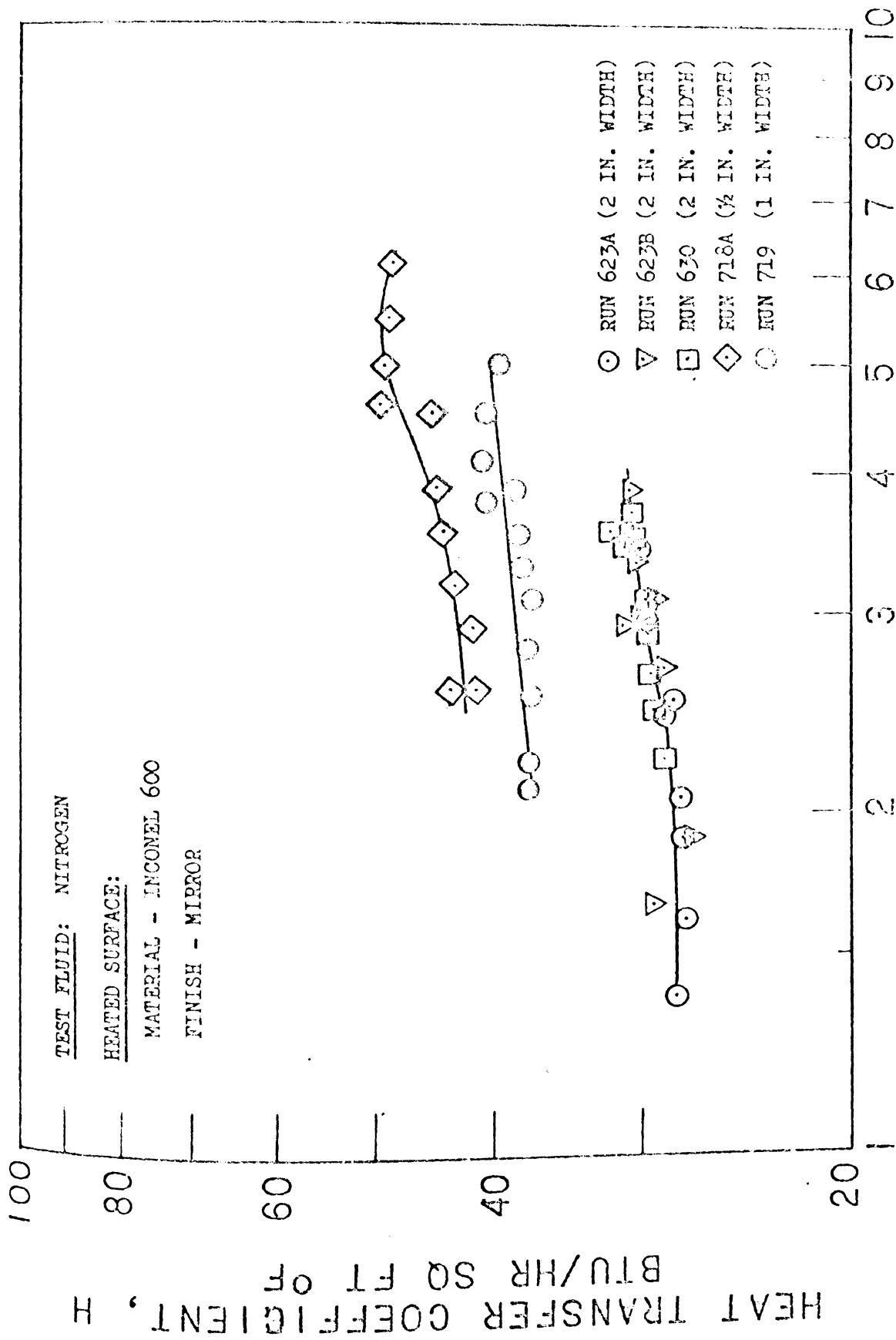


FIGURE 30 - H versus q/A for N_2 on Inconel Horizontal Surfaces

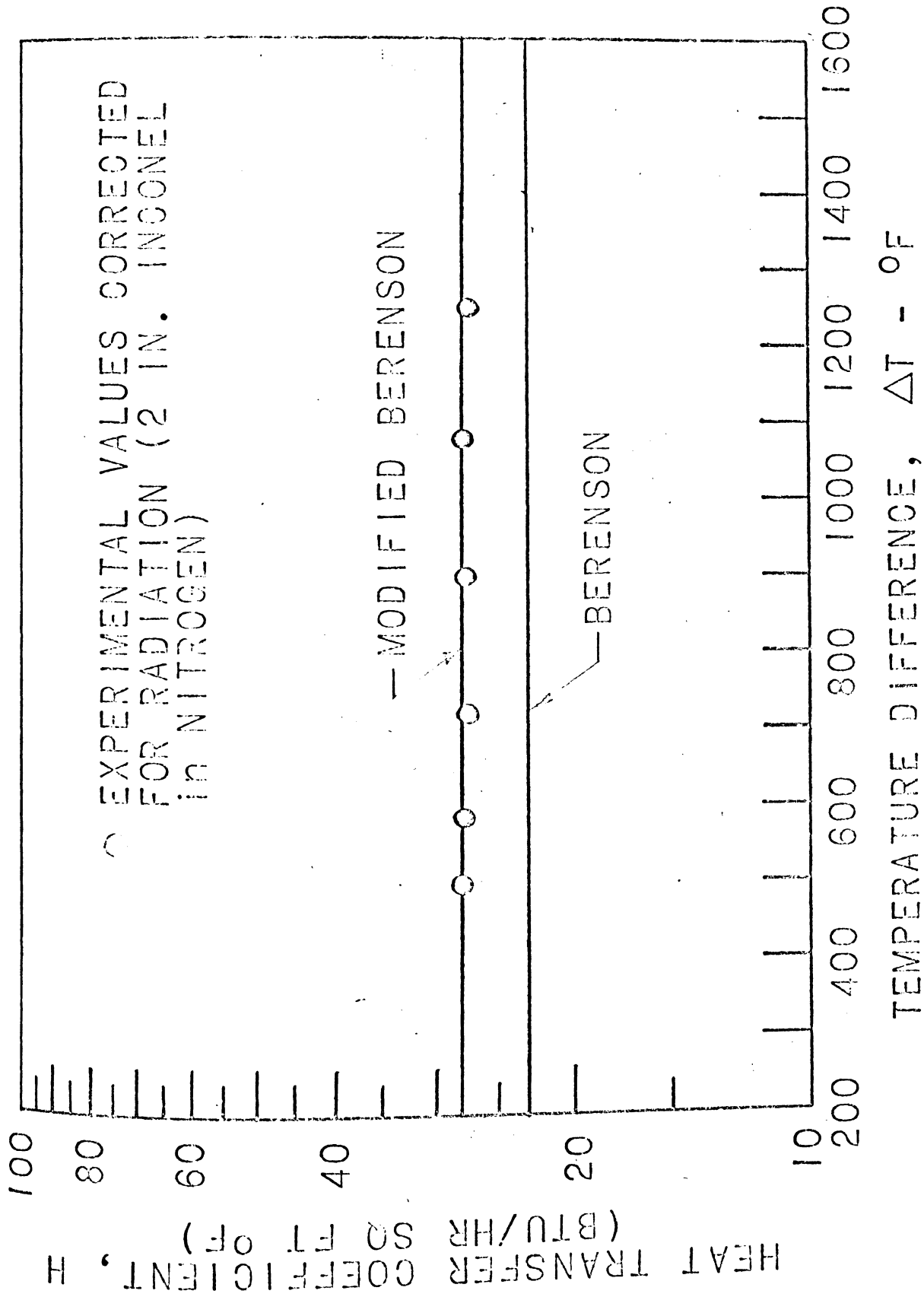


FIGURE 31 - Modified Berenson Equation

$$h = .512 \left[\frac{K_{vf}^3 h_{fg} \rho_{vf} (\rho_l - \rho_v) g}{\mu_{vf} g_c \Delta T \left[\frac{g_c \sigma}{g(\rho_l - \rho_v)} \right]} \right]^{1/4} \quad (12)$$

This is a justifiable modification, since the original value of Berenson's coefficient was not obtained as part of his theoretical derivation, but was obtained from existing experimental data.

Effect of Surface Roughness

Several theoretical investigators have stated that surface roughness should not affect the stable film boiling curve. ^{(10), (14)} They further state that the important reason that the roughness cannot have an effect is because the liquid never touches the heated surface in stable film boiling.

The 1.0 in. heated surfaces used in this experimental investigation have the width dimension only approximately twice the value calculated for the most dangerous wavelength. Therefore, according to Taylor Instability Criteria (see Appendix A) there exists the possibility that the vapor film will not be uniformly supported in this direction, and the boiling liquid may occasionally touch the heated surface. Investigation of Figure 26 for 1.0 in. wide heated surfaces suggests a possible roughness effect. The trend observed is opposite to that expected, if any was expected at all. It is suggested that the roughness acts as a holding agent for the vapor film, and actually helps support it in the width direction; therefore, accounting for the reduction in heat flux as compared to a smooth surface in nitrogen.

Figures 14 and 16 show that no surface roughness effect is observed

in refrigerant-11. It was observed in all refrigerant-11 tests that a deposit formed on the heated surface early in the test. This deposit would cover the roughened surface and make its outer appearance identical to a smooth surface with deposits. Therefore, the boiling results are, as expected, the same for roughened and unroughened surfaces in refrigerant-11.

Effect of Surface Size

In the literature it is generally accepted that a flat horizontal plate can be assumed infinite for a particular fluid if its smallest dimension is greater than ten times the most dangerous wavelength for the fluid. ⁽⁴⁾ The 0.5 and 1.0 in. heated surfaces employed in this investigation are well below this lower limit, and therefore a surface size effect is expected similar to the diameter effect which occurs with cylindrical heaters. Investigation of Figures 16, 17, and 18 for refrigerant-11 and Figure 22 for nitrogen will suggest a surface size effect. This effect is possibly exaggerated by the one-dimensional method of calculating heat losses out the insulated side of the heated surface.

Effect of Surface Material

Figure 26, which includes Inconel and Kanthal heated surfaces, displays no surface material effect. Theoretical investigators have predicted that such an effect should not appear in stable film boiling.

Effect of Surface Orientation

In Figure 27 the results of a test with the heater turned face downward are presented. The best fit curve for a similar heater turned face upwards

is included for comparison. By turning the heater upside down the gravity vector has been rotated 180° ; this figure therefore indicated a gravity effect also. There is a definite effect and no attempt is made here to explain it; but only to observe that it did indeed occur, and indicate that more work is needed in this area before a true understanding can be achieved.

Effect of Fluid Properties

The density, viscosity, surface tension, heat of vaporization, and thermal conductivity are all fluid properties which affect boiling performance. No theoretical analysis could be completed without a proper understanding of the effect of these properties on the boiling phenomenon. Investigation of the thermophysical properties for refrigerant-11 and nitrogen in Appendix D will justify the similarities and differences observed in the boiling characteristics of the two fluids as presented in the results. It is suggested that the modified Berenson equation takes best account of the important boiling parameters.

Experimental Accuracy

Some error must be tolerated in all experimental investigations. This investigation was no exception.

One source of error is the induced emf due to the direct attachment of a thermocouple to an electrically heated plate.⁽³⁵⁾ No error occurs if the thermocouple junctions are points. However, the thermocouple junctions are finite in size and therefore a voltage drop is present across the junction. It was originally planned to correct the data for the induced signal. An experimental investigation of the magnitude of this emf was made by reversing the current at a

given equilibrium point and yielded a good indication of the error for a single thermocouple. However, because of different orientations of the thermocouples as they were spot welded to the heater, no single calibration or correction curve could be obtained. It was also observed that the errors were somewhat self-cancelling due to random attachment of the thermocouple junctions. It was therefore decided that, for this investigation, any error due to the induced emf would be accepted and its maximum value reported. The resulting average temperature of the test plate could be in error by as much as $\pm 50^{\circ}\text{F}$, although this is neither known nor expected to have been the case. The expected error is less than this value.

The "average" plate temperature used was the simple arithmetic average of the six thermocouples attached to the plate. Because of the relatively large temperature variation with position (on the order of 100°F) on the heater under some boiling conditions, this average may not represent the mean value of the surface temperature.

Heat loss through the transite insulation backing was determined by instrumenting the backing with thermocouples as a heat meter. The accuracy of this method of determining the heat loss through the backing decreases as the width of the heater decreases. Using three temperature locations (essentially two heat meters in series) in the backing indicated that for the 1.0 and 2.0 inch wide heaters, heat loss measurements were accurate to 10%. For future work with half-inch heaters a complete three-dimensional temperature profile within the backing will be needed for accurate determination of this heat loss.

Precision instruments were used for measuring the current, voltage drop across the test section, and thermocouple emfs. Errors introduced because of the limitation on accuracy and readability of these instruments were small compared to the errors introduced by other factors as mentioned above.

CONCLUSIONS AND RECOMMENDATIONS

It is concluded that:

1. There may be a surface size and roughness effect in stable film boiling for horizontal heated surfaces with one dimension near the most dangerous wavelength.
2. The heated surface material does not affect the stable film boiling region.
3. The orientation of the heated surface with respect to the g vector does affect boiling performance in the stable film region.
4. Film boiling performance for horizontal heated surfaces can be accurately predicted using the modified Berenson equation (12).
5. The heat transfer coefficients predicted by Chang's equation serve as an upper limit to the data observed in refrigerant-11.

It is recommended that:

1. Further work be performed with several fluids in all areas reported to further verify the data, especially with the heated surface facing downward.
2. A drop test apparatus be designed in conjunction with the present apparatus to test the effect of reduced gravity fields on stable film boiling.
3. The apparatus be modified to study the effect of oscillation upon the stable film region.
4. The present apparatus be instrumented to study burnout phenomenon of low thermal capacity flat plates.

REFERENCES

1. Nukiyama, "The Maximum and Minimum Values of the Heat Q Transmitted From Metal to Boiling Water Under Atmospheric Pressure," Int. J. Heat Mass Transfer, Vol. 9, 1966, p. 1419.
2. Jens, "Boiling Heat Transfer: What is Known About It," ASME, December 1954.
3. Kreith, Principles of Heat Transfer, International Textbook Company, Scranton, Pennsylvania, 1966, 2nd ed., Chap. 10, p. 449.
4. Berenson, "Transition Boiling Heat Transfer from a Horizontal Surface," MIT Technical Report No. 17, 1960.
5. Gottfried, Lee and Bell, "The Leidenfrost Phenomenon: Film Boiling of Liquid Droplets on a Flat Plate," Int. J. Heat Mass Transfer, Vol. 9, 1966, p. 1167.
6. Bromley, "Heat Transfer in Stable Film Boiling," Chemical Engineering Progress, Vol. 46, 1950.
7. Chang, "Wave Theory of Heat Transfer in Film Boiling," Journal of Heat Transfer, Vol. 81, 1959, p. 1.
8. Zuber, "Hydrodynamic Aspects of Boiling Heat Transfer " AECU-4439, 1959.
9. Berenson, "Experiments on Pool-Boiling Heat Transfer," Int. J. Heat Mass Transfer, Vol. 5, 1962, p. 985.
10. Berenson, "Film Boiling Heat Transfer From a Horizontal Surface," ASME Paper No. 60-WA-147, 1961.
11. Hosler and Westwater, "Film Boiling on a Horizontal Plate", ASME, April 1962.
12. Class, DeHaan, Piccone and Cost, "Boiling Heat Transfer to Liquid Hydrogen from Flat Surfaces," Int. Adv. in Cry. Eng., Vol. 5, 1959, p. 254.
13. Manson, "A Periodic Nonuniform Heat Transfer Mechanism in Film Boiling," Journal of Heat Transfer, Feb. 1967, p. 111.
14. Brentari and Smith, "Nucleate and Film Pool Boiling Design Correlations for O₂, N₂, H₂ and He," Int. Adv. in Cry. Eng., Vol. 10, 1964 p. 325.

15. Cole, "Investigation of Transient Pool Boiling Due to Sudden Large Power Surge," NACA Technical Note No. 3885, 1956.
16. McAdams, Heat Transmission, McGraw-Hill Book Co., Inc., New York, N. Y., 1954, p. 387.
17. Rohsenow and Choi, Heat, Mass and Momentum Transfer, Prentice-Hall Inc., Englewood Cliff, New Jersey, 1961, p. 231.
18. Holman, Heat Transfer, McGraw-Hill Book Company Inc., New York, N. Y., 1963, Chap. 9, p. 208.
19. Jakob, Heat Transfer, John Wiley and Sons, Inc., New York, N. Y., Vol. 1, 1958, p. 652.
20. Parker and Boggs, Fluid Mechanics and Heat Transfer, Preliminary Edition Oklahoma State University, 1966.
21. Tong, Boiling Heat Transfer and Two-Phase Flow, John Wiley and Sons, Inc., New York, N. Y., 1965, Chap. 2.
22. Houchin and Lienhard, "Boiling Burnout in Low Thermal Capacity Heaters," ASME Paper No. 66-WA/HT-40, 1966.
23. Usikin and Siegel, "An Experimental Study of Boiling in Reduced and Zero Gravity Fields," Journal of Heat Transfer, 1961, p. 243.
24. Change, "A Theoretical Analysis of Heat Transfer in Natural Convection and in Boiling," ASME Paper No. 56-A42, Oct. 1957.
25. DiCicco and Schoenhals, "Heat Transfer in Film Boiling with Pulsating Pressures", ASME Paper No. 63-WA-75, 1964.
26. Grossmann and Hauser, "Heat Transfer from Wire to Subcooled and Boiling Water," Int. J. Heat Mass Transfer, Vol. 7, 1964, p. 211.
27. Flynn, Draper and Roos, "The Nucleate and Film Boiling Curve of Liquid Nitrogen at one Atmosphere," Int. Adv. in Cry. Eng., Vol. 7, 1961, p. 539.
28. Rhea, "Boiling Heat Transfer from an Oscillating Sphere with a Cryogenic Fluid at Atmospheric Pressure and Standard Gravity," Ph.D. Thesis, Kansas State University, 1967.
29. Levy, "Generalized Correlation of Boiling Heat Transfer," Journal of Heat Transfer, Vol. 81, 1959, p. 37.

30. Forster and Grief, "Heat Transfer to a Boiling Liquid - Mechanisms and Correlations," Journal of Heat Transfer, Feb. 1959, p. 43.
31. Rohsenow, "A Method of Correlating Heat Transfer Data for Surface Boiling of Liquids," ASME Paper No. 51-A-110, 1951.
32. Taylor, "The Instability of Liquid Surfaces When Accelerated in a Direction Perpendicular to Their Plane, I," Proceedings, Royal Society of London, Vol. 21, Series A, 1950, p. 192.
33. Lamb, Hydrodynamics, Dover Publications, New York, N. Y., 1915, p. 455.
34. Milne-Thomson, Theoretical Hydrodynamics, The MacMillan Company, New York, N. Y., 1960, Chap. XIV, p. 388.
35. Davenport, Magee and Leppert, "Thermocouple Attachment to a Direct-Current Heater," Journal of Heat Transfer, May 1962, p. 187.
36. Allred and Blount, "Experimental Studies of Taylor Instability," LA-1600, Nov. 1953.
37. Perry, Chemical Engineers Handbook, McGraw-Hill Book Co., Inc., New York, 1950, 3rd Ed., p. 229, 371.
38. Chelton and Mann, "Cryogenic Data Book," WADC Technical Report 59-8, 1959.

APPENDIX A

DISCUSSION OF APPLIED HYDRODYNAMICS

Hydrodynamics is a branch of physics which deals with the problems associated with fluids in motion. Several authors, such as Berenson,⁽¹⁰⁾ Chang⁽⁷⁾ and Zuber,⁽⁸⁾ have drawn upon different phases of hydrodynamic theory to arrive at models to represent film boiling from a flat plate. The fact that solid-vapor and vapor-liquid interfaces coexist in film boiling makes the problem very interesting. Berenson⁽⁴⁾ and Zuber have also investigated the application of hydrodynamic theory to the transition boiling region, where a triple solid-vapor-liquid interface has been proven to exist.⁽¹⁾

The following is a brief presentation of the ideas, assumptions, and to a lesser degree the mathematics set forth in the literature concerning the application of hydrodynamics to boiling at the burnout point and in the stable film region. This presentation will draw upon the works of Berenson,⁽⁴⁾ Zuber,⁽⁸⁾ and Chang.⁽⁷⁾

Taylor - Helmholtz Instability

Taylor⁽³²⁾⁽³⁶⁾ was the first to study the problem of a liquid vapor interface subjected to small sinusoidal perturbations. Taylor visualizes a fluid of density ρ_1 existing at an interface. The heavier fluid is above the lighter fluid ($\rho_2 > \rho_1$). Both fluids are experiencing the pull of gravity and also an added acceleration in the opposite direction. Berenson interprets Taylor's results to state that, when the acceleration is directed from the lighter to the heavier fluid, an instability will exist, that is, the interface will periodically

rupture with time. Hosler and Westwater⁽¹¹⁾ say that 'Taylor' s results show that, when the acceleration is directed from the heavier to the lighter fluid, an instability will arise. There seems to be some question on the interpretation of 'Taylor' s results. The present interpretation is that there are two acceleration factors of importance, the acceleration due to gravity and an acceleration resulting from the buoyancy effect of the lower fluid.

In the literature several terms associated with a discussion of film boiling, such as critical wavelength, most dangerous wavelength and criteria for stability, are at best not universally or uniformly applied and understood. Possibly it is unfortunate that the name Taylor Instability has come into wide use, because this instability must exist in order for a system to operate in stable film boiling. That is to say that stable film boiling is characterized by the mathematics of Taylor Instability.

The basic mathematics of hydrodynamics for two phase interfaces subjected to small perturbations can be found in several texts.^{(33), (34)} The usual assumption is made that the liquid-vapor interface is subjected to the following small perturbation:

$$N = N_o e^{-i\omega t} \cos mx \quad , \quad (\text{A-1})$$

where the wave number is defined as follows :

$$m = \frac{2\pi}{\lambda} \quad . \quad (\text{A-2})$$

By making the appropriate simplifications applicable to a two phase interface above a flat horizontal plate, the irrotational flow kinematic equation yields the following frequency equation describing the oscillation of the interface:

$$\omega^2 = \frac{g_c \sigma m^3}{\rho_1 + \rho_v} - \frac{g(\rho_1 - \rho_v)m}{\rho_1 + \rho_v} \quad (A-3)$$

This equation assumes that the effect of vapor velocity and depth are negligible.

The condition for stability is that ω be real. Inspection of the interface equation shows that when ω is imaginary the oscillation will grow with time and the interface must rupture. Therefore, the left hand side of equation (A-3) is set equal to zero to find the range of instability.

$$\frac{g_c \sigma m^3}{\rho_1 + \rho_v} = \frac{g(\rho_1 - \rho_v)m}{\rho_1 + \rho_v} ;$$

$$m = \left[\frac{g}{g_c} \frac{(\rho_1 - \rho_v)}{\sigma} \right]^{1/2} = \frac{2\pi}{\lambda} , \text{ and}$$

therefore the critical wavelength,

$$\lambda_c = 2\pi \left[\frac{g_c}{g} \frac{\sigma}{(\rho_1 - \rho_v)} \right]^{1/2} \quad (A-4)$$

The term wavelength as used here means the distance between the antinodes of vibration of the interface or the distance between the bubble release areas. Examination of the above criteria for stability yields the fact that wavelengths longer than λ_c cannot exist in a system experiencing film boiling from a flat plate. In stable film boiling the wavelength and amplitude decrease, and the frequency increases as the surface temperature rises. There is a continuum of wavelengths that can exist in stable film boiling, but only one wavelength, the most dangerous wavelength, has the maximum growth rate. Thus, the derivative of ω^2 with respect to m is taken which gives

$$\lambda_d = 2\pi \left[\frac{3g_c}{g} \frac{\sigma}{(\rho_l - \rho_v)} \right]^{1/2}; \quad (A-5)$$

therefore,

$$\lambda_d = \sqrt{3} \lambda_c.$$

Hosler and Westwater have shown experimentally that the minimum wavelength present at the Leidenfrost point is λ_c , and the average wavelength present is λ_d . With this in mind an experimenter could design a flat strip heater to have a minimum point in stable film boiling at any desired position along the film boiling curve for an infinite plate.

Fluid properties have a significant effect upon λ_d . Property values used for Refrigerant-11 and Nitrogen are listed below:

Nitrogen

$$\rho_l = 50.44 \text{ #/cu.ft.}$$

$$\rho_v = 0.225 \text{ #/cu.ft.}$$

$$\sigma = 5.67 \cdot 10^{-4} \text{ #/ft.}$$

$$\lambda_d = .439 \text{ in.}$$

Refrigerant-11

$$\rho_l = 91.3 \text{ #/cu.ft.}$$

$$\rho_v = 0.307 \text{ #/cu.ft.}$$

$$\sigma = 1.30 \cdot 10^{-3} \text{ #/ft.}$$

$$\lambda_d = .494 \text{ in.}$$

The density and surface tension of the liquid were taken at saturation temperature for the liquid and the vapor density was evaluated using the perfect gas law at the average film temperature.

Berenson has greatly expanded this Taylor Instability theory to develop equations (1) and (3).

It is interesting to think about what is actually happening to a system in film boiling at the Leidenfrost point. At this point the surface temperature

is just sufficient to generate enough vapor to support the interface at the existing wavelength. An understanding of the transition region can be developed with this simple model. If the temperature is lowered to slightly below the Leidenfrost point, hydrodynamic effects demand the break-up of the vapor film, but the temperature is too high to allow stable nucleate boiling and transition boiling occurs. In the transition region the vapor generated is too large for stable film boiling to exist and too small for nucleate boiling to exist continuously at any given point.

In conclusion, a brief discussion of the physical boiling phenomena governed by Helmholtz Instability will be included. Zuber has extensively discussed the flooding effect which takes place at the burnout point. This flooding effect is mathematically described with the application of Helmholtz Instability Criteria. In the nucleate region at high heat fluxes columns of vapor form in the boiling liquid. As the temperature of the heater goes up, more and more vapor is being carried away from the heater surface; therefore the columns of vapor become larger in diameter and begin to rub against one another. At the burnout point the surface becomes flooded with vapor columns, and the relative velocity and surface tension effects of the columns cause them to coalesce into a continuous vapor blanket. If the system were temperature controlled it would oscillate between nucleate and film boiling as the temperature was increased slightly past the burnout point. It is with the mathematics associated with these ideas that Zuber has developed equation (7).

APPENDIX B

EXPERIMENTAL DATA

TABLE IV

BOILING RESEARCH DATA AND RESULTS TABULATION SHEETTEST NO. (Date) 529 AMBIENT TEMPERATURE 82°F REFERENCE JUNCTION Room Temperature, 82°FFLUID Refrigerant - 11HEATER Material: Kanthal A-1 Size: 1.0x4.125x0.010 Surface Condition: Smooth; 5-8 μin. rms.

Run No.	1	2	3	4	5
Current amperes	118.1	144.4	131.8	116.4	105.5
Voltage Drop across Heater volts	3.13	4.19	4.03	3.60	3.28
Average Heater Temperature, T_H °F	1106	1452	1276	1106	948
Average Bulk Temperature, T_B °F	75	75	75	75	75
Temperature Drop in Backing °F	124	222	179	126	103
Power Supplied to Test Section Btu/hr sq ft	44,100	72,000	63,100	49,900	41,200
Heat Loss through Backing Btu/hr sq ft	3,730	6,678	5,384	3,790	3,098
Temperature Difference, ΔT °F ($T_H - T_B$)	1,031	1,377	1,201	1,031	873
Boiling Heat Flux, Q/A Btu/hr sq ft	40,370	65,322	57,716	45,110	38,102
Heat Transfer Coefficient, h Btu/hr sq ft °F	39.15	47.43	46.05	44.72	43.64

BOILING RESEARCH DATA AND RESULTS TABULATION SHEET

TEST NO. (Date) 603 AMBIENT TEMPERATURE 80°F REFERENCE JUNCTION 32°F

FLUID Refrigerant - 11

HEATER Material: Kanthal A-1 Size: 1.0 x 4.17 x 0.010 Surface Condition: Smooth: 5-8 μ in. rms.

Run No.	1	2	3	4				
Current amperes	125.4	112.3	102.0	95.6				
Voltage Drop across Heater volts	3.36	3.03	2.77	2.61				
Average Heater Temperature, T_H °F	1000	878	765	693				
Average Bulk Temperature, T_B °F	75	75	75	75				
Temperature Drop in Backing °F	289	285	223	166				
Power Supplied to Test Section Btu/hr sq ft	49,100	39,700	32,800	29,100				
Heat Loss through Backing Btu/hr sq ft	9,260	9,140	7,150	5,320				
Temperature Difference, ΔT °F ($T_H - T_B$)	925	803	690	618				
Boiling Heat Flux, Q/A Btu/hr sq ft	39,840	30,560	25,650	23,780				
Heat Transfer Coefficient, h Btu/hr sq ft °F	43.1	33.0	37.2	38.4				

BOILING RESEARCH DATA AND RESULTS TABULATION SHEET

TEST NO. (Date) 605 AMBIENT TEMPERATURE 80°F REFERENCE JUNCTION 32°F

FLUID Refrigerant - 11

HEATER Material: Kanthal A-1 Size: 1.0 x 4.17 x 0.010 Surface Condition: Smooth; 5-8 μ in. rms.

Run No.	1	2	3	4	5			
Current amperes	125.0	120.0	109.0	100.0	93.0			
Voltage Drop across Heater volts	3.36	3.21	3.00	2.70	2.50			
Average Heater Temperature, T_H °F	1019	990	878	756	705			
Average Bulk Temperature, T_B °F	75	75	75	75	75			
Temperature Drop in Backing °F	314	302	245	185	165			
Power Supplied to Test Section Btu/hr sq ft	48,900	44,800	38,100	31,400	27,100			
Heat Loss through Backing Btu/hr sq ft	10,100	9,680	7,850	5,940	5,290			
Temperature Difference, ΔT °F ($T_H - T_B$)	944	915	803	681	630			
Boiling Heat Flux, Q/A Btu/hr sq ft	37,600	33,800	28,460	23,220	19,540			
Heat Transfer Coefficient, h Btu/hr sq ft °F	39.9	37.0	35.5	34.1	31.0			

BOILING RESEARCH DATA AND RESULTS TABULATION SHEET

TEST NO. (Date) 621 AMBIENT TEMPERATURE 89°F REFERENCE JUNCTION -320°F

FLUID Nitrogen

HEATER Material: Kanthal A-1 Size: 1.0 x 4.0 x 0.010 Surface Condition: Smooth; 5-8 μ in. rms.

Run No.	1	2					
Current amperes	97.5	96.0					
Voltage Drop across Heater volts	2.55	2.50					
Average Heater Temperature, T_H °F	348	325					
Average Bulk Temperature, T_B °F	-320	-320					
Temperature Drop in Backing °F	190	194					
Power Supplied to Test Section Btu/hr sq ft	30,500	29,400					
Heat Loss through Backing Btu/hr sq ft	5,680	5,840					
Temperature Difference, ΔT °F ($T_H - T_B$)	668	645					
Boiling Heat Flux, Q/A Btu/hr sq ft	24,820	23,530					
Heat Transfer Coefficient, h Btu/hr sq ft °F	37.2	33.5					

BOILING RESEARCH DATA AND RESULTS TABULATION SHEET

TEST NO. (Date) 623A AMBIENT TEMPERATURE 85°F REFERENCE JUNCTION -320°F

FLUID Nitrogen

HEATER Material: Inconel - 600 Size: 2.0 x 4.09 x 0.005 Surface Condition: Mirror Finish

Run No.	1	2	3	4	5	6	7	8
Current amperes	160.1	174.5	186.7	161.8	147.0	138.7	129.0	117.5
Voltage Drop across Heater volts	3.10	3.40	3.65	3.15	2.87	2.72	2.50	2.31
Average Heater Temperature, T_H °F	532	684	824	580	433	367	267	176
Average Bulk Temperature, T_B °F	-320	-320	-320	-320	-320	-320	-320	-320
Temperature Drop in Backing °F	177	191	209	176	150	118	105	80
Power Supplied to Test Section Btu/hr sq ft	29,800	35,600	40,750	30,600	25,300	22,600	19,350	16,300
Heat Loss through Backing Btu/hr sq ft	5,310	5,750	6,270	5,300	4,500	3,540	3,160	2,400
Temperature Difference, ΔT °F ($T_H - T_B$)	852	1,004	1,144	900	753	687	597	496
Boiling Heat Flux, q/A Btu/hr sq ft	24,490	29,850	34,480	25,300	20,800	19,060	16,190	13,900
Heat Transfer Coefficient, h Btu/hr sq ft °F	28.7	29.8	30.1	27.6	27.7	27.7	27.7	27.7

BOILING RESEARCH DATA AND RESULTS TABULATION SHEET

TEST NO. (Date) 623B AMBIENT TEMPERATURE 85°F REFERENCE JUNCTION -320°F

FLUID Nitrogen

HEATER Material: Inconel - 600 Size: 2.0 x 4.09 x 0.005 Surface Condition: Mirror Finish

Run No.	1	2	3	4	5	6	7	8
Current amperes	168.7	171.7	175.0	180.5	193.7	162.5	137.6	127.5
Voltage Drop across Heater volts	3.32	3.38	3.45	3.57	3.85	3.20	2.71	2.51
Average Heater Temperature, T_H °F	626	680	744	786	938	619	376	252
Average Bulk Temperature, T_B °F	-320	-320	-320	-320	-320	-320	-320	-320
Temperature Drop in Backing °F	135	154	164	169	195	140	107	80
Power Supplied to Test Section Btu/hr sq ft	33,600	34,800	36,200	38,700	44,700	31,200	22,400	19,200
Heat Loss through Backing Btu/hr sq ft	4,060	4,700	4,940	5,080	5,850	4,200	3,220	2,400
Temperature Difference, ΔT °F ($T_H - T_B$)	946	1,000	1,064	1,106	1,258	939	696	572
Boiling Heat Flux, Q/A Btu/hr sq ft	29,540	30,100	31,260	33,620	38,850	27,000	19,180	17,800
Heat Transfer Coefficient, h Btu/hr sq ft °F	31.2	30.1	29.4	33.4	33.9	27.8	21.3	29.4

BOILING RESEARCH DATA AND RESULTS TABULATION SHEETTEST NO. (Date) 623B (cont'd) AMBIENT TEMPERATURE 85°F REFERENCE JUNCTION -320°FFLUID NitrogenHEATER Material: Inconel - 600 Size: 2.0 x 4.09 x 0.005 Surface Condition: Mirror Finish

Run No.	9	10	11				
Current amperes	158.0	145.0	132.0				
Voltage Drop across Heater volts	3.10	2.85	2.58				
Average Heater Temperature, T_H °F	368	248	142				
Average Bulk Temperature, T_B °F	-320	-320	-320				
Temperature Drop in Backing °F	113	112	97				
Power Supplied to Test Section Btu/hr sq ft	29,400	24,800	20,400				
Heat Loss through Backing Btu/hr sq ft	3,400	3,370	2,920				
Temperature Difference, ΔT °F ($T_H - T_B$)	688	568	462				
Boiling Heat Flux, q/A Btu/hr sq ft	26,000	21,430	17,480				
Heat Transfer Coefficient, h Btu/hr sq ft °F	27.8	37.7	37.8				

BOILING RESEARCH DATA AND RESULTS TABULATION SHEET

TEST NO. (Date) 629 AMBIENT TEMPERATURE 80°F REFERENCE JUNCTION -320°F

FLUID Nitrogen

HEATER Material: Kanthal A-1 Size: 1.0 x 4.09 x 0.010 Surface Condition: Smooth; 5-8 μ in. rms.

Run No.	1	2	3	4	5	6	7	8
Current amperes	95.0	100.0	102.0	99.2	93.0	89.5	84.7	81.7
Voltage Drop across Heater volts	2.50	2.63	2.72	2.63	2.51	2.41	2.29	2.20
Average Heater Temperature, T_H °F	383	510	426	409	328	275	230	189
Average Bulk Temperature, T_B °F	-320	-320	-320	-320	-320	-320	-320	-320
Temperature Drop in Backing °F	209	228	235	225	197	180	164	141
Power Supplied to Test Section Btu/hr sq ft	28,540	31,605	33,340	31,351	28,051	25,919	23,308	21,599
Heat Loss through Backing Btu/hr sq ft	6,287	6,858	7,069	6,768	5,956	5,414	4,933	4,241
Temperature Difference, ΔT °F ($T_H - T_B$)	703	830	746	729	648	595	550	509
Boiling Heat Flux, Q/A Btu/hr sq ft	22,253	24,747	26,235	24,583	22,095	20,505	18,375	17,350
Heat Transfer Coefficient, h Btu/hr sq ft °F	31.65	29.81	35.16	32.72	34.09	34.46	33.40	34.10

BOILING RESEARCH DATA AND RESULTS TABULATION SHEET

TEST NO. (Date) 630 AMBIENT TEMPERATURE 85°F REFERENCE JUNCTION -320°F

FLUID Nitrogen

HEATER Material: Inconel - 600 Size: 2.0 x 4.09 x 0.005 Surface Condition: Mirror Finish

Run No.	1	2	3	4	5	6	7	8
Current amperes	182.5	181.7	183.7	182.5	188.2	174.0	167.5	161.7
Voltage Drop across Heater volts	3.61	3.60	3.61	3.60	3.72	3.41	3.30	3.16
Average Heater Temperature, T_H °F	782	789	819	813	878	719	651	582
Average Bulk Temperature, T_B °F	-320	-320	-320	-320	-320	-320	-320	-320
Temperature Drop in Backing °F	135	151	133	133	128	151	143	135
Power Supplied to Test Section Btu/hr sq ft	39,585	39,303	39,845	39,476	42,065	35,651	33,212	30,701
Heat Loss through Backing Btu/hr sq ft	4,061	4,542	4,783	4,783	4,933	4,542	4,301	4,061
Temperature Difference, ΔT °F ($T_H - T_B$)	1,102	1,109	1,139	1,133	1,198	1,039	971	902
Boiling Heat Flux, Q/A Btu/hr sq ft	35,524	34,761	35,062	34,693	37,132	31,109	28,911	26,640
Heat Transfer Coefficient, h Btu/hr sq ft °F	32.23	31.34	30.78	30.82	30.99	29.94	29.77	29.53

BOILING RESEARCH DATA AND RESULTS TABULATION SHEET

TEST NO. (Date) 630(cont'd) AMBIENT TEMPERATURE 85°F REFERENCE JUNCTION -320°F

FLUID Nitrogen

HEATER Material: Inconel - 600 Size: 2.0 x 4.09 x 0.005 Surface Condition: Mirror Finish

Run No.	9	10	11				
Current amperes	156.0	150.0	150.0				
Voltage Drop across Heater volts	3.05	2.90	2.90				
Average Heater Temperature, T_H °F	521	459	457				
Average Bulk Temperature, T_B °F	-320	-320	-320				
Temperature Drop in Backing °F	127	126	125				
Power Supplied to Test Section Btu/hr sq ft	23,588	26,137	26,137				
Heat Loss through Backing Btu/hr sq ft	3,820	3,790	3,760				
Temperature Difference, ΔT °F ($T_H - T_B$)	841	779	777				
Boiling Heat Flux, Q/A Btu/hr sq ft	24,768	22,347	22,377				
Heat Transfer Coefficient, h Btu/hr sq ft °F	29.45	28.68	28.79				

BOILING RESEARCH DATA AND RESULTS TABULATION SHEET

TEST NO. (Date) 704 AMBIENT TEMPERATURE 83°F REFERENCE JUNCTION -320°F

FLUID Nitrogen

HEATER Material: Inconel - 600 Size: 2.0 x 4.16 x 0.005 Surface Condition: Mirror Finish

Run No.	1	2	3	4	5			
Current amperes	108.5	110.0	113.7	116.5	169.7			
Voltage Drop across Heater volts	2.13	2.15	2.24	2.30	3.40			
Average Heater Temperature, T_H °F	217	246	306	327	985			
Average Bulk Temperature, T_B °F	-320	-320	-320	-320	-320			
Temperature Drop in Backing °F	86	85	96	93	84			
Power Supplied to Test Section Btu/hr sq ft	27,385	28,025	30,180	31,752	68,372			
Heat Loss through Backing Btu/hr sq ft	2,537	2,557	2,888	2,797	2,527			
Temperature Difference, ΔT °F ($T_H - T_B$)	537	566	626	647	1305			
Boiling Heat Flux, Q/A Btu/hr sq ft	24,798	25,468	27,292	28,955	65,845			
Heat Transfer Coefficient, h Btu/hr sq ft °F	45.17	44.99	43.59	44.73	50.45			

BOILING RESEARCH DATA AND RESULTS TABULATION SHEET

TEST NO. (Date) 706 AMBIENT TEMPERATURE 85°F REFERENCE JUNCTION -320°F

FLUID Nitrogen

HEATER Material: Kanthal A-1 Size: 1.0 x 4.09 x 0.010 Surface Condition: Sand blasted; 40-60 μin. rm

Run No.	1	2	3	4	5	6	7	8
Current amperes	100.0	92.5	88.0	85.0	83.7	87.5	91.2	96.2
Voltage Drop across Heater volts	2.44	2.27	2.17	2.08	2.05	2.15	2.24	2.38
Average Heater Temperature, T_H °F	574	472	414	364	349	394	440	507
Average Bulk Temperature, T_B °F	-320	-320	-320	-320	-320	-320	-320	-320
Temperature Drop in Backing °F	108	95	84	73	68	73	80	89
Power Supplied to Test Section Btu/hr sq ft	29,321	25,232	22,948	21,246	20,619	22,606	24,548	27,513
Heat Loss through Backing Btu/hr sq ft	3,249	2,853	2,527	2,196	2,045	2,196	2,406	2,677
Temperature Difference, ΔT °F ($T_H - T_B$)	894	792	734	684	669	714	760	827
Boiling Heat Flux, Q/A Btu/hr sq ft	26,072	22,374	20,421	19,050	18,574	20,410	22,142	24,836
Heat Transfer Coefficient, h Btu/hr sq ft °F	29.15	28.25	27.82	27.85	27.76	28.58	29.13	30.09

TEST NO. (Date) 706 (con't) AMBIENT TEMPERATURE 85°F REFERENCE JUNCTION -320°F

FLUID Nitrogen

HEATER Material: Kanthal A-1 Size: 1.0 x 4.09 x 0.010 Surface Condition: Sand blasted; 40-60 μin.rms.

Run No.	9	10	11	12	13	14	15
Current amperes	97.5	100.0	92.5	85.0	81.2	80.0	75.5
Voltage Drop across Heater volts	2.40	2.44	2.30	2.11	2.01	1.99	1.89
Average Heater Temperature, T_H °F	529	559	452	366	314	285	234
Average Bulk Temperature, T_B °F	-320	-320	-320	-320	-320	-320	-320
Temperature Drop in Backing °F	97	96	84	73	64	62	52
Power Supplied to Test Section Btu/hr sq ft	28,120	29,321	25,566	21,552	19,613	19,131	17,147
Heat Loss through Backing Btu/hr sq ft	2,918	2,888	2,527	2,195	1,925	1,865	1,564
Temperature Difference, ΔT °F ($T_H - T_B$)	849	879	772	686	634	605	554
Boiling Heat Flux, q/A Btu/hr sq ft	25,202	26,433	23,039	19,356	17,688	17,266	15,583
Heat Transfer Coefficient, h Btu/hr sq ft °F	29.58	30.07	29.89	28.81	27.69	28.53	27.12

TEST NO. (Date) 711 AMBIENT TEMPERATURE 91°F REFERENCE JUNCTION -320°F

FLUID Nitrogen

HEATER Material: Kanthal A-1 Size: 0.5 x 4.09 x 0.010 Surface Condition: Smooth; 5-8 μ in. rms.

Run No.	1	2	3	4	5	6	7	8
Current amperes	59.2	69.5	62.5	57.5	54.0	50.5	49.0	46.0
Voltage Drop across Heater volts	3.17	3.70	3.33	3.05	2.90	2.71	2.61	2.48
Average Heater Temperature, T_H °F	157	429	254	158	108	48	10	-35
Average Bulk Temperature, T_B °F	-320	-320	-320	-320	-320	-320	-320	-320
Temperature Drop in Backing °F	42	88	73	91	90	94	54	37
Power Supplied to Test Section Btu/hr sq ft	45,057	61,742	49,970	42,106	37,600	32,858	30,706	27,391
Heat Loss through Backing Btu/hr sq ft	1,263	2,647	2,196	2,737	2,707	2,828	1,624	1,113
Temperature Difference, ΔT °F ($T_H - T_B$)	477	749	574	478	428	368	330	285
Boiling Heat Flux, q/A Btu/hr sq ft	43,794	59,095	47,774	39,369	34,893	30,030	29,082	25,278
Heat Transfer Coefficient, h Btu/hr sq ft °F	91.81	78.89	83.23	80.35	81.52	81.60	85.12	92.23

BOILING RESEARCH DATA AND RESULTS TABULATION SHEET

TEST NO. (Date) 717 AMBIENT TEMPERATURE 85°F REFERENCE JUNCTION 32°F

FLUID Refrigerant - 11

HEATER Material: Kanthal A-1 Size: 1.0 x 4.06 x 0.010 Surface Condition: Sand blasted; 50-90 μ in. rms.

Run No.	1	2	3	4	5	6	7	8
Current amperes	148.2	137.0	128.7	121.0	112.5	132.5	140.5	145.5
Voltage Drop across Heater volts	4.06	3.83	3.64	3.44	3.20	3.90	4.30	4.60
Average Heater Temperature, T_H °F	1,378	1,279	1,180	1,089	957	1,258	1,268	1,449
Average Bulk Temperature, T_B °F	75	75	75	75	75	75	75	75
Temperature Drop in Backing °F	221	240	217	192	159	258	237	268
Power Supplied to Test Section Btu/hr sq ft	72,786	63,474	56,670	50,352	43,549	62,511	73,084	80,965
Heat Loss through Backing Btu/hr sq ft	6,647	7,219	6,527	5,775	4,783	7,761	7,129	8,964
Temperature Difference, ΔT °F ($T_H - T_B$)	1,303	1,204	1,105	1,014	882	1,183	1,193	1,374
Boiling Heat Flux, Q/A Btu/hr sq ft	66,139	56,255	50,143	44,577	37,766	54,750	65,955	72,001
Heat Transfer Coefficient, h Btu/hr sq ft °F	50.75	45.72	45.37	43.95	42.81	45.28	55.28	52.40

BOILING RESEARCH DATA AND RESULTS TABULATION SHEET

TEST NO. (Date) 717(con't) AMBIENT TEMPERATURE 85°F REFERENCE JUNCTION 32°F

FLUID Refrigerant - 11

HEATER Material: Kanthal A-1 Size: 1.0 x 4.06 x 0.010 Surface Condition: Sand blasted; 50-90 μ in.rms.

Run No.	9							
Current amperes	155.5							
Voltage Drop across Heater volts	5.29							
Average Heater Temperature, T_H °F	1,645							
Average Bulk Temperature, T_B °F	75							
Temperature Drop in Backing °F	327							
Power Supplied to Test Section Btu/hr sq ft	99,509							
Heat Loss through Backing Btu/hr sq ft	9,836							
Temperature Difference, ΔT °F ($T_H - T_B$)	1570							
Boiling Heat Flux, Q/A Btu/hr sq ft	89,673							
Heat Transfer Coefficient, h Btu/hr sq ft °F	57.11							

TEST NO. (Date) 718A AMBIENT TEMPERATURE 87°F REFERENCE JUNCTION -320°F

FLUID Nitrogen

HEATER Material: Inconel - 600 Size: 0.5 x 3.91 x 0.005 Surface Condition: Mirror Finish

Run No.	1	2	3	4	5	6	7	8
Current amperes	39.2	45.8	52.0	57.0	59.2	62.0	65.0	55.5
Voltage Drop across Heater volts	2.68	3.15	3.63	4.05	4.22	4.44	4.73	4.00
Average Heater Temperature, T_H °F	-25	103	304	598	684	793	937	655
Average Bulk Temperature, T_B °F	-320	-320	-320	-320	-320	-320	-320	-320
Temperature Drop in Backing °F	197	260	228	399	428	476	523	353
Power Supplied to Test Section Btu/hr sq ft	26,434	36,303	47,498	58,089	62,862	69,269	77,363	55,862
Heat Loss through Backing Btu/hr sq ft	8,422	7,821	9,866	12,002	12,874	14,318	15,732	10,618
Temperature Difference, ΔT °F ($T_H - T_B$)	295	423	624	918	1,004	1,113	1,257	975
Boiling Heat Flux, q/A Btu/hr sq ft	14,012	28,482	37,632	46,087	49,988	54,951	61,631	45,244
Heat Transfer Coefficient, h Btu/hr sq ft °F	41.25	72.9	93.3	112.5	119.7	129.0	147.0	107.5

BOILING RESEARCH DATA AND RESULTS TABULATION SHEET

TEST NO. (Date) 718A(cont'd) AMBIENT TEMPERATURE 87°F REFERENCE JUNCTION -320°F

FLUID Nitrogen

HEATER Material: Inconel - 600 Size: 0.5 x 3.91 x 0.005 Surface Condition: Mirror Finish

Run No.	9	10	11	12	13	14
Current amperes	51.5	49.5	46.7	45.0	42.0	41.5
Voltage Drop across Heater volts	3.68	3.51	3.31	3.19	2.96	2.89
Average Heater Temperature, T_H °F	546	483	417	377	299	274
Average Bulk Temperature, T_B °F	-320	-320	-320	-320	-320	-320
Temperature Drop in Backing °F	289	261	228	225	178	142
Power Supplied to Test Section Btu/hr sq ft	47,689	43,718	38,894	36,121	31,282	30,178
Heat Loss through Backing Btu/hr sq ft	8,693	7,851	6,858	6,765	5,354	4,271
Temperature Difference, ΔT °F ($T_H - T_B$)	866	803	737	697	619	594
Boiling Heat Flux, q/A Btu/hr sq ft	38,996	35,867	32,036	29,356	25,928	25,907
Heat Transfer Coefficient, h Btu/hr sq ft °F	45.65	44.35	43.45	42.11	41.58	43.61

TABLE XVII

BOILING RESEARCH DATA AND RESULTS TABULATION SHEETTEST NO. (Date) 718B AMBIENT TEMPERATURE 90°F REFERENCE JUNCTION 32°FFLUID Refrigerant - 11HEATER Material: Inconel-600 Size: 0.5 x 3.91 x 0.005 Surface Condition: Mirror Finish

Run No.	1	2	3	4	5	6	7	8
Current amperes	57.0	53.5	50.0	48.0	45.0	52.5	57.0	61.0
Voltage Drop across Heater volts	4.12	3.85	3.62	3.47	3.13	3.84	4.12	4.45
Average Heater Temperature, T_H °F	867	801	701	668	568	715	872	980
Average Bulk Temperature, T_B °F	75	75	75	75	75	75	75	75
Temperature Drop in Backing °F	336	247	209	186	166	230	274	346
Power Supplied to Test Section Btu/hr sq ft	59,093	51,828	45,545	41,912	35,442	50,729	59,093	68,305
Heat Loss through Backing Btu/hr sq ft	10,107	7,430	6,287	5,595	4,993	6,918	8,242	10,408
Temperature Difference, ΔT °F ($T_H - T_B$)	792	726	626	593	493	640	797	905
Boiling Heat Flux, Q/A Btu/hr sq ft	48,986	44,398	39,258	36,317	30,449	43,811	50,851	57,897
Heat Transfer Coefficient, h Btu/hr sq ft °F	61.85	61.15	62.71	61.24	61.76	68.45	63.80	63.97

BOILING RESEARCH DATA AND RESULTS TABULATION SHEET

TEST NO. (Date) 718B(cont'd) AMBIENT TEMPERATURE 90°F REFERENCE JUNCTION 32°F

FLUID Refrigerant - 11

HEATER Material: Inconel - 600 Size: 0.5 x 3.91 x 0.005 Surface Condition: Mirror Finish

Run No.	9	10	11	12	13	14	15	16
Current amperes	63.0	65.0	59.5	54.0	58.0	62.0	66.2	67.0
Voltage Drop across Heater volts	4.62	4.80	4.43	4.00	4.33	4.60	4.99	5.09
Average Heater Temperature, T_H °F	1,010	1,036	926	779	894	971	1,064	1,073
Average Bulk Temperature, T_B °F	75	75	75	75	75	75	75	75
Temperature Drop in Backing °F	369	390	335	271	320	364	420	431
Power Supplied to Test Section Btu/hr sq ft	73,239	78,509	66,325	54,352	63,194	71,765	83,121	85,813
Heat Loss through Backing Btu/hr sq ft	11,100	11,731	10,077	8,152	9,626	10,949	12,634	12,965
Temperature Difference, ΔT °F ($T_H - T_B$)	935	961	851	704	819	896	989	998
Boiling Heat Flux, Q/A Btu/hr sq ft	62,139	66,778	56,248	46,200	53,568	60,816	70,487	72,848
Heat Transfer Coefficient, h Btu/hr sq ft °F	66.45	69.48	66.09	65.62	65.40	67.87	71.27	72.99

BOILING RESEARCH DATA AND RESULTS TABULATION SHEET

TEST NO. (Date) 718B(cont'd) AMBIENT TEMPERATURE 90°F REFERENCE JUNCTION 32°F

FLUID Refrigerant - 11

HEATER Material: Inconel - 600 Size: 0.5 x 3.91 x 0.005 Surface Condition: Mirror Finish

Run No.	17						
Current amperes	68.5						
Voltage Drop across Heater volts	5.72						
Average Heater Temperature, T_H °F	1,161						
Average Bulk Temperature, T_B °F	75						
Temperature Drop in Backing °F	455						
Power Supplied to Test Section Btu/hr sq ft	98,594						
Heat Loss through Backing Btu/hr sq ft	13,686						
Temperature Difference, ΔT °F ($T_H - T_B$)	1086						
Boiling Heat Flux, Q/A Btu/hr sq ft	84,908						
Heat Transfer Coefficient, h Btu/hr sq ft °F	78.18						

BOILING RESEARCH DATA AND RESULTS TABULATION SHEET

TEST NO. (Date) 719 AMBIENT TEMPERATURE 85°F REFERENCE JUNCTION -320°F

FLUID Nitrogen

HEATER Material: Inconel - 600 Size: 1.0 x 4.03 x 0.005 Surface Condition: Mirror Finish

Run No.	1	2	3	4	5	6	7	8
Current amperes	83.0	84.0	87.5	91.2	93.7	98.0	100.8	105.5
Voltage Drop across Heater volts	3.17	3.22	3.34	3.51	3.62	3.83	3.99	4.20
Average Heater Temperature, T_H °F	251	233	278	399	468	606	685	790
Average Bulk Temperature, T_B °F	-320	-320	-320	-320	-320	-320	-320	-320
Temperature Drop in Backing °F	228	223	224	136	146	256	256	283
Power Supplied to Test Section Btu/hr sq ft	32,076	32,974	35,628	39,025	41,351	45,758	49,031	54,018
Heat Loss through Backing Btu/hr sq ft	6,858	6,708	6,738	7,099	7,400	7,700	7,700	8,513
Temperature Difference, ΔT °F ($T_H - T_B$)	571	553	598	719	788	926	1,005	1,110
Boiling Heat Flux, Q/A Btu/hr sq ft	25,218	26,266	28,890	31,926	33,951	38,058	41,331	45,505
Heat Transfer Coefficient, h Btu/hr sq ft °F	44.16	47.49	48.31	44.40	43.08	41.09	41.12	40.99

BOILING RESEARCH DATA AND RESULTS TABULATION SHEET

TEST NO. (Date) 719(cont'd) AMBIENT TEMPERATURE 85°F REFERENCE JUNCTION -320°F

FLUID Nitrogen

HEATER Material: Inconel - 600 Size: 1.0 x 4.03 x 0.005 Surface Condition: Mirror Finish

Run No.	9	10	11	12	13	14	15	16
Current amperes	110.8	97.5	93.0	90.5	87.5	83.2	79.5	74.2
Voltage Drop across Heater volts	4.42	3.88	3.69	3.54	3.42	3.25	3.09	2.87
Average Heater Temperature, T_H °F	942	693	606	552	512	429	366	275
Average Bulk Temperature, T_B °F	-320	-320	-320	-320	-320	-320	-320	-320
Temperature Drop in Backing °F	309	240	207	195	177	158	143	119
Power Supplied to Test Section Btu/hr sq ft	59,703	46,119	41,836	39,056	36,482	32,964	29,947	25,961
Heat Loss through Backing Btu/hr sq ft	9,295	7,219	6,227	5,866	5,324	4,753	4,301	3,580
Temperature Difference, ΔT °F ($T_H - T_B$)	1,262	1,013	926	872	832	749	686	595
Boiling Heat Flux, Q/A Btu/hr sq ft	50,408	38,900	35,609	33,190	31,158	28,211	25,646	22,381
Heat Transfer Coefficient, h Btu/hr sq ft °F	39.94	38.40	38.45	38.10	37.44	37.66	37.38	37.61

BOILING RESEARCH DATA AND RESULTS TABULATION SHEET

TEST NO. (Date) 719(cont'd) AMBIENT TEMPERATURE 85°F REFERENCE JUNCTION -320°F

FLUID Nitrogen

HEATER Material: Inconel - 600 Size: 1.0 x 4.03 x 0.005 Surface Condition: Mirror Finish

Run No.	17						
Current amperes	71.7						
Voltage Drop across Heater volts	2.77						
Average Heater Temperature, T_H °F	237						
Average Bulk Temperature, T_B °F	-320						
Temperature Drop in Backing °F	106						
Power Supplied to Test Section Btu/hr sq ft	24,211						
Heat Loss through Backing Btu/hr sq ft	3,188						
Temperature Difference, ΔT °F ($T_H - T_B$)	557						
Boiling Heat Flux, Q/A Btu/hr sq ft	21,023						
Heat Transfer Coefficient, h Btu/hr sq ft °F	37.74						

BOILING RESEARCH DATA AND RESULTS TABULATION SHEET

TEST NO. (Date) 721 AMBIENT TEMPERATURE 86°F REFERENCE JUNCTION 32°F

FLUID Refrigerant - 11

HEATER Material: Inconel - 600 Size: 2.0 x 4.12 x 0.005 Surface Condition: Mirror Finish

Run No.	1	2	3	4				
Current amperes	176.7	170.5	163.5	154.5				
Voltage Drop across Heater volts	3.45	3.35	3.20	3.02				
Average Heater Temperature, T_H °F	960	915	857	801				
Average Bulk Temperature, T_B °F	75	75	75	75				
Temperature Drop in Backing °F	102	98	82	68				
Power Supplied to Test Section Btu/hr sq ft	36,400	34,000	31,200	27,800				
Heat Loss through Backing Btu/hr sq ft	3,350	2,950	2,470	2,045				
Temperature Difference, ΔT °F ($T_H - T_B$)	885	840	782	726				
Boiling Heat Flux, Q/A Btu/hr sq ft	33,050	31,050	28,730	25,755				
Heat Transfer Coefficient, h Btu/hr sq ft °F	37.4	37.0	36.7	35.4				

APPENDIX C

STATISTICAL DATA ANALYSIS

NITROGEN 0.5 I

LEAST SQUARES POLY COEFF. ARE:

A(0)= -0.94967770E 04
 A(1)= 0.57441800E 05

DELTA T	HEAT FLUX	CALC. HEAT FLUX	% DEVIATION	H
0.91799970E 03	0.46090000E 05	0.43387230E 05	5.8641	50.2070
0.10039990E 04	0.49990000E 05	0.48291210E 05	3.3983	49.7909
0.11129990E 04	0.54950000E 05	0.54426230E 05	0.9532	49.3711
0.12569990E 04	0.61630000E 05	0.62393240E 05	-1.2384	49.0294
0.07499970E 03	0.45240000E 05	0.46643810E 05	-3.1030	46.4000
0.86599970E 03	0.39000000E 05	0.40394860E 05	-3.5766	45.0247
0.80299970E 03	0.35970000E 05	0.36742050E 05	-2.4312	44.6700
0.73499970E 03	0.32040000E 05	0.32883070E 05	-2.6313	43.4735
0.69699970E 03	0.29350000E 05	0.30528230E 05	-4.0144	42.1090
0.61899970E 03	0.25930000E 05	0.25901460E 05	0.1101	41.8902
0.59399970E 03	0.25910000E 05	0.24408760E 05	5.7940	43.6195

AVERAGE DEVIATION = 3.01041100 % DEGREE = 1

TABLE XX

Statistical Data for 0.5 in. Inconel in Nitrogen

NITROGEN 1.0 I

LEAST SQUARES POLY COEFF. ARE:

A(0)= -0.37860580E 04
 A(1)= 0.43374440E 05

DELTA T	HEAT FLUX	CALC. HEAT FLUX	% DEVIATION	H
0.92599970E 03	0.38060000E 05	0.36286640E 05	4.6594	41.1015
0.10049990E 04	0.41330000E 05	0.39742720E 05	3.8405	41.1244
0.11099990E 04	0.45510000E 05	0.44382460E 05	2.4776	41.0000
0.12619990E 04	0.50410000E 05	0.51192330E 05	-1.5519	39.9445
0.10129990E 04	0.38900000E 05	0.40994380E 05	-3.0704	38.4008
0.92599970E 03	0.35610000E 05	0.36286640E 05	-1.9002	38.4557
0.87199970E 03	0.33190000E 05	0.33941410E 05	-2.2640	38.0619
0.83199970E 03	0.31160000E 05	0.32213170E 05	-3.3799	37.4519
0.74899970E 03	0.28210000E 05	0.28651480E 05	-1.5650	37.6636
0.68599970E 03	0.25650000E 05	0.25970010E 05	-1.2476	37.3907
0.59499970E 03	0.22380000E 05	0.22130250E 05	1.1159	37.6134
0.55699970E 03	0.21020000E 05	0.20538550E 05	2.2904	37.7379
AVERAGE DEVIATION =			2.44688600 %	DEGREE = 1

TABLE XXI

Statistical Data for 1.0 in Inconel in Nitrogen

NITROGEN 2.0 T

LEAST SQUARES POLY COEFF. ARE:

A(0) = 0.13750370E 05
 A(1) = -0.242299880E 05
 A(2) = 0.60840220E 05
 A(3) = -0.20292820E 05

DELTA T	HEAT FLUX	CALC. HEAT FLUX	% DEVIATION	H
0.85109970E 03	0.24490000E 05	0.24609100E 05	-0.4823	28.7441
0.10030000E 04	0.29850000E 05	0.30160530E 05	-1.0403	29.7311
0.11430090E 04	0.34480000E 05	0.35237360E 05	-2.1955	30.1399
0.89909970E 03	0.25300000E 05	0.26327600E 05	-4.0620	28.1111
0.75200070E 03	0.20800000E 05	0.21247600E 05	-2.1520	27.6228
0.68600070E 03	0.19060000E 05	0.19188090E 05	-0.6721	27.7438
0.58600070E 03	0.16190000E 05	0.16395520E 05	-1.2694	27.5909
0.49500070E 03	0.13900000E 05	0.14220240E 05	-2.3039	28.0242
0.04500070E 03	0.29540000E 05	0.28011850E 05	5.1731	31.2262
0.10000000E 04	0.30100000E 05	0.30012100E 05	0.2920	30.1000
0.10630090E 04	0.31200000E 05	0.32375920E 05	-3.7690	29.3233
0.11050090E 04	0.33620000E 05	0.32897850E 05	-0.8264	30.3978
0.12570090E 04	0.33850000E 05	0.38894260E 05	-0.1139	30.8924
0.93300070E 03	0.27000000E 05	0.27753910E 05	-2.7923	28.7540
0.69500070E 03	0.19180000E 05	0.19459300E 05	-1.4562	27.5575
0.57100070E 03	0.15800000E 05	0.16012750E 05	-4.6860	29.3706
0.11010000E 04	0.35520000E 05	0.33754470E 05	4.9705	32.3323
0.11090090E 04	0.34760000E 05	0.34005050E 05	2.1719	31.3436
0.11390090E 04	0.35060000E 05	0.35063480E 05	-0.0105	30.7814
0.11320000E 04	0.34600000E 05	0.34854140E 05	-0.4732	30.6178
0.11970000E 04	0.37130000E 05	0.37051310E 05	0.2119	30.9933
0.10390000E 04	0.31110000E 05	0.31456530E 05	-1.1130	30.9423
0.97000070E 03	0.23910000E 05	0.23936320E 05	-0.0911	29.7224
0.90100070E 03	0.25640000E 05	0.26400290E 05	-0.8998	29.5264
0.94000070E 03	0.24770000E 05	0.24221140E 05	2.2158	29.4530
0.77900070E 03	0.22350000E 05	0.22101370E 05	1.1124	28.6906
0.77600070E 03	0.22380000E 05	0.22034900E 05	1.5420	28.8031

AVERAGE DEVIATION = 1.79149600 % DEGREE = 3

TABLE XXII

Statistical Data for 2.0 in. Inconel in Nitrogen

R-11 0.5 I

LEAST SQUARES POLY COEFF. ARE:

A(0)= 0.56492880E 02
 A(1)= 0.16038780E 00

HEAT FLUX	H	CALC. H	% DEVIATION
0.48989980E 05	0.61950000E 02	0.64970050E 02	-3.5894
0.44399990E 05	0.61149990E 02	0.63390670E 02	-3.6642
0.39259990E 05	0.62710000E 02	0.62766020E 02	-0.0893
0.36319980E 05	0.61240000E 02	0.62473370E 02	-2.0140
0.30449990E 05	0.61759990E 02	0.62029870E 02	-0.4370
0.43809990E 05	0.68449990E 02	0.63311660E 02	7.5067
0.50849980E 05	0.63800000E 02	0.64378000E 02	-0.9060
0.57899990E 05	0.63970000E 02	0.65716290E 02	-2.7299
0.62139990E 05	0.66449990E 02	0.66651450E 02	-0.3032
0.66779930E 05	0.69479990E 02	0.67787010E 02	2.4366
0.56250000E 05	0.66089990E 02	0.65378910E 02	1.0761
0.46199990E 05	0.65619990E 02	0.63643410E 02	3.0122
0.53569980E 05	0.65399990E 02	0.64862280E 02	0.8222
0.60819980E 05	0.64839990E 02	0.66349820E 02	-2.3285
AVERAGE DEVIATION = 2.20822600 %			DEGREE = 1

TABLE XXIII

Statistical Data for 0.5 in. Inconel in Refrigerant-11

R-11 1.0 K

LEAST SQUARES POLY COEFF. ARE:

A(0) = 0.23496670E 02
 A(1) = 0.52384100E 00
 A(2) = -0.16617430E-02

HEAT FLUX	H	CALC. H	% DEVIATION
0.4036000E 05	0.30140000E 02	0.42014400E 02	-7.3167
0.6531000E 05	0.47420000E 02	0.50517340E 02	-6.5093
0.5771000E 05	0.48050000E 02	0.48143200E 02	-0.1942
0.4610000E 05	0.44720000E 02	0.44156240E 02	1.2382
0.3800000E 05	0.42630000E 02	0.41125510E 02	5.7619
0.3933000E 05	0.43100000E 02	0.41800000E 02	2.0955
0.3055000E 05	0.38000000E 02	0.38004570E 02	-0.0120
0.2564000E 05	0.37100000E 02	0.35822780E 02	3.7022
0.2370000E 05	0.38300000E 02	0.34058750E 02	8.9616
0.3750000E 05	0.36000000E 02	0.40026680E 02	-2.5732
0.3370000E 05	0.37000000E 02	0.30378200E 02	-6.4281
0.2345000E 05	0.35500000E 02	0.37086530E 02	-4.4691
0.2321000E 05	0.34100000E 02	0.34606300E 02	-1.7487
0.1953000E 05	0.31000000E 02	0.32028610E 02	-6.2214
0.6513000E 05	0.50750000E 02	0.50764250E 02	-0.0281
0.5625000E 05	0.46720000E 02	0.47660040E 02	-2.0202
0.5013000E 05	0.45360000E 02	0.45600150E 02	-0.5072
0.4457000E 05	0.43060000E 02	0.42605680E 02	0.8060
0.3776000E 05	0.46270000E 02	0.40004300E 02	4.2411
0.5475000E 05	0.45270000E 02	0.47160420E 02	-1.0219
0.6595000E 05	0.55270000E 02	0.50710180E 02	8.2667
0.7200000E 05	0.52300000E 02	0.52682000E 02	-0.1582
0.8966000E 05	0.57110000E 02	0.57296460E 02	-0.3265

AVERAGE DEVIATION = 3.3224600 % DFGRFF = 2

TABLE XXIV

Statistical Data for 1.0 in. Kanthal in Refrigerant-11

R-11 2.0 I

LEAST SQUARES POLY COEFF. ARE:

A(0) = 0.46777800E 01
A(1) = 0.19194050E 01
A(2) = -0.28158620E-01

HEAT FLUX	H	CALC. H.	% DEVIATION
0.33049980E 05	0.37399990E 02	0.37345590E 02	0.1454
0.31049980E 05	0.37000000E 02	0.37139870E 02	-0.3780
0.28729980E 05	0.36699990E 02	0.36585110E 02	0.3130
0.25759990E 05	0.35399990E 02	0.35429350E 02	-0.0829
AVERAGE DEVIATION =		0.22986510 %	DEGREE = 2

TABLE XXV

Statistical Data for 2.0 in. Inconel in Refrigerant-11

LEAST SQUARES POLY COEFF. ARE:

A(0)= 0.12596290E 02
 A(1)= 0.23432780E 02

DELTA T	H	CALC. H	% DEVIATION
0.10300000E 04	0.39140000E 02	0.43721110E 02	-11.6759
0.13760000E 04	0.47420000E 02	0.51896640E 02	-9.3963
0.12000000E 04	0.48050000E 02	0.47717130E 02	0.6928
0.10300000E 04	0.44720000E 02	0.43721110E 02	2.2336
0.87200000E 03	0.43630000E 02	0.40034820E 02	8.2612
0.92400000E 03	0.43100000E 02	0.41245100E 02	4.3027
0.20200000E 03	0.39000000E 02	0.38410140E 02	-1.0703
0.68000000E 03	0.37100000E 02	0.35798460E 02	3.7676
0.61700000E 03	0.38300000E 02	0.34141490E 02	11.0898
0.94300000E 03	0.39000000E 02	0.41698030E 02	-4.4813
0.91400000E 03	0.37000000E 02	0.41012110E 02	-10.8436
0.80200000E 03	0.35500000E 02	0.33410140E 02	-8.1976
0.68000000E 03	0.34100000E 02	0.35591040E 02	-4.3726
0.62000000E 03	0.31000000E 02	0.34417260E 02	-11.0234
0.13020000E 04	0.50750000E 02	0.50129530E 02	1.2226
0.12030000E 04	0.46720000E 02	0.47787930E 02	-2.2858
0.11040000E 04	0.45360000E 02	0.45456780E 02	-0.1013
0.10130000E 04	0.43960000E 02	0.43323220E 02	1.4485
0.98100000E 03	0.42800000E 02	0.40244000E 02	5.9937
0.11820000E 04	0.45270000E 02	0.47202570E 02	-2.1879
0.11920000E 04	0.55270000E 02	0.47528410E 02	14.0224
0.13730000E 04	0.52300000E 02	0.51815270E 02	1.1159
0.15690000E 04	0.57110000E 02	0.56496810E 02	1.0737

AVERAGE DEVIATION = 5.25914400 % DEGREE = 1

TABLE XXVI

Statistical Data for 1.0 in. Kanthal in Refrigerant-11

APPENDIX D

THERMOPHYSICAL PROPERTIESRefrigerant-11Density in (lbs. _m/cu. ft.)

$$\rho_l = 91.3$$

$$\rho_v = \frac{P}{RT}, \text{ where } P \text{ is pressure in (lbs.}_f\text{/sq.ft.)}, \text{ and } R = 11.21$$

(ft. lbs._f/lbs._m^oF). The temperature, T, is the mean temperature of the vapor film. (^oR)

Latent Heat of Vaporization in (BTU/lbs._m). (11)

$$h_{fg} = 78.3$$

$$h'_{fg} = 78.3 \left[1 + (34C_{pv} \Delta T / 78.3) \right]^2$$

h'_{fg} includes the sensible heat added to vapor due to the fact that the average temperature of the vapor is above the saturation temperature.*

Vapor Thermal Conductivity in (BTU/hr.ft.^oF) (11)

$$K_{vf} = 0.0048 + 1.14 \cdot 10^{-5} T \text{ where } T \text{ is the average temperature}$$

of the vapor film in ^oF.

Vapor Viscosity in (lbs._f hr./sq.ft.)

{ See Perry's Handbook }⁽³⁷⁾

*

Chang's equation for the prediction of heat transfer coefficients does not include the sensible heat added to the vapor film in his λ value. Therefore, to add a degree of reality to Chang's equation h'_{fg} values were calculated and used instead of the simple latent heat of vaporization, λ , that he suggests.

Surface Tension in (lbs._f/ft.)

$$\sigma = 1.3 \cdot 10^{-3}$$

Vapor Specific Heat in (BTU/lbs._m °F)

(See Perry's Handbook)⁽³⁷⁾

Nitrogen

Density in (lbs._m/cu.ft.)

$$\rho_l = 50.47$$

$$\rho_v = \frac{P}{RT}, \text{ where } P \text{ is pressure in (lbs._f/sq.ft.), and } R = 55.2$$

(ft.lbs._f/lbs._m °F). The temperature T, is the mean temperature

the vapor film. (°R)

Latent Heat of Vaporization in (BTU/lbs._m).⁽³⁸⁾

$$h_{fg} = 86.0$$

$$h'_{fg} = 86.0 + .224(T + 320), \text{ where } T \text{ is the average temperature}$$

of the vapor film. (°F)

Vapor Thermal Conductivity in (BTU/hr.ft. °F)

$$K_{vf} = (241.9) (6.15) 10^{-6} T/1 + (235.5/T) (10^{-\frac{12}{T}})$$

where T is in °K.

Vapor Viscosity in (lbs._fhr./sq. ft.)

See Perry's Handbook⁽³⁷⁾

Surface Tension in (lbs._f/ft.)

$$\sigma = 5.67 \cdot 10^{-4}$$

VITA

The author of this thesis, Kenneth Martin Ragsdell, was born on September 3, 1942, in Jacksonville, Illinois. He attended elementary and secondary schools in St. Louis, Missouri, and was graduated from Wellston High School in June of 1960.

He entered the University of Missouri School of Mines and Metallurgy in the fall of 1960, and completed one year. On February 14, 1962 he married Miss Janet Anna Norton, and they moved to Rolla in the fall of 1963 so he could resume his studies at the University. He received his bachelor of science degree in Mechanical Engineering in June, 1966, and immediately thereafter entered the graduate school at the University of Missouri at Rolla.